

Threshold and Symmetric Functions over Bitmaps

TR-14-001, Dept of CSAS

Owen Kaser
Dept. of CSAS
UNBSJ
Saint John, NB

Daniel Lemire
LICEF, TELUQ
Université du Québec
Montreal, QC

June 12, 2021

Threshold and symmetric functions over bitmaps

Owen Kaser and Daniel Lemire

June 12, 2021

Abstract

Bitmap indexes are routinely used to speed up simple aggregate queries in databases. Set operations such as intersections, unions and complements can be represented as logical operations (`and`, `or`, `not`). However, less is known about the application of bitmap indexes to more advanced queries. We want to extend the applicability of bitmap indexes. As a starting point, we consider symmetric Boolean queries (e.g., threshold functions). For example, we might consider stores as sets of products, and ask for products that are on sale in 2 to 10 stores. Such symmetric Boolean queries generalize intersection, union, and T-occurrence queries.

It may not be immediately obvious to an engineer how to use bitmap indexes for symmetric Boolean queries. Yet, maybe surprisingly, we find that the best of our bitmap-based algorithms are competitive with the state-of-the-art algorithms for important special cases (e.g., MergeOpt, MergeSkip, DivideSkip, ScanCount). Moreover, unlike the competing algorithms, the result of our computation is again a bitmap which can be further processed within a bitmap index.

We review algorithmic design issues such as the aggregation of many compressed bitmaps. We conclude with a discussion on other advanced queries that bitmap indexes might be able to support efficiently.

1 Introduction

There are many applications to bitmap indexes, from conventional databases (e.g., Oracle [3]) all the way to information retrieval [9] and including on column stores [37]. We are primarily motivated by the application of bitmap indexes to common databases (i.e., row stores). In this case, it has long been established that bitmap indexes can

This report is intended to be viewed electronically and uses fonts and colours that make it unsuited for viewing on paper.

Table 1: Algorithms considered in this report.

Algorithm	Source	Section
SCANCOUNT	[25]	§ 4.2
HASHCNT	variant of SCANCOUNT	§ 4.2
MGOPT	[35]	§ 4.3
DSK	[25]	§ 4.3
LOOPED	novel	§ 4.5
TREEADD	novel	§ 4.4.2
SSUM	related to [33]	§ 4.4.2
CSVCKT	novel	§ 4.4.2
SRTCCT	novel	§ 4.4.1
SOPCKT	novel	§ 4.4
RBMRG	modified from [23]	§ 4.1
WHEAP	[35]	§ 4.3
WMGSK	[25]	§ 4.3
W2CTA	novel	§ 4.2.2
W2CTN	novel	§ 4.2.2
W2CTI	novel	§ 4.2.2
WSORT	novel	§ 4.2.1

speed up several queries corresponding, e.g., to intersections or unions (such as `SELECT * WHERE A=1 AND B=2`). We show that these good results extend to the more advanced queries we want to consider.

Since bitmap indexes are widely used and basic Boolean operators over the bitmaps have been found useful in answering queries, our broad goal is to investigate how to integrate symmetric Boolean functions (in particular, threshold functions such as the Majority function) into the set of operations supported on bitmaps. This would permit queries that arbitrarily combine such complex functions and the standard operations permitted on bitmaps (OR, AND, XOR, perhaps NOT) and so forth.

Of course, the set of basic operations (typically depending whether NOT is provided) may be sufficient to synthesize any required function, symmetric or otherwise. However, the efficiency of such approaches is not clear. To our knowledge, it has never been investigated in depth: the exception is Rinfret et al. [33] where two algorithms are compared on a closely related problem.

The concrete contribution of this report is a study of an extensive set of alternative algorithms (see Table 1) to compute threshold functions over bitmap indexes. Many of the alternatives can be generalized to handle arbitrary symmetric Boolean functions. The theoretical analyses of these alternatives are summarized in Tables 3 and 4. The notation used in the tables can be found in Table 2.

We shall see that the characteristics of the bitmaps, such as the number of ones or the number of distinct runs, have a major effect in determining the superior alternatives. This is determined by extensive experiments described in § 5. To obtain results that correspond to a practical applications of bitmap indexes, we focus on using threshold functions over bitmap indexes to answer *similarity* queries.

Similarity Queries: A similarity query presents a prototypical item. We determine the criteria that this item meets, and then seek all items that meet (at least) T of these criteria. For example, if a user liked a given movie, he might be interested in other similar movies (e.g., same director, or same studio, or same leading star, or same date of release). As part of a recommender system, we might be interested in identifying quickly all movies satisfying at least T of these criteria.

Similarity queries could be used to study the vocabulary of a corpus of texts. Items are vocabulary words, and the occurrence within a given text is a binary attribute. Given a word such as “pod”, we will seek words that occur in many of the same texts that “pod” occurs in. We might thus find “whale” and “pea”, besides many words that occur in almost every text. Once filtered of words that occur commonly across the corpus, we might produce information that would interest a literary analyst or linguist.

Similarity queries have previously been used with approximate string matching [25, 35]. In this case, items are small chunks of text, and the occurrence of a particular q -gram is a criterion². In this previous work, each q -gram has a sorted list of integers that specify the chunks of text containing it. Ferro et al. [12] solve a very similar problem, but instead use a bitmap for each q -gram³. Montaneri and Puglisi [28] extend the bitmap approach to detect near-duplicate documents arriving over time.

A generalization of a similarity query presents *several* prototypical items, then determines the criteria met by at least one of them. We then proceed as before, finding all items in the database that meet at least T of the criteria.

Another generalization allows criteria to be assigned different weights, to reflect their relative importance. In our recommender system, we might want to give more weight to having the right director than the right movie studio.

Once the criteria have been defined, it is possible to use SQL to handle the rest of the query. For instance, one might use a query⁴ like

```
SELECT * FROM movies WHERE  
IF (Lead=" Sean_Penn " ,1 ,0) +
```

²Their experiments used $q = 3$.

³Their experiments used $q = 2$.

⁴MySQL syntax used. Some databases use IIF or CASE instead of IF.

```

IF ( Studio="Paramount" , 1 , 0 ) +
IF ( Director="Ridley_Scott" , 1 , 0 ) > 2

```

Assuming you have a bitmap index, can you do better than the row-scan that would be done by a typical database engine?

Formulation We take N sorted sets over a universe of r distinct values. For our purposes, we represent sets as bitmaps using r bits. See Table 2.

The sum of the cardinalities of the N sets is B . We apply a threshold T ($1 \leq T \leq N$), seeking those elements that occur in at least T sets. Because the cases $T = 1$ and $T = N$ correspond to intersections and unions, and are well understood, we assume that $2 \leq T \leq N - 1$. These queries are often called T -overlap [26, 5] or T -occurrence [25, 18] queries. We show that, indeed, bitmap indexes can be used to speed up T -overlap queries (when compared with a row-store scan, see § 3).

We can map a T -overlap query to a query over bitmaps using a Boolean threshold function: given N bits, the T -threshold function returns true if at least T bits are true, it returns false otherwise. A (unary) bitmap index over a table has as many bitmaps as there are distinct attribute values. Each attribute value (say value v of attribute a) has a bitmap that encodes the set of row-ids (rids) that satisfy the criterion $v = a$. A T -overlaps query seeks rids that occur in at least T of N chosen sets. Since each set is encoded as a bitmap, we need to compute a bitwise threshold function over the N chosen bitmaps.

Threshold functions are a subset of the symmetric Boolean functions. They include the majority function: given N bits, the majority function returns true when $\lceil N/2 \rceil$ or more bits are true, and it returns false otherwise.

We denote the processor's native word length as W (currently⁵ $W = 64$ is typical). An uncompressed bitmap will have $\lceil r/W \rceil$ words. If you have N bitmaps, then you have $N \lceil r/W \rceil$ words. To simplify, we assume $\log N < W < r$ as well⁶ as $\log r \leq W$, which would typically be the case in the applications we envision. Also, we assume that $B \geq N$, which would be true if there is no empty bitmap.

For the remainder of the paper we assume that a bitmap index has been created over the table, where each attribute value is represented by a bitmap (compressed or otherwise). Perhaps the index is smaller than the original table and can fit in main memory; if not, we assume that at least the N bitmaps involved in the threshold query can be simultaneously stored in memory. Thus, even if the N bitmaps must be initially loaded from disk, we only consider in-memory computation. For even larger datasets, we could assume that the table has been horizontally fragmented

⁵Common 64-bit PCs have SIMD instructions that work over 128-bit (SSE and AVX) and 256-bit (AVX2) vectors. These instructions might be used automatically by compilers and interpreters.

⁶In this paper, $\log n$ means $\log_2 n$.

Table 2: Notation used in analyses.

Symbol	Meaning
N	Number of bitmaps in query
N_{\max}	Maximum value of N allowed
T	Minimum threshold
r	length of bitmaps (largest index covered)
B_i	i^{th} bitmap
\mathcal{B}	$\{B_i\}$
$ B_i $	number of ones in i^{th} bitmap
B	$\sum_i B_i $
B'	number of ones not in $T - 1$ largest bitmaps
B''	number of ones not in L largest bitmaps
L	number of long bitmaps reserved in DSK
RUNCOUNT	number of runs of zeros and ones in collection of bitmaps
$\vartheta(T, \mathcal{B})$	threshold function over bitmaps
$\vartheta(T, \{b_1, \dots, b_N\})$	threshold function over bits b_i
W	machine word size

(the fragments would be much larger than with a row store), such that, for any fragment, any N bitmaps fit in memory. This paper does not consider external-memory algorithms that can compute thresholds without using much main memory.

Lower Bound: Towards a lower bound for the problem, note if the output indicates that X entries meet the threshold, we must have processed input such that at least TX predicate-satisfaction events have been observed. If each such observation triggers $\Omega(1)$ work (as it does with SCANCOUNT (§ 4.2), when a counter is incremented), this implies an $\Omega(TX)$ lower bound. However, this leaves open the possibility of using bit-level parallelism (readily available in bitmap inputs) to process several events per machine operation. (See § 4.4.) It also leaves open the possibility of using Run Length Encoding (RLE), whereby many consecutive events can be succinctly represented and processed together. We present such an approach later in § 4.1.

While it might superficially appear that a lower-bound could be based on a need to read the entire input, note that sometimes there is no such need. For instance, suppose the threshold is T and we have already processed $N - 1$ of our N input bitmaps. It is only necessary to inspect the last bitmap at positions where the current count is $T - 1$. Other positions already achieve the threshold, or have no possibility of achieving it. The strategy of skipping portions of the input has been

Table 3: Time and memory complexity of some threshold algorithms over **uncompressed** bitmap indexes. Our memory bounds exclude storage for the input and output bitmaps. The RBMRG is based on run-length encoding and is thus omitted. Factor rN/W is required to read all the input one word at a time. We assume that $rN/W \gg N \log N$. Actual bitmap libraries may detect that a bitmap has no ones past some word and thus run faster.

Algorithm	Time complexity (big-Oh)	Space complexity (big-Oh)		Comment
		horizontal	vertical	
SCANCOUNT	$rN/W + B$	W	r	
HASHCNT	expected $rN/W + B$	W	B	
WHEAP	$rN/W + B \log N$	N	N	
WMGSK	$rN/W + B \log N$	N	N	Note ¹
MGOPT	$r(N - T)/W + B'(\log(N - T) + T)$	$N - T$	$N - T$	
DSK	$r(N - L)/W + B''(\log(N - L) + L)$	$N - L$	$N - L$	
LOOPED	rNT/W	T	rT/W	Note ²
TREEADD	rN/W	N	rN/W	Note ³
SSUM	rN/W	N	rN/W	Note ³
CSVCKT	rN/W	N	$r \log(N)/W$	
SRTCKT	$\log^2(N)rN/W$	$N \log^2 N$	$rN \log^2(N)/W$	Note ³
SOPCKT	$N^T rN/W$	N^T	rN^T/W	Note ³
w2CTN	$rN/W + BN$	WN	B	
w2CTA	$rN/W + BN$	WN	B	Note ⁴
w2CTI	$rN/W + BN$	WN	B	Note ⁴
wSORT	$rN/W + B \log WN$	WN	B	Note ⁵

¹ Pruning can allow skipping portions of all bitmaps, so rN/W and B can be reduced, depending on data.

² While fewer than $7N$ temporary bitmaps are generated, register-allocation techniques would usually be able to share space between temporaries. In many cases, space for $o(N)$ bitmaps would suffice.

³ Register allocation should be able to greatly reduce the actual space requirements.

⁴ Pruning can reduce the amount of temporary data processed, but every input bitmap is completely scanned. w2CTI prunes more than w2CTA.

⁵ Vertical implementation would sort B values, for a time of $O(rN/W + B \log B)$.

used in prior algorithms noted in Table 1. Theoretically, they typically assume the ability to do random access on the input, so we can jump over irrelevant portions. The sorted-list-of-integers representation facilitates this kind of action, as do uncompressed bitmaps. However, word-aligned compressed bitmap representations typically do not support the required access in constant time [42]. Nevertheless, we have been able to adapt this idea to compressed bitmaps: it may require more than constant time to skip over input, but we can do the work in a small fraction of the time it would take to process otherwise.

Table 4: Time and memory complexity of some threshold algorithms over RLE-compressed bitmap indexes. We assume that one can iterate over the ones in a RLE-compressed bitmap in $\Theta(1)$ time per one. Horizontal or iterator-based implementations are not considered.

Algorithm	Time complexity bound (big-Oh)	Space (big-Oh)	Comment
SCANCOUNT	$r + B$	r	Note ¹
HASHCNT	expected $B + (B/T) \log(B/T)$	B	Note ²
WHEAP	$B \log N$	N	
WMGSK	$B \log N$	N	Note ³
MGOPT	$B'(\log(N - T) + T) + B - B'$	N	Note ³
DSK	$B''(\log(N - L) + L) + B - B''$	N	Note ⁴
LOOPED	NT basic bitmap operations	T bitmaps	
TREEADD	N basic bitmap operations	N bitmaps	Note ⁵
SSUM	N basic bitmap operations	N bitmaps	Note ⁵
CSVCKT	N basic bitmap operations	$\log N$ bitmaps	
SRTCCT	$N \log^2 N$ basic bitmap ops	$N \log^2 N$ bitmaps	Note ⁵
SOPCKT	N^T basic bitmap ops	N^T bitmaps	Note ⁵
RBMRG	RUNCOUNT $\log N$	N	
W2CTN	BN	B	
W2CTA	BN	B	Note ⁶
W2CTI	BN	B	Note ⁶
WSORT	$B \log B$	B	

¹ Access pattern is efficient.

² Access pattern is inefficient.

³ Pruning can reduce B .

⁴ Pruning can reduce B'' and B .

⁵ With register allocation, the space complexity would typically be much lower than the value shown, which merely bounds the number of temporary bitmaps created.

⁶ Pruning reduces N .

2 Background

We next consider relevant background on bitmaps, Boolean functions and two major implementation approaches for bitmap operations.

2.1 Bitmaps

We consider compressed and uncompressed bitmaps. The *density* of a bitmap is the fraction of its bits that are ones. A bitmap with very low density is *sparse*, and such bitmaps arise in many applications.

Uncompressed Bitmaps An uncompressed bitmap represents a sorted set S over $\{0, 1, \dots, r\}$ using $\lceil (r + 1)/W \rceil$ consecutive words. The W bits in the first word

record which values in $[0, W - 1]$ are present in S . The bits in the second word record the values in $[W, 2W - 1]$ that are in S , and so forth. For example, the set $\{1, 2, 7, 9\}$ is represented as 10000110 00000010 with $W = 8$; the number of ones is equal to the cardinality of the set.

Uncompressed bitmaps have the advantages of a fixed size (updates do not change the size) and an efficient membership test. However, if r is large, the bitmap occupies many words—even if it is representing a set with few elements.

The Java library contains a `BITSET` class [16] which implements an uncompressed bitmap data structure. In most respects, it is an uncompressed bitmap, but it does not have a fixed size. The number of words it occupies is $\lceil (\hat{r} + 1) / W \rceil$, where $\hat{r} = \max S$. Note that \hat{r} might be much less than r ; also note that if a new element larger than \hat{r} is inserted into S , the `BITSET` may need to grow. Not storing the trailing empty words is an optimization that would slightly complicate operations over a `BITSET`. But in the case of an AND operation between a `BITSET` representing S_1 (with largest value \hat{r}_1) and one representing S_2 (with largest value \hat{r}_2), bitwise AND instructions would only need to be done over $\lceil (\min(\hat{r}_1, \hat{r}_2) + 1) / W \rceil$ words, rather than $\lceil (r + 1) / W \rceil$. Similar optimizations are possible for OR and XOR. One consequence is that the speed of an operation over `BITSETs` depends on the data involved.

Compressed Bitmaps In many situations where bitmaps are generated, the processes creating the bitmaps generate long runs of consecutive zeros (and sometime long runs of ones). The number of such runs is called the `RUNCOUNT` of a bitmap, or of a collection of bitmaps [22].

Though there are alternatives [29], the most popular compression techniques are based on the (word-aligned) RLE compression model inherited from Oracle (BBC [3]): WAH [40], Concise [7], EWAH [23]), COMPAX [14]. These techniques typically use special marker words to compress fill words: sequences of W bits made of all ones or all zeros. When accessing these formats, it is necessary to read every word to determine whether it indicates a sequence of fill words, or a *dirty* word (W consecutive bits containing a mix of ones and zeros). The EWAH format supports a limited form of skipping because it uses marker words not only to mark the length of the sequences of fill words, but also to indicate the length of the sequences of dirty words. Because of this feature, it is possible to skip runs of dirty words when using EWAH.

Compressed bitmaps are often appropriate for storing sets that cannot be efficiently handled by uncompressed bitmaps. For instance, consider the bitmap consisting of a million zeros followed by a million ones. This data has two runs (`RUNCOUNT=2`) but a million ones. It can be stored in only a few words.

RLE compressed bitmaps are not an efficient way to store extremely sparse data that does not have dense clusters. Sparse data with very long runs of zeros between elements will result in a marker word and a dirty word for each one bit. This would be even less efficient than explicitly listing the set elements.

Software libraries for compressed bitmaps will typically include an assortment of basic Boolean operations that operate directly on the compressed bitmaps. One would expect to find operations for AND, OR, and often one finds XOR, AND-NOT, and NOT. Some libraries support only binary operations, whereas others support *wide* queries (for instance, a “wide” AND would allow us to intersect four bitmaps in a single operation, rather than having to AND bitmaps together pairwise). Even if intersection is eventually implemented by pairwise operations, the wide query allows the library to decide how to schedule the pair-at-a-time operations, and this may lead to a performance gain [41].

2.2 Boolean Functions and Circuits

For relevant background on Boolean functions, see Knuth’s book [21]. Boolean functions can be computed by Boolean circuits that compose some basic set of operators, such as NOT and binary AND and OR.

Some Boolean functions are *symmetric*. These functions are unchanged under any permutation of their inputs. I.e., a symmetric function is completely determined if one knows the number of ones (the Hamming weight) in its inputs. An example symmetric function outputs 0 iff the Hamming weight of its inputs is a multiple of 2: this is the XOR function. Another example is the function that indicates whether the Hamming weight of its inputs is less than 5. The “delta” function indicates whether the Hamming weight of its inputs is some specified value, and another symmetric function indicates whether between 5 and 8 of its inputs are ones.

Some Boolean functions are monotone; changing an input of such a function from 0 to 1 can never cause the output to go from 1 to 0. It is well known that the set of monotone Boolean functions equals the set of Boolean functions that can be implemented using only AND and OR operators.

2.3 Threshold Functions

Threshold functions are those Boolean functions that are both symmetric and monotone. Such a function indicates whether the Hamming weight of its inputs exceeds some threshold T . Function $\vartheta(T, \{b_1, \dots, b_N\})$ denotes the function that outputs 1 exactly when at least T of its N inputs are 1. Several well-known functions are threshold functions: Note that $\vartheta(1, \{b_1, \dots, b_N\})$ is merely a wide OR,

$\vartheta(N, \{b_1, \dots, b_N\})$ is merely a wide AND, and $\vartheta(\lceil N/2 \rceil, \{b_1, \dots, b_N\})$ is the majority function. Efficient compressed bitmap algorithms for wide AND, OR and XOR have been studied before [41].

Knuth [21, 7.1.1&7.1.2] discusses threshold functions and symmetric functions, as well as techniques by which general symmetric functions can be synthesized from threshold functions.

There are a number of identities involving threshold functions that might be useful to a query optimizer, if thresholds were incorporated into database engines. For instance, we have that

$$\overline{\vartheta(T, \{b_1, \dots, b_N\})} = \vartheta(N - T, \{\bar{b}_1, \dots, \bar{b}_N\}).$$

If the efficiency of a threshold algorithm depends on the density of its inputs, this identity can be helpful, because it can convert very dense bitmaps into sparse bitmaps, or vice-versa.

In general, threshold functions may permit weights on the various inputs. However, if the weights are positive integers, we can simply replicate input b_i so that it occurs w_i times. In this way we give the input an effective weight of w_i . This approach may be practical if weights are small. Otherwise, the resulting threshold query may be impractically wide.

Unweighted threshold functions (in the guise of T -overlap queries) have been used for approximate searching. Specifically, Sarawagi and Kirpal [35] show how to avoid unnecessary and expensive pairwise distance computations (such as edit-distance computations) by using threshold functions to screen out items that cannot be approximate matches. Their observation was that strings s_1 and s_2 must have many (T) q -grams in common, if they have a chance of being approximate matches to one another. Given s_1 and seeking suitable s_2 values, we take the set of q -grams of s_1 . Each q -gram is associated with a set of the words (more specifically, with their record ids) that contain that q -gram at least once. Taking these N sets, we do a threshold function to determine values s_2 that can be compared more carefully against s_1 . Using q -grams, Sarawagi and Kirpal showed that $T = |s_1| + q - 1 - kq$ will not discard any string that might be within edit distance k of s_1 . In applications where k and q are small but the strings are long, this will create queries where $T \approx N$.

2.4 Horizontal and Vertical Implementations

Implementations of bitmap operations can be described as “horizontal” or “vertical”. The former implementation produces its output incrementally, and can be stopped early. The latter implementation produces the entire completed bitmap. Horizontal approaches would be preferred if the output of the algorithm is to be

consumed immediately, as we may be able to avoid storing the entire bitmap. As well, the producer and consumer can run in parallel. Vertical implementations may be simpler and have less overhead. If the output of the algorithm needs to be stored because it is consumed more than once, there may be no substantial space advantage to a horizontal implementation.

With uncompressed bitmaps, a particularly horizontal implementation exists: a word of each input is read, after which one word of the output is produced.

3 An index is better than no index

Algorithm 1 Row-scanning approach over a row store.

Require: A table with D attributes. A set κ of $N \leq D$ attributes, and for each such attribute a desired value. Some threshold T .

- 1: s a set, initially empty
 - 2: **for** each row in the table **do**
 - 3: **for** each attribute k in κ **do**
 - 4: **if** attribute k of the row has the desired value **then**
 - 5: increment counter c
 - 6: **if** $c \geq T$ **then**
 - 7: add the row (via a reference to it) to s
 - 8: return the set of matching rows s
-

Perhaps a simple T-occurrence query can be more effectively answered without using a bitmap index. In that case, our work would be of less value⁷. Algorithm 1 shows such an approach, and Table 5 shows that it is outperformed on both compressed and uncompressed bitmaps by one of the algorithms studied (SCANCOUNT, which is often outperformed by other bitmap algorithms).

If $D \gg N$ and the N attributes involved in the computation are scattered throughout the record, the row-scanning approach will not make good use of the memory system—few of the N important attributes will be in any given cache line.

Moreover, interesting datasets often do not fit in main memory. Horizontal partitioning could be used, loading a group of rows, operating on them, then loading the next group of rows. This will still suffer from the inefficiencies inherent in row stores.

It is reassuring to see that a bitmap index can answer our queries faster than they would be computed from the base table. We made 30 trials, using the first

⁷ Good algorithms over bitmaps would still be essential, in the event that the T-occurrence operation is required over a set of computed bitmaps, for which no corresponding table exists.

Table 5: Time (ms) required for queries. Top: Random attributes. Bottom: similarity query.

Algorithm	CENSUSINCOME	KINGJAMES10D
EWAH SCANCOUNT	5214	1017
BITSET SCANCOUNT	5168	805
Row Scan (no index)	21,275	5114
EWAH SCANCOUNT	15,913	3590
BITSET SCANCOUNT	16,999	3574
Row Scan (no index)	23,129	5063

10^4 rows of a dataset (CensusIncome, described in § 5.2) with 42 attributes. We randomly chose one value per attribute and randomly chose a threshold between 2 and 41.

In Table 5 we see that using either a BITSET or EWAH index for this query is four times better than scanning the table. The advantage persists, but is smaller, when a similarity query is done. The results are consistent if we use the first 10^4 rows of a 10-attribute dataset⁸ (KINGJAMES10D [39]).

4 Approaches for Threshold Functions

This report focuses on threshold functions but notes approaches that generalize easily to handle all symmetric functions. It also notes approaches that can be modified to support delta queries or interval queries.

4.1 RBMRG

Algorithm RBMRG is a refinement of an algorithm presented in Lemire et al. [23], and it works for bitmaps that have been run-length encoded. See Algorithm 2. The approach considers runs similarly to integer intervals. For each point, the set of intervals containing it is the same as the set of intervals containing its neighbour, unless the point or its neighbour begins a run. Each bitmap provides a sorted sequence of intervals. Heap H enables us to quickly find, in sorted order, those points where intervals begin (and the bitmaps involved). At such points, we calculate the function on its revised inputs; in the case of symmetric functions such as threshold,

⁸ The other real datasets used for experiments in § 5 had hundreds to many thousands of binary attributes; it would have been unreasonable to test a row store with them. KINGJAMES10D was selected because we had used it in prior work and it was derived from text data, as were the unsuitable datasets used in our experiments.

this can be done very quickly. As we sweep through the data, we update the current count. Whenever a new interval of ones begins, the count increases; whenever a new interval of zeros begins, the count decreases. For regions where no interval changes, the function will continue to have the same value. Assuming $\log L \leq W$, the new value of a threshold function can be determined in $\Theta(1)$ time whenever an interval changes. (The approach can be used with Boolean functions in general, but evaluating a Boolean function over N inputs may be required even when only one input has changed, taking more than constant time.)

Every run passes through a N -element heap, giving a running time that is in $O(\text{RUNCOUNT} \log N)$. One can implement the N required iterators in $O(1)$ space each, leaving a memory bound of $O(N)$.

The algorithm would be a reasonable addition to compressed bitmap index libraries that are RLE-based. We have added it to JavaEWAH library [24] as of version 0.8.

As an extreme example where this approach would excel, consider a case where each bitmap is either entirely ones or entirely zeros. Then $\text{RUNCOUNT} = N$, and in $O(N \log N)$ time we can compute the output, regardless of r or B .

Algorithm 2 Algorithm RBMRG.

INPUT: N bitmaps B_1, \dots, B_N

$I_i \leftarrow$ iterator over the runs of identical bits of B_i

$\Gamma \leftarrow$ a new buffer to store the aggregate of B_1, \dots, B_N (initially empty)

$\gamma \leftarrow$ the bit value determined by $\gamma(I_i, \dots, I_N)$

$H \leftarrow$ a new N -element min-heap storing ending values of the runs and an indicator of which bitmap

$a' \leftarrow 0$

while some iterator has not reached the end **do**

 let a be the minimum of all ending values for the runs of I_1, \dots, I_N , determined from H

 append run $[a', a]$ to Γ with value γ

$a' \leftarrow a + 1$

for iterator I_i with a run ending at a (selected from H) **do**

 increment I_i while updating γ

 let b be the new run-ending value for I_i

if b exists **then**

 increase the key of the top item in H from a to b

The EWAH implementation of RBMRG processes runs of clean words as described. If the interval from a' to a corresponds to N_{clean} bitmaps with clean runs, of which k are clean runs of ones, the implementation distinguishes three cases:

1. $T - k \leq 0$: the output is 1, and there is no need to examine the $N - N_{\text{clean}}$ bitmaps that contain dirty words. This pruning will help cases when T is small.
2. $T - k > N - N_{\text{clean}}$: the output is 0, and there is no need to examine the dirty words. This pruning will help cases when T is large.
3. $1 \leq T - k \leq N - N_{\text{clean}}$: the output will depend on the dirty words. We can do a $(T - k)$ -threshold over the $N - N_{\text{clean}}$ bitmaps containing dirty words.

We process the $N - N_{\text{clean}}$ dirty words as follows. If $T - k = 1$ (resp. $T - k = N - N_{\text{clean}}$), we compute the bitwise OR (resp. AND) between the dirty words. Otherwise, if $T - k \geq 128$, we always use SCANCOUNT using 64 counters (see § 4.2). Otherwise, we compute the number of ones (noted β) in the dirty words. This can be done efficiently in Java since the `Long.bitCount` function on desktop processors is typically compiled to fast machine code. If $2\beta \geq (N - N_{\text{clean}})(T - k)$, we use the LOOPED algorithm (§ 4.5), otherwise we use SCANCOUNT again. We arrived at this particular approach by trial and error: we find that it gives reasonable performance.

4.2 Counter-Based Approaches

In information retrieval, it is common practice to solve threshold queries using sets of counters [30]. The simple SCANCOUNT algorithm of Li et al. [25] uses an array of counters, one counter per item. The input is scanned, one bitmap at a time. If an item is seen in the current bitmap, its counter is incremented. A final pass over the counters can determine which items have been seen at least T times. In our case, items correspond to positions in the bitmap. If the maximum bit position is known in advance, if this position is not too large, and if you can efficiently iterate the bit positions in a bitmap, then SCANCOUNT is easily coded. These conditions are frequently met when the bitmaps represent the sets of rids in a table that is not exceptionally large.

SCANCOUNT and other counter-based approaches can handle arbitrary symmetric functions, since one can provide a user-defined function mapping $[0, N]$ to Booleans. However, optimizations are possible when more sophisticated counter-based approaches compute threshold functions.

To analyze SCANCOUNT, note that it requires $\Theta(r)$ counters. We assume $N < 2^W$, so each counter occupies a single machine word. Even if counter initialization can be avoided, each counter is compared against T . (An alternative is to compare only after each increment [25], but since the counters achieve T in an

unpredictable order, a sorting phase is required before the compressed bitmap index is constructed. In many cases, this extra overhead would be excessive.) Also, the total number of counter increments is B . Together, these imply a time complexity of $\Theta(r + B)$ and a space complexity of $\Theta(r)$, for compressed bitmaps. For uncompressed bitmaps, we potentially have to wade through regions that store only zeros and do not contribute toward B . This adds an extra Nr/W term to the time⁹. Aside from the effect of N on B (on average, a linear effect), note that this algorithm does not depend on N .

The SCANCOUNT approach fits modern hardware well: note that the counters will be accessed in sequence, during the N passes over them when they are incremented. Given that 16 `int` counters fit into a typical 64-byte cache line, the performance improvement from fewer increments is likely to be small until average selectivity of $a_j = v_j$ drops to values near $1/16$. (Far below that value and we may find two successively accessed counters are in different cache lines. Well above it, and two successively accessed counters are likely to be in the same cache line, and we will not get a cache miss on both.)

Experimentally, we found that using `byte` counters when $N < 128$ usually brought a small (perhaps 15%) speed gain compared with `int` counters. Perhaps more importantly, this also quarters the memory consumption of the algorithm. One can also experiment with other memory-reduction techniques: for instance, if $T < 128$, one could use a saturating 8-bit counter. Experimentally, we found that the gains usually were less than the losses to make the additional conditional check (needed to avoid incrementing the counter once it had achieved either T or the maximum byte values). (In the special case where $T = 1$, that is, when we want to compute the union, the SCANCOUNT array could use *single-bit* counters. These counters would effectively be an uncompressed bitmap. Indeed, the JavaEWAH library [24] uses this observation in its OR implementation.)

Based on our experimental results, the SCANCOUNT Java implementation used in § 5 switches between `byte`, `short` and `int` counters based on N , but does not use the saturating-count approach.

SCANCOUNT fails when the bitmaps have extreme r values. If we restrict ourselves to bitmaps that arise within a bitmap index, this implies that we have indexed a table with an extreme number of rows. However, hashing can be employed to use an approach like SCANCOUNT on data where r is especially large. Algorithm HASHCNT uses a map from integers (items) to integers (their counts). We only

⁹This is easily done if one assumes an $O(1)$ instruction to compute the number of leading zeros in a W -bit word. For instance, the x86 has a `lzcnt` instruction and the ARM has `clz`. Otherwise, there are approaches that use $O(\log W)$ operations [38, 5.3], and it appears the OpenJDK implementation of `Integer.numberOfLeadingZeros()` uses such an approach. Without the assumption of an $O(1)$ instruction, the term Nr/W would become $\frac{Nr \log W}{W}$.

need counters for as many distinct items as actually exist in our data (which could be at most B). In Java, we can use `HashMap` from the `java.util` package. Unfortunately, the constant-factor overheads in hashing are significantly higher than merely indexing an array. Also, `SCANCOUNT` indexes the array of counters in N ascending passes, which should lead to good cache performance. Hashing will scatter accesses to boxed Integer objects that could be anywhere in memory. Somewhat higher-performance int-to-int hash maps are found in libraries such as GNU Trove [10]. However, hashing would still lead to random-looking accesses through a large array, and poor cache performance should be anticipated. Note also that, with compression, the output bitmap must be constructed in sorted order. Since there can be at most B/T ones in the output bitmap, we have an $O(\frac{B}{T} \log \frac{B}{T})$ cost for construction.

4.2.1 Sorting to Count

Algorithm `WSORT` counts by converting each bitmap into a (presorted) list of positions, concatenating such lists, sorting the result, and then scanning to see which items are repeated at least T times in the large sorted list. If we process uncompressed bitmaps horizontally, this naïve approach may work well enough, especially given that sorting libraries are typically very efficient. In the worst case, in one horizontal step our bitmap fragments have WN ones, requiring that we use $O(WN \log(WN))$ time to sort, and requiring $O(WN)$ space. Over the entire horizontal computation, we use $O(B \log(WN))$ time. (We have that $B = WN$ in the our worst-case scenario. But in others, WN is an upper bound on the number of ones in a horizontal step, and B is the total number of ones in all horizontal steps.) However, if we are not using horizontal computation, we unpack B data items and sort them in $\Theta(B \log B)$ time.

4.2.2 Mergeable-Count structures

A common approach to computing intersections and unions of several sets is to do it two sets at a time. To generalize the idea to symmetric queries, we represent each set as an array of values coupled with an array of counters. For example, the set $\{1, 14, 24\}$ becomes $\{1, 14, 24\}, \{1, 1, 1\}$ where the second array indicates the frequency of each element (respectively). If we are given a second set $(\{14, 24, 25, 32\})$, we supplement it with its own array of counters $\{1, 1, 1, 1\}$ and can then merge the two: the result is the union of two sets along with an array of counters $(\{1, 14, 24, 25, 32\}, \{1, 2, 2, 1, 1\})$. From this final answer, we can deduce both the intersection and the union, as well as other symmetric operations.

Algorithm `w2CTN` takes this approach. Given N inputs, it orders them by

increasing length and then merges each input, starting with the shortest, into an accumulating total. A worst-case input would have all inputs of equal length, each containing B/N items that are disjoint from any other input. At the i^{th} step the accumulating array of counters will have Bi/N entries and this will dominate the merge cost for the step. The total time complexity for this worst-case input is $\Theta(\sum_{i=1}^{N-1} Bi/N) = \Theta(BN)$. The same input ends up growing an accumulating array of counters of size B . If this algorithm is implemented “horizontally” on uncompressed bitmaps, the maximum temporary space would be bounded by the maximum number of ones that can appear in N words of size W .

Algorithms w2CTA and w2CTI are refinements. Although they end up reading their entire inputs, during the merging stages they can discard elements that cannot achieve the required threshold. For instance, w2CTA checks the accumulating counters after each merge step. If there are i inputs left to merge, then any element that has not achieved a count of at least $T - i$ can be pruned. Algorithm w2CTI does such pruning *during* the merge step, rather than including elements and then discarding them during a post-processing step after merging each pair of sets. Because these two algorithms prune data during the processing, it might be advantageous to work from the small sets: this increases the probability that data will be pruned earlier. Hence we order input bitmaps by increasing cardinality and then merge each input, starting with the shortest, into an accumulating total.

In many cases, this pruning is beneficial. However, it does not help much with the worst-case input, if $T = 2$. We cannot discard any item until the final merge is done, because the last input set could push the count (currently 1) of any accumulated item to 2, meeting the threshold.

4.3 T-occurrence algorithms for integer sets

Others [25, 35] have studied the case when the data is presented as sorted lists of integers rather than bitmaps. The initial application was with approximate search, to help discover all terms with a small edit distance to a user-supplied term. It is not clear that these techniques could be applied in a more general setting, to compute symmetric functions other than threshold functions.

Specifically, we consider

1. wHEAP [35],
2. MGOPT [35],
3. wMGSK [25],
4. DSK [25].

For details of these algorithms, see the papers that introduced them. The WHEAP approach essentially uses an N -element min-heap that contains one element per input, unless the input has been exhausted. Using the heap, it merges the sorted input sequences. As items are removed from the heap, we count duplicates and thereby know which elements had at least T duplicates. This approach can be used for arbitrary symmetric functions. It requires that we process the ones in each bitmap, inserting (and then removing) the position of each into an N element min-heap. This determines the space bound. If the bitmap is uncompressed, we have an additional time cost of Nr/W to find the B ones. The total time cost is thus $O(B \log N)$ for compressed bitmaps and $O(Nr/W + B \log N)$ for uncompressed, done vertically. Horizontal processing does not change the time or space use.

The remaining algorithms are also based around heaps, but are designed to exploit characteristics of real data, such as skew. Algorithm MGOPT sets aside the largest $T - 1$ bitmaps. Any item contained only in these bitmaps cannot meet the threshold. Then it uses an approach similar to WHEAP with threshold 1. For each item found, say with count t , it checks whether at least $T - t$ instance of the item are found in the largest $T - 1$ bitmaps. The items checked for are an ascending sequence. If one of the largest bitmaps is asked to check whether item x occurs, and then is later asked whether item y occurs, we know that $y > x$. Items between x and y in the big list will never be needed, and can be skipped over without inspection. When the data is provided as a sorted list of integers, a doubling/bootstrapping binary-search procedure can find the smallest value at least as big as y without needing to scan all values between x and y . We can consider the portions skipped to have been “pruned”.

As noted in § 2.1, providing random access is not a standard part of a RLE-based compressed bitmap library, although it is essentially free for uncompressed bitmaps. However, with certain compressed bitmap indexes it is possible to “fast forward”, skipping portions of the index in a limited way: JavaEWAH uses the fact that we can skip runs of dirty words (e.g., when computing intersections). It should be possible, through auxiliary data structures to skip even more effectively at the expense of memory usage [27, 34]. However, such auxiliary data structures do not always improve performance [9]. The alternative is to convert from bitmap representation to sorted array, apply the classic algorithm, then convert the result back into a bitmap. The overheads of such an approach would be expected to be unattractive.

To bound the running time, we can distinguish the $B - B'$ ones in the $T - 1$ largest bitmaps from the B' ones in the remaining $N - T + 1$ bitmaps. A heap of size $O(N - T)$ is made of the $N - T + 1$ remaining bitmaps, and $O(B')$ items will pass through the heap, at a cost of $O(1 + \log(N - T))$ each. As each item is removed from the heap, it will be sought in $O(T)$ bitmaps. With uncompressed

bitmaps, this costs $O(T)$.

With compressed bitmaps, the situation is more complicated. Because the items sought are in ascending order, the $T - 1$ bitmaps will each be processed in a single ascending scan that handles all the searches. Each of the $B - B'$ ones in the remaining bitmaps should cost us $O(1)$ effort. Thus we obtain a bound of $O(B'(\log(N - T) + T) + B - B')$ for the time complexity of MGOPT on an compressed bitmap. With uncompressed bitmaps, we add a $r(N - T)/W$ term that accounts for looking for the ones in the $N - T + 1$ smallest bitmaps, but we can deduct the $B - B'$ term, as we do not need to wade through all positions in the T lists. We obtain a bound of $O(r(N - T)/W + B'(\log(N - T) + T))$.

This analysis does not take fully into account the effect of pruning, because even the compressed bitmaps might be able to skip many of the $B - B'$ ones as we “fast forward” through the largest $T - 1$ bitmaps. Since these are the *largest* bitmaps, if T is close to N or if the sizes (number of ones) in the bitmaps vary widely, pruning could make a large difference. This depends on the data.

Algorithm WMGSK is a different modification of the heap-based algorithm. When removing copies of an item from the heap, if there are not enough copies to meet the threshold, we remove some extra items. This is done in such a way that the extra items removed (and not subsequently re-inserted) could not possibly meet the threshold. They are pruned. Moreover, inspection of the heap yields a lower-bound on the next possible item that can meet the threshold. Each input can then be advanced to (or beyond) that item. Items skipped are pruned, and will avoid the overheads of being inspected and (especially) inserted into the heap. As with MGOPT the effectiveness of such pruning depends heavily on the characteristics of the data. Our bound for WMGSK does not reflect the improvements that pruning might bring in some cases; we use the same bounds as WHEAP.

Algorithm DSK is essentially a hybrid of WMGSK and MGOPT. It uses both methods of pruning. However, rather than following MGOPT and choosing the $T - 1$ largest sets, it chooses the L largest sets. Parameter L is a tuning parameter, and choosing an appropriate value of L for a given threshold query is problematic. The authors suggest a heuristic approach whereby another tuning parameter μ is determined experimentally, for a given type of queries against a given dataset. From μ and the length of the longest input, an appropriate value of L can often be determined by a heuristic formula. We found this approach unsatisfactory in our experiments, as the best μ for one query against a dataset often differed substantially from the best μ for a similar query. (See § 5.8.2 for some detail on appropriate values for μ on our datasets.) The effectiveness of DSK is definitely affected by μ , though perhaps by less than a factor of five over a reasonable range of values. Choosing appropriate μ and hence L values will be a difficulty for any engineer planning to use DSK, especially if the input datasets are not available for prior

analysis. Nonetheless, DSK might be considered to reflect the state-of-the-art for the T -occurrence problem, at least as it arises in approximate string searches.

The running-time bound for DSK is obtained using reasoning similar to that for MGOPT. If there are $B - B''$ ones in the largest L bitmaps, then each of the remaining B'' ones will pass through the heap and trigger searches in the L largest bitmaps. For uncompressed bitmaps, this will result in $O(B''L)$ work for all the searches. For compressed bitmaps, it will result in $O(B''L + (B - B''))$ work for all the searches. For the right data, less than $B - B''$ items may be scanned during the searches on compressed bitmaps, as with MGOPT. Algorithm DSK also has the pruning opportunities of WMGSK, whereby some of the B'' ones are skipped. Thus, our running-time bound for DSK on uncompressed bitmaps is $O(r(N - L)/W + B''(\log(N - L) + L))$. For compressed bitmaps, we do not have the $r(N - L)/W$ cost to wade through the $N - L$ smallest bitmaps, looking for ones. However, we will potentially face a cost of $O(B - B'')$ while fast-forwarding through the largest L lists. As with MGOPT, data-dependent pruning could reduce the $B - B''$ term. As with WMGSK, the multiplicative B'' factor can be reduced by data-dependent pruning. For compressed bitmaps, we end up with a bound of $O(B''(\log(N - L) + L) + (B - B''))$.

For an analysis of space, note that MGOPT and DSK partition the inputs into two groups. Regardless of group, each compressed bitmap input will have an iterator constructed for it. For uncompressed bitmaps, only the first group (small bitmaps) needs the iterator and auxiliary storage. For either kind of bitmap, the first group go into a heap that accepts one element per input. Thus we end up with a memory bound of $O(N)$, which can be refined to $O(N - T)$ (for MGOPT on uncompressed bitmaps) or $O(N - L)$ (for DSK on uncompressed bitmaps).

4.4 Boolean synthesis

A typical bitmap implementation provides a set of basic operations, typically AND, OR, NOT and XOR, and frequently ANDNOT. Since it is possible to synthesize any Boolean function using AND, OR and NOT gates in combination, any desired bitmap function can be “compiled” into a sequence of primitive operations. One major advantage is that this approach allows us to use a bitmap library as a black box, although it is crucial that the primitive operations have efficient algorithms and implementations.

Unfortunately, it is computationally infeasible to determine the fewest primitive operations except in the simplest cases. However, there are several decades of digital-logic-design techniques that seek to implement circuits using few components. Also, Knuth has used exhaustive techniques to determine the minimal-gate circuits for all symmetric functions of 4 and 5 variables ([21, Figs. 9&10, 7.1.2]).

Table 6: Number of gates in Knuth’s minimum-gate constructions for $N = 4$ and $N = 5$

T	$N = 4$	$N = 5$
1	3	4
2	7	not shown
3	7	9
4	3	10
5	–	4

Table 7: Number of 2-input operations for $N = 4$ and $N = 5$, Knuth’s optimal solution, our sideways-sum adder, our sorter, and the LOOPED approach

T	$N = 4$				$N = 5$			
	Opt	Add	Sort	Loop	Opt	Add	Sort	Loop
1	3	11	3	3	4	14	12	4
2	7	9	7	9	not shown	12	12	12
3	7	11	7	13	9	14	12	18
4	–	–	–	–	10	11	12	22

(Following Knuth, we assume an ANDNOT operation.) But Intel SSE or AVX supports AND NOT, as do several bitmap libraries (EWAH included). Specifically, Intel has the `pandn` and `vpandn` instructions; however it does not look like the standard x86 instruction set has AND NOT. Results are given in Table 6 and are often significantly smaller than those we will obtain from our more general constructions.

We need to be concerned with both running time and memory consumption. Based on Knuth’s exhaustive analysis, all 4-input symmetric ($N = 4$) functions can be evaluated in the minimum amount of memory possible for each, without increasing the number of operations[21, 7.1.2]. Knuth does not give an algorithm for minimum-memory evaluation, which is probably due to its close relationship to the known NP-hard Register Sufficiency problem [15, A11.1.P01] [36]. (We have a restricted version of Register Sufficiency—we only need to compute one output, rather than an output for each root of the expression dag. However, one could take a multi-rooted expression dag, introduce a new node x and make each (former) root become a child of x . The resulting dag has a single root, and the registers required for evaluation would not have changed from the original dag.)

See Table 7 and 8 for information on a number of threshold circuits discussed later in this section. The sideways-sum adder needed 5 gates for ($N = 3, T = 2$) and the tree adder needed only 4. However, for all larger values of N and T , the

Table 8: Gates (i.e., operations) for adders and sorter for some larger N and T . Note how the sorter circuit behaves with T .

N	T	Adders		Sorter
		Tree	S. Sum	
43	30	272	192	480
85	12	562	398	1216
120	105	806	580	1907
323	14	2226	1586	7518
329	138	2272	1620	9052
330	324	2275	1623	7549
786	481	5467	3905	28945
786	776	5461	3899	24233

sideways-sum adder used fewer gates. For $N > 25$, it used about 40% fewer gates. (Perhaps surprisingly, on BITSETS the dataset determined which of the two adders was fastest, as discussed in § 5.7.) The asymptotically larger sorting-based circuits indeed are larger even for modest N , although they are optimal for the $N = 4$ cases.

Consider uncompressed bitmaps using a word size W , and assume that all logic operations take unit time. Then a logic circuit with C gates can obtain a batch of W threshold results with C operations. For instance, on a 64-bit architecture, our sorting circuit for 511 inputs uses about 15 k gates. Thus in 15,000 bitwise operations we can compute 64 threshold results, or 234 operations per result. Wording individually, it would take more binary operations than this to reduce 511 inputs to a single output. With a larger W , such as provided by SSE and AVX extensions, the advantage of this approach increases. However, this analysis ignores the fact that, given a limited number of registers, the CPU must spend some time loading bit vectors from main memory and storing intermediate results there. Note, however, that this approach is essentially horizontal, in that no more than W bits from each input, or each intermediate result, needs to be stored at a time.

With RLE compressed bitmaps, the primitive operations do not all have the same computational cost. For instance, consider a bitmap B_1 that consists of a single long run of zeros and a bitmap B_2 that contains a single long run of ones, and a bitmap B_3 that contains alternating zeros and ones. The operations $\text{AND}(B_1, B_3)$ and $\text{OR}(B_2, B_3)$ are fast operations that do not require any copying or bitwise machine operations. However, $\text{OR}(B_1, B_3)$ and $\text{AND}(B_2, B_3)$ will be expensive operations—if B_3 is mutable, then a copy must be made of it. We see that it is simplistic to assume a cost model based on the uncompressed lengths of the bitmaps,

or one that merely counts the number of bitmap operations.

Sum-of-Products circuits We implemented classic un-minimized Sum-of-Products circuits to allow computation of arbitrary N -input Boolean functions over bitmaps. This became our SOPCKT algorithm. If the function is known to be monotone, negative literals can be omitted from the Sum-of-Products circuit. Note that threshold functions are monotone; this realization of them consists of $\binom{N}{T}$ different T -input AND gates, whose results are the input to a single $\binom{N}{T}$ -input OR gate. These approaches can result in huge circuits, and this is unavoidable: since none of the AND terms is contained within another of the AND terms, a corollary noted by Knuth [21, Corollary Q, § 7.1.1] of a result of Quine [32] implies that no other Sum-of-Products circuit for the function can be smaller.

If we replace each high-input gate by two input gates, we require $\binom{N}{T}(T - 1)$ AND gates and $\binom{N}{T} - 1$ OR gates, for a total of $\binom{N}{T}T - 1$ gates. Comparing with Knuth’s results in Table 6, the result is optimal for $N = 4$ or $N = 5$ if $T = 1$, and reasonable when $N = 4$, $T = 2$ (11 gates versus 7). If $T = N - 1$ it requires $\Theta(T^2)$ gates. Experimentally, it often performs reasonably well in these conditions, but otherwise the $\binom{N}{T}$ factor makes the result impractical.

We also implemented techniques specialized for symmetric functions, obtaining a sorting-based algorithm, SRTCKT. We also obtain two adder-based algorithms, TREEADD and SSUM.

4.4.1 Sorting

A sorting circuit [20, 5.3.4] for Booleans maps a N -bit Boolean input to a N -bit Boolean output, where the output is $1^k 0^{N-k}$ if the input had Hamming weight k . Boolean sorting circuits are usually depicted as comparator-based sorting networks, but each comparator is simply a 2-input AND operation and a 2-input OR operation [21, 7.1.1]. It is then simple to compute whether threshold T has been achieved: simply use the T^{th} output bit from the sorting circuit. In general, for symmetric functions one could determine whether the input had **exactly** Hamming weight T by ANDing the T^{th} output with the negation of the $T + 1^{st}$ output. (This is the delta function.) One could then OR together the appropriate collection of these ANDNOT gates to synthesize any desired symmetric function. Interval functions (to recognize whether the Hamming weight of the inputs is within an interval) are also achieved by the ANDNOT approach.

There is no known general procedure to obtain a minimum-comparator sorting circuit [20, 5.3.4]. Asymptotically, the AKS construction [1] yields circuits with $O(N \log N)$ comparators, but the hidden constants make this approach impractical.

For modest size inputs, the construction used in Batcher’s Even-Odd sort is well known to use few comparators (see [20, 5.3.4.(11)]) even though asymptotically it will generate circuits of size $\Theta(N \log^2 N)$. We used Batcher’s sort for our `SRTCKT` algorithm. It requires only that the bitmap library provide 2-input AND and OR primitives. Intermediate results are frequently reused many times.

4.4.2 Adding

Another approach is to compute the Hamming weight of the input by summing all the input bits. We present two such approaches, and the first uses a tree of adders. (See Fig. 1.) The leaves of the tree consist of 1-bit adders (half adders, requiring an AND and an XOR operation) producing a 2-bit sum. Then these 2-bit sums are added to obtain 3-bit sums. Multi-bit adders use the ripple-carry technique, where summing two x -bit numbers uses $2x - 1$ AND operations, $2x - 1$ XOR operations and $x - 1$ OR operations. The final outcome is a $\log N + 1$ -bit binary number representing the Hamming weight of the N inputs. (When N is not a power of 2, we pad with zero inputs and then using a constant-propagation pass to simplify the resulting circuit.)

This $\log N + 1$ -bit quantity is then compared to T using a \geq circuit. Since it operates over $O(\log N)$ inputs and N inputs involved in the Hamming weight computation, it is not crucial to have the most efficient method of computing \geq . However, if T is a power of 2, it is easy to compute the threshold function from the Hamming weight using an OR function: for instance, to see if the 4-bit number $b_3b_2b_1b_0$ is at least 2, compute $b_1|b_2|b_3$.

This approach can be generalized if T is not a power of two; a *magnitude comparator* circuit [4] can determine whether the bit-string for the Hamming weight lexicographically exceeds the bit-string for $T - 1$. As various designs for such circuits exist, we proceed to derive and analyze our circuit to compare a quantity to a constant.

Consider two bit strings $b_{n-1}b_{n-2} \cdots b_0$ and $a_{n-1}a_{n-2} \cdots a_0$, where we have $n = \lfloor \log 2N \rfloor$. The first is greater if there is some $0 \leq j < n$ where $b_j > a_j$ and the two bit strings have $b_k = a_k$ for all $k > j$. If we define $\text{prefix_match}(j) = \bigwedge_{k=j+1}^{n-1} (b_k \equiv a_k)$ then $b_{n-1}b_{n-2} \cdots b_0 > a_{n-1}a_{n-2} \cdots a_0$ can be computed as $\bigvee_{j=0}^{n-1} \text{prefix_match}(j) \wedge b_j \wedge \neg a_j$. The prefix values can be computed with n XOR and n ANDNOT operations with

$$\begin{aligned} \text{prefix_match}(n) &= 1, \\ \text{prefix_match}(k) &= \text{prefix_match}(k+1) \wedge \neg(b_k \oplus a_k). \end{aligned}$$

Altogether $5n - 1$ bitwise operations (AND, ANDNOT, XOR, OR) are used to determine the truth value of the inequality $b_{n-1}b_{n-2} \cdots b_0 > a_{n-1}a_{n-2} \cdots a_0$.

We can do better because $T - 1$ (whose binary representation is the second bit string, $a_{n-1} \cdots a_0$) is a constant.

- First, OR terms drop out for positions j where $a_j = 1$, leaving us with $\bigvee_{j|a_j=0} \text{prefix_match}(j) \wedge b_j$.
- Second, the previous expression does not need `prefix_match` for the trailing ones in $T - 1$; they no longer appear in our expression and there is no 0 to their right. (The `prefix_match` value required for a 0 is indirectly calculated from `prefix_match` values for all positions to the left of the 0.)
- Third, we can redefine `prefix_match(j)` as $\bigwedge_{\substack{j < k < n \\ \wedge a_k = 1}} b_k$. Thus, if $T - 1 = 101100_2$, `prefix_match(2)` no longer checks that the other bit string starts with 101. Instead, it matches 101 or 111. In the latter case, the bit string is already known to exceed $T - 1$.

For an example, consider $T - 1 = 0010100111_2$ with $n = 10$. We compute $b_9 \vee b_8 \vee (\text{prefix_match}(6) \wedge b_6) \vee (\text{prefix_match}(4) \wedge b_4) \vee (\text{prefix_match}(3) \wedge b_3)$, where `prefix_match(6)` = b_7 , `prefix_match(4)` = $b_5 \wedge b_7 = b_5 \wedge \text{prefix_match}(6)$ and `prefix_match(3)` = $b_5 \wedge b_7 = \text{prefix_match}(4)$. Thus, we get the formula $b_9 \vee b_8 \vee (b_6 \wedge b_7) \vee (b_4 \wedge b_5 \wedge b_7) \vee (b_3 \wedge b_5 \wedge b_7)$. Since $b_5 \wedge b_7$ is a shared sub-expression, we need only 8 operations in this case, which less than $n = 10$.

With these optimizations, computing all required `prefix_match` values needs one AND for every 1 bit except for the trailing ones and the first one: for each of these 1 bits no gate is required. We also need a single wide OR that takes an input for each of the zeros (there must be a 0 and a 1 in the binary representation of $T - 1$) in $T - 1$. That OR input is computed as a 2-input AND; as a minor optimization, the leading zeros in $T - 1$ can omit the AND, because they would use a `prefix_match` value that would be 1. To count operations, let $\nu(T - 1)$ denote the Hamming weight when $T - 1$ is written in binary, let $\text{nto}(T - 1)$ denote the number of trailing ones, and $\text{nlz}(T - 1)$ denote the number of leading zeros. Therefore, the number of zeros in $T - 1$ is $n - \nu(T - 1)$. Thus, computing the `prefix_match` values needs $\max(0, \nu(T - 1) - \text{nto}(T - 1) - 1)$ ANDs. We need to “OR” $n - \nu(T - 1)$ items, requiring $n - \nu(T - 1) - 1$ two-input OR gates. The items are computed by $n - \nu(T - 1) - \text{nlz}(T - 1)$ AND gates. In total we use at most $2n - \nu(T - 1) - \text{nlz}(T - 1) - \text{nto}(T - 1) - 1$ operations; i.e., between 0 (when $T - 1 = 011 \cdots 1$) and $2n - 3$ (when $T - 1 = 100 \cdots 0$). The similar comparator circuit presented by Ashenden [4] can also be simplified when a values are constant. The worst case value of T gives a circuit whose size is similar to ours, but the best case is not as good.

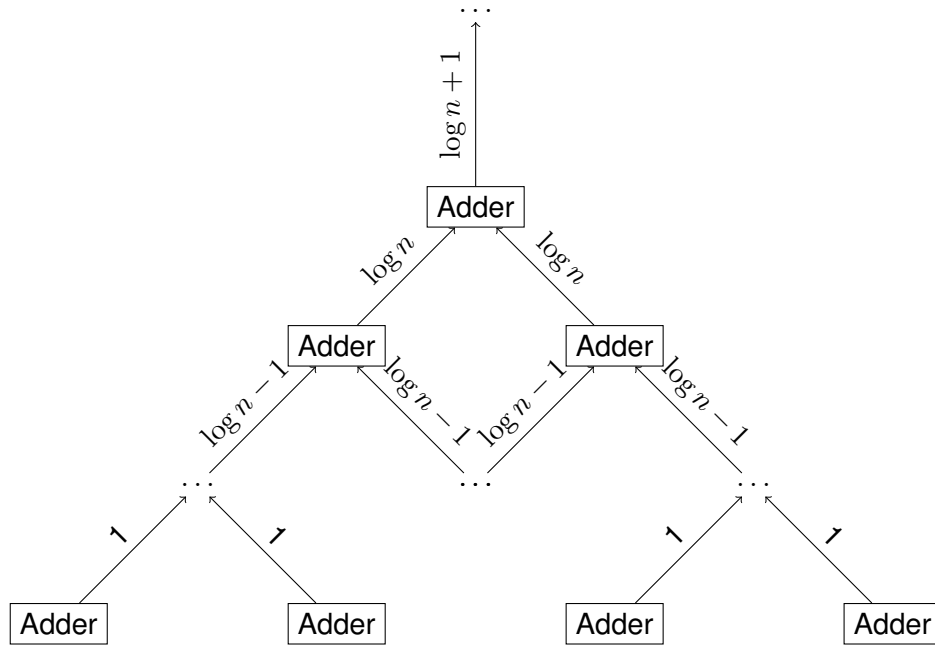


Figure 1: A tree of adders to compute the Hamming weight of an input, where the input length is a power of two.

There is an alternative way to compare two $\log N$ -bit quantities, T and the Hamming weight, with approximately $7 \log N$ gates: use an adder to sum $-T$ and the Hamming weight; then inspect the sign of the result. Considering the algorithms introduced later in this section, we used this approach in the implementation of CSVCKT, but otherwise our TREEADD and SSUM algorithms used the previous approach.

For general symmetric functions, one could use a sum-of-products circuit over the $1 + \lceil \log N \rceil$ -bit number that gives the Hamming weight of the inputs. Knuth [21, 7.1.2] observes that since he has calculated the minimum number of gates (7) to realize any 4-input Boolean function, we immediately can realize any symmetric Boolean function of $N \leq 15$ inputs using $7 + c(N)$ gates, where $c(N)$ is the number of gates used by our adder tree.

To determine $c(N)$ when $N = 2^k$ is a power of two, note that we use 2^{k-1} half-adders in the first level of the adder tree. The 2^{k-2} resultant 2-bit numbers are added in the second levels, using a half-adder and a full adder for each 2-bit sum. In the third level, we require 2^{k-3} 3-bit adders, each containing two full adders and a half adder. In general, the i^{th} level contains 2^{k-i} adders that each require

$i - 1$ full adders and a half adder. The final level is level $k = \log N$. Since a half-adder requires two gates and a full adder requires five, we obtain a total gate count of

$$c(2^k) = \sum_{i=1}^k 2^{k-i} (5(i-1) + 2) = 7N - 5 \log N - 7.$$

For the first few powers of 2 this yields

$$\begin{array}{rcccccc} N = & 2 & 4 & 8 & 16 & 32 \\ c(N) = & 2 & 11 & 34 & 85 & 192 \end{array} \cdot$$

4.4.3 Sideways Sum

Knuth describes an alternative “sideways sum” circuit to compute the Hamming weight of a vector of bits [21, 7.1.2]. This circuit consists of $O(\log N)$ levels. The first level takes a collection C_1 of bits of weight 1, and as output produces a single weight-1 bit, z_0 , and a collection C_2 of bits of weight 2. The Hamming weights are preserved: i.e., $z_0 + 2 \text{ hamming}(C_2) = \text{hamming}(C_1)$. The second level takes C_2 and produces a single weight-2 bit, z_1 , and a collection C_3 of bits of weight 3. Again, Hamming weights are preserved: $2z_1 + 4 \text{ hamming}(C_3) = 2 \text{ hamming}(C_2)$. Note that bits z_1 and z_0 are the least significant bits of $\text{hamming}(C_1)$. Subsequent levels are similar, and the Hamming weight of the N input bits is specified by the z bits. Fig. 2 shows how input bits of weight 2^x are used to compute the single weight- 2^x bit z_x and the output bits of weight 2^{x+1} .

Compared to the tree of adders, the sideways-sum arrangement of full- and half-adders results in somewhat fewer gates (bounded by $5N$ rather than $7N$). For N a power of 2, it has $s(N)$ gates, where

$$\begin{array}{rcccccc} N = & 2 & 4 & 8 & 16 & 32 \\ s(N) = & 2 & 9 & 26 & 63 & 140 \end{array} \cdot$$

If all bitwise operations take the same amount of time, this circuit should always outperform the tree of adders. However, when computing over compressed bitmaps, we did find cases where certain inputs favoured the larger circuit (§ 5).

4.4.4 Compiling or interpreting circuits

Implementation using the circuit-based approach can be done in several ways. Regardless, at some point an appropriate circuit needs to be constructed. We used a directed, acyclic graph whose nodes are labelled by the associated Boolean operator. The N inputs to this circuit are associated with the N bitmaps.

A straightforward vertical implementation then simulates the circuit, processing the circuit’s nodes in topological order, propagating values from inputs towards

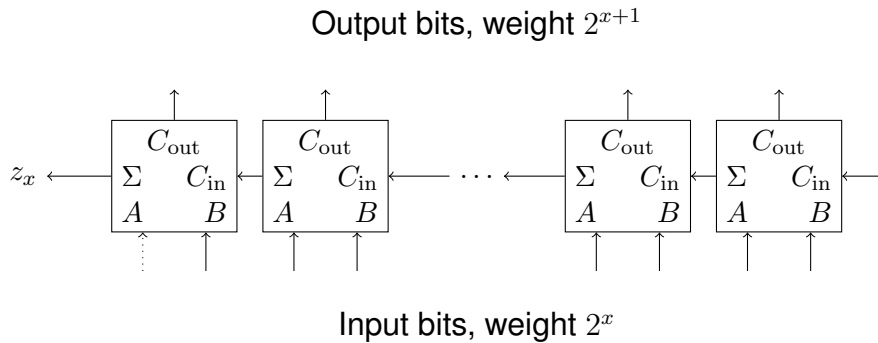


Figure 2: One layer in the sideways sum circuit, similar to that discussed by Knuth. Note that this is not a “ripple carry” arrangement: the **sum** bit from a full adder becomes the carry-in input of the next full (or half) adder. Whether the leftmost adder is a full or a half adder depends on whether the number of input bits is even.

the output. When a node is processed, its inputs will be associated with bitmaps. We apply the node’s operation to these bitmaps, and then associate the resultant bitmap to the node’s output. Since the output of a node can become the input of several nodes, some book-keeping would be necessary to know when the storage occupied by an intermediate bitmap can be reclaimed.

An alternative approach generates straight-line code from the circuit (again, processing the nodes in topological order). See Appendix B for sample C++ code. With this approach, we can do a compiler-type analysis to determine the point when an intermediate value is last used. The straight-line code could then include operations to reclaim storage occupied by no-longer-useful intermediate results. Having obtained such code, it can be compiled and executed. An initial implementation that machine-generated Java code ran into a limitation of the Java Virtual Machine: there is a fixed, and relatively small, maximum size for the JVM byte code of any method.

Our third approach generates our own byte-code (operations for AND, OR, XOR, reclaim, and so forth). A trivial byte-code interpreter then processes this straight-line byte code. This is the implementation adopted for the experiments.

One might also consider a horizontal implementation. It would be straightforward to produce groups of W bits of an uncompressed “array of bits” bitmap by any of the approaches given above. With compressed bitmaps, it is considerably more difficult. One reason is that two RLE-compressed bitmaps may never have runs that begin at the same location. Another is that operations over RLE-compressed bitmaps gain efficiency by skipping portions of their input. For instance, if B_1 begins with a run of a thousand zeros, an AND operation using B_1 may skip the

corresponding portion of its other input.

The JavaEWAH library allows iterator-based basic operations (AND, OR, etc.), which take and produce iterators. Each iterator has the ability to skip portions, as noted above. If the circuit were a tree (no output connects to more than one input) we can compose iterators according to the circuit. For instance, the circuit corresponding to

```
AND (OR (b1, b2) , b3)
```

gives rise to something like

```
EWAHIterator it_b1 = b1.iterator()
EWAHIterator it_b2 = b2.iterator()
EWAHIterator temp1 = iteratorOR(it_b1, it_b2)
EWAHIterator it_b3 = b3.iterator()
EWAHIterator result = iteratorAND(temp1, it_b3)
```

The `result` iterator can then be made to yield its values. Unfortunately, this approach does not handle shared sub-expressions well. (Consider what would happen if the last statement were `iteratorAND(temp1, it_b1)`.) A solution would need to buffer the results produced by an iterator, in case that iterator's results are needed by several consumers. Moreover, different portions of the iterator's output may be skipped by the different consumers. While it is not impossible to envision solutions to this problem, they seem infeasibly expensive. We have implemented an alternative approach that unfolds a circuit with sharing into a tree—one that can be exponentially larger. This approach is infeasible for the adder and sorting circuits. However, the (mostly impractical) Sum-of-Products circuit is a tree, except near the leaves. The resulting iterator-based threshold function could be used when $\binom{N}{T}$ is small. Since this is rarely the case, we do not report performance results of this approach.

4.4.5 Tabulating circuits

There may be considerable overhead in constructing the required circuit, whether it be an adder, a sorter or the sum-of-products construction. In our implementations, we first construct the circuit. In the case of the sorting circuit, we are interested only in the T^{th} output. Yet we have generated all the other outputs, as well as the subcircuits that affect only the unused outputs. In the case of the tree-adder circuit we introduce constant zero inputs, which end up being passed into our gates. Some of the circuit constructions can generate unary AND, OR or XOR gates. Therefore, after constructing a circuit with these deficiencies, we then apply a variety of post-processing optimizations. First, a reachability analysis removes all

gates that are not in the “fan” of the one desired output: i.e., a gate whose output has no path to the overall circuit output is useless and it is removed. We then apply a simple constant-propagation pass that simplifies the circuits using such rules as $\text{AND}(x_1, \dots, x_k, 0) \rightarrow 0$ and $\text{OR}(x_1, \dots, x_k, 0) \rightarrow \text{OR}(x_1, \dots, x_k)$. These simplifications can produce unary gates, which can be removed: $\text{XOR}(x_1) \rightarrow x_1$ and so forth.

We do not propose that circuits be computed dynamically, at run time. Instead, circuits can be pre-computed and stored. Indeed, we do not need to generate a circuit for all $\Theta(N_{\max}^2)$ possible combination of N and T . Observe that if we have a circuit for $N = 16, T = 8$, we can use it to solve a variety of other threshold problems. For instance, if we wish to compute $N = 10, T = 7$, we can add five additional padding bitmaps that contain only zeros. We can also add one additional padding bitmap that contains only ones. We now have 16 bitmaps, and the threshold of 8 can be achieved with the padding bitmaps iff the threshold of 7 could be achieved on the original 10 bitmaps.

The general rule is that a circuit for N and T can be used, with appropriate padding, to compute any threshold problem with N' inputs and a threshold of T' , iff

1. $N' \leq N$ and
2. $T' \in [T - (N - N'), T]$

If we want to compute all values of T from 2 to $N_{\max} - 1$, note that none of these (N, T) pairs covers another. However, together they do cover all other pairs. Thus, we can tabulate $N_{\max} - 2$ circuits.

Nevertheless, if $N' \ll N_{\max}$, we will do a great deal of extra work to answer the query. We can tabulate $O(N_{\max} \log N_{\max})$ circuits if we choose all T values for $N = 2, 4, 8, \dots, 2^{\lceil \log N \rceil}, N$. This guarantees that we can answer any query for N' with a value of N where $N' \leq N < 2N$.

We can further reduce the size of the tabulated circuits by taking advantage of the similarity between the Sorter circuits for (N, T) and (N, T') . Both are based on minor optimizations applied to the same N -input Even-Odd mergesort circuit: if we know a particular value of T , we currently prune out the portions of the circuit that compute the outputs used for other values of T . Instead, we can forgo this optimization. With one circuit for N inputs, we compute all possible T values. Choosing $N = 2, 4, 8, \dots, 2^{\lceil \log N_{\max} \rceil}, N_{\max}$, we see that $\Theta(\log N_{\max})$ circuits can be tabulated and handle all queries. The *total* size of these circuits will $\Theta(N_{\max} \log^2 N_{\max})$.

The Adder circuits also offers a similar opportunity. Ignoring any pruning of portions unused for a particular value of T , the basic adder tree (or sideways-sum

circuit) is the same for all N -input Adder circuits. If we then compare for $\geq T$ using the $O(\log N)$ -gate subtract-and-check-the-sign circuit, the exact same circuit can be used for all T , since the $\Theta(\log N)$ bits for $-T$ can be inputs. Thus, the total tabulated size to handle one choice of N and any value of T is $\Theta(N)$. Choosing $N = 2, 4, 8, \dots, 2^{\lceil \log N_{\max} \rceil}, N_{\max}$, we have a total size bound of $\Theta(N_{\max})$ for all our tabulated circuits.

4.5 LOOPED Algorithm

We can develop a threshold algorithm for individual binary variables b_1, b_2, \dots, b_N by observing that

$$\vartheta(1, \{b_1\}) = b_1 \text{ and}$$

$$\vartheta(T, \{b_1\}) = \text{false if } T > 1 \text{ and}$$

$$\vartheta(T, \{b_1, b_2, \dots, b_N\}) = \vartheta(T, \{b_1, \dots, b_{N-1}\}) + \vartheta(T-1, \{b_1, \dots, b_{N-1}\}) \cdot b_N$$

In words: we can achieve a given threshold T over N bits, either by achieving it over $N-1$ bits, or by having a 1-bit for b_N and achieving threshold $T-1$ over the remaining $N-1$ bits.

We can then use bit-level parallelism to express this as a computation over bit vectors and a loop can compute the result specified by the recurrence. Note that $\Theta(NT)$ bit-vector operations are used, but we need only $O(T)$ working bitmaps during the computation, in addition to our N inputs.

Essentially, Algorithm 3 tabulates $\vartheta(T, \{b_1, \dots, b_N\})$ (using a table with rows for N and columns for T) by filling in the table row-wise. At the end of the k^{th} iteration, C_j stores $\vartheta(j, \{b_1, \dots, b_k\})$.

Although one can understand this as a computation over a recursively defined circuit, the tabulation-based implementation avoids circuit-based overheads present in the adder or sorting circuits.

The number of binary bitmap operations is $2NT - N - T^2 + T - 1$ and depends linearly on T , which is unusual compared with our other algorithms. Referring to Table 7, we see that even for $(N = 4, T = 3)$ this circuit uses twice as many bitmap operations as SSUM. Nevertheless, in experiments we have seen that this algorithm can sometime outperform SSUM. Indeed, the number of bitmap operations is not necessarily a good predictor of performance when using compressed bitmaps. It depends on the dataset.

4.5.1 CSVCKT algorithm

The CSVCKT algorithm also does not use an explicit circuit, but is inspired by a carry-save increment approach described by Ellingsen [11]. As with SSUM and TREEADD, we construct a “vertical counter” and then look for items whose counts

Algorithm 3 LOOPED algorithm.

Require: N bitmaps B_1, B_2, \dots, B_N , a threshold parameter T

- 1: create T bitmaps C_1, C_2, \dots, C_T initialized with false bits
 - 2: $C_1 \leftarrow B_1$
 - 3: **for** $i \leftarrow 2$ **to** N **do**
 - 4: **for** $j \leftarrow \min(T, i)$ **down to** 2 **do**
 - 5: $C_j \leftarrow C_j \vee (C_{j-1} \wedge B_i)$
 - 6: $C_1 \leftarrow C_1 \vee B_i$
 - 7: **return** C_T
-

exceed T . The approach is to maintain $\lfloor \log 2N \rfloor$ counter digits, using a redundant encoding scheme where each counter digit can have value 0, 1 or 2, encoded respectively as 00, as 01 or 10, and as 11. Hence we need two bitmaps for each counter digit. The redundantly encoded vertical counter is used as an accumulator, to which the input bitmaps are successively added. With a conventional binary encoding rather than the redundant encoding, we would have to do about $5 \log N$ bitmap operations every time a new bitmap is added to the counter—we need to update all bitmaps in the counter and each such update needs the five operations that make up a full adder. The advantage of the redundant encoding is that it permits one to (usually) avoid propagating changes to all counter digits. Frequently, changes need to be made to the least significant digit. Half as frequently, changes need to be made to the next-least significant digit, and so forth. Even though the individual positions may be maintaining different count values, it is sufficient to propagate changes on a fixed schedule that sees an amortized 2 digits updated for every bitmap added to the accumulator. (This fixed schedule corresponds to the bit changes from a counter that increments by one in every cycle, and the amortized number of such digit updates is asymptotically 2 per cycle [8].) Thus we need approximately $2 \times 5 \times N$ bitmap operations to build the final vertical counter using this redundant encoding.

It is easy to recover a vertical counter that uses a conventional binary encoding from this redundant encoding. For each digit, we merely sum the encoding's two bits, plus any carry from converting the previous digit. The result is the binary digit, plus possibly a carry for the next stage. This requires $O(\log N)$ bitmap operations.

Then any method for comparing the counter against T can be used. As an alternative to the approach used for SSUM, we show the approach where we subtract T from the counter and check that the result is non-negative. A minor optimization is possible: of the difference bits V_i , only the sign bit ($V_{1+\lfloor \log 2N \rfloor}$) needs to be computed. Thus, the body of the final **for** loop either consists of an AND operation or consists of an OR and an ANDNOT operation.

Pseudocode for this approach is given in Algorithm 4. We used an additional small optimization in our implementation that is not reflected in the pseudocode: when the first two bitmaps are added into the total, they directly become the first encoded digit. Then the `time` variable starts out at 1 rather than 0.

Given the ease of implementing the approach, it appears that it may be a reasonable alternative to `SSUM` (which uses $\approx 5N$ bitmap operations) or `TREEADD` (which uses $\approx 7N$ bitmap operations), depending on the cost of the operations.

Algorithm 4 CSvCKT algorithm; see [11] for the first parts.

Require: input bitmaps B_1, B_2, \dots, B_N , integer threshold T with $2 \leq T < N$
create $1 + \lfloor \log 2N \rfloor$ bitmap pairs $\langle C_1^1, C_1^2 \rangle, \langle C_2^1, C_2^2 \rangle, \dots, \langle C_{\lfloor \log 2N \rfloor}^1, C_{\lfloor \log 2N \rfloor}^2 \rangle,$
 $\langle C_{\lfloor \log 2N \rfloor + 1}^1, C_{\lfloor \log 2N \rfloor + 1}^2 \rangle$ of empty bitmaps (initialized with false bits)
 $t \leftarrow 0$ { t is “time”} {Add each bitmap to accumulating carry-save counter}
for $i \leftarrow 1$ **to** N **do**
 $c \leftarrow B_i$
 $t \leftarrow t + 1$; $x \leftarrow$ number of trailing zeros in t
 for $p \leftarrow 1$ **to** x **do**
 $a \leftarrow C_p^1$; $b \leftarrow C_p^2$; $C_p^1 \leftarrow$ an empty bitmap
 $s \leftarrow a \oplus b$; $C_p^2 \leftarrow s \oplus c$; $c \leftarrow (a \wedge b) \vee (c \wedge s)$
 $C_{x+1}^1 \leftarrow c$
 {convert redundant representation to two’s complement}
create $1 + \lfloor \log 2N \rfloor$ empty bitmaps $V_1, V_2, \dots, V_{1+\lfloor \log 2N \rfloor}$
 $c_{\text{in}} \leftarrow$ an empty bitmap
for $i \leftarrow 1$ **to** $\lfloor \log 2N \rfloor$ **do**
 $a \leftarrow C_i^1$; $b \leftarrow C_i^2$
 $s \leftarrow a \oplus b$; $V_i \leftarrow s \oplus c_{\text{in}}$; $c_{\text{in}} \leftarrow (a \wedge b) \vee (c_{\text{in}} \wedge s)$
 {Compare the vertical counter to T (subtract T and check sign)}
Let $T_{\lfloor \log 2N \rfloor + 1}, T_{\lfloor \log 2N \rfloor}, \dots, T_2, T_1$ be the bits in the two’s complement binary representation of $-T$
 $c_{\text{in}} \leftarrow$ an empty bitmap
for $i \leftarrow 1$ **to** $1 + \lfloor \log 2N \rfloor$ **do**
 $a \leftarrow V_i$
 if $T_i = 1$ **then**
 $s \leftarrow \neg a$; $V_i \leftarrow s \oplus c_{\text{in}}$; $c_{\text{in}} \leftarrow a \vee (c_{\text{in}} \wedge s)$
 else
 $s \leftarrow a$; $V_i \leftarrow s \oplus c_{\text{in}}$; $c_{\text{in}} \leftarrow c_{\text{in}} \wedge s$
 {use the sign bit of the difference we just computed}
return $\neg V_{1+\lfloor \log 2N \rfloor}$

5 Detailed Experiments

We conducted extensive experiments on the various threshold algorithms, using both uncompressed bitmaps and EWAH compressed bitmaps. Our experiments involved both synthetic and real datasets. On the real datasets, the various bitmaps in the index vary drastically in characteristics such as density. We discuss this in more detail before giving the experimental results.

5.1 Platform:

Experimental results were gathered on a two identical desktops with Intel Core i7 2600 (3.40 GHz, 8 MB of L3 CPU cache) 3.4 GHz processors with 16 GB of memory (DDR3-1333 RAM with dual channel). Because all algorithms are benchmarked after the data has been loaded in memory, disk performance is irrelevant.

One system was running Ubuntu 12.04LTS with Linux kernel 3.2, and the other ran Ubuntu 12.10 with Linux kernel 3.5. During experiments, we disabled dynamic overclocking (Turbo Boost) and dynamic frequency scaling (SpeedStep). Software was written in Java (version 1.7), compiled and run using OpenJDK (IcedTea 2.3.10) and the OpenJDK 64-bit server JVM. We believe that results obtained on either system are comparable; even if there is some speed difference, the result should not favour one algorithm over another. We used the JavaEWAH software library [24], version 0.8.1, for our EWAH compressed bitmaps. It includes support for the RBMRG algorithm. Our measured times were in wall-clock milliseconds. All our software is single-threaded.

Our measured times were in wall-clock milliseconds. Since our reported times vary by six orders of magnitude (from about 10^{-1} to 10^5 ms) we used an adaptive approach, rather than repeat the computation a fixed number of times. To do this, the computation was attempted. If it completed in less than 10^3 ms, we ran the computation twice (restarting the timing). If that completed too fast, we then repeated the computation four times, and so forth, until the computation had been repeated enough times to take at least 10^3 ms.

5.2 Real data

Real data tests were done using IMDB-3gr, IMDB-2gr, PGDVD-3gr, PGDVD-2gr, PGDVD and CensusIncome.¹⁰ Some statistics for each dataset are given in Table 9.

The first two are based on descriptions of a dataset used in the work of Li et al. [25], in an application looking for actor names that are at a small edit distance from a (possibly misspelt) name. The list of actor names used is obtained from the

¹⁰See <http://lemire.me/data/symmetric2014.html>.

Internet Movie Database project. Although the data is available for noncommercial use, the terms of its distribution may not permit us to make the data publicly available. Thus, Appendix A gives a detailed explanation of how this dataset was obtained. (Others can follow the steps and obtain a similar dataset.) Each actor name became a record and we extracted its q -grams (for $q \in \{2, 3\}$). Essentially, for each q -gram that occurs in at least one name, we recorded the list of record-ids where the actor’s name contained at least one occurrence of the q -gram. Whereas the work of Li et al. [25] would have computed results over the sorted lists of integers, we followed the approach of Ferro et al. [12] and represented each sorted list of integers by a bitmap: in our case either an uncompressed bitmap (BITSET) or an EWAH compressed bitmap. Whereas Li et al. chose $q = 3$, Ferro et al. chose $q = 2$. We used both values of q . There is at least one bigram that is *extremely* common in this data: most actor names are given as a surname, a comma, a space, and a forename. Such a format will contain the comma-space bigram. Therefore, there is at least one bitmap that is very dense, and this may help explain why algorithms did not always behave similarly on the two datasets.

The PGDVD-3gr and PGDVD-2gr datasets are similar to the IMDB datasets, except instead of actor names, we formed q -grams from chunks of text from the Project Gutenberg DVD [31]. Each chunk was obtained by concatenating paragraphs until we accumulated at least 1000 characters. We rejected any paragraph with over 20 000 characters—this protected us from some content on the Project Gutenberg DVD. (Unfortunately, the DVD contains not only the desired natural-language texts of out-of-copyright books, but it also contains the human genetic code and also the digits of π and other irrational constants.)

The PGDVD dataset is based on the vocabulary present in the Project Gutenberg DVD. The text in the 11,118 suitable text files on the DVD was tokenized into maximal sequences of alphabetic characters. Tokens longer than 20 characters were discarded; the human genome files created such long tokens. The remaining distinct tokens (there were more than 2 million of them) were considered to be words, although not all of them are in English. We formed a dataset with a row for every word, and a column (corresponding to a bitmap) for each of the 11,118 files. The bitmap for a file contained a 1 whenever that file contained the associated word at least once. Such bitmaps should be highly compressible, because words that first occur within a given text will occupy contiguous portions of the bitmaps.

Whereas an inverted index over the DVD would have a set for each word (indicating the files that contain the word), we have a set for each file. Thus our PGDVD dataset can be considered an “uninverted” index, or the transpose of an inverted index. Similarity queries on such a dataset will yield words that often occur in the same files/books as a query word. We suspect that a useful tool for a literary analyst could use this approach, and the development of this dataset was motivated by

Table 9: Characteristics of real datasets. Overall bitmap density is the number of ones, divided by the product of the number of rows and the number of bitmaps.

Dataset	Rows	Attributes	Bitmaps	Average Density	
				Overall	Similarity
IMDB-2gr	1,783,816	4276	4276	4.5×10^{-3}	1.3×10^{-1}
IMDB-3gr	1,783,816	50,663	50,663	4.1×10^{-4}	3.0×10^{-2}
PGDVD	2,439,448	11,118	11,118	2.9×10^{-4}	6.1×10^{-3}
PGDVD-2gr	3,513,575	755	755	2.8×10^{-1}	7.0×10^{-1}
PGDVD-3gr	3,513,575	20,247	20,247	2.8×10^{-2}	3.6×10^{-1}
CensusIncome	199,523	42	103,419	4.1×10^{-4}	5.6×10^{-1}

some of our prior work [19].

We also chose a more conventional dataset with many attributes, CensusIncome [23, 13]. A conventional bitmap index was built, having a bitmap for every attribute value. One attribute is responsible for 99,800 of the bitmaps; the remaining 3619 bitmaps are much denser than these 99,800.

5.3 Synthetic data

We also experimented with smaller synthetic datasets. One difficulty is that threshold queries for moderately large T almost always return an empty set (except for the row selected for the similarity query), which may not be very realistic.

Each random bitmap represented a set with 10,000 entries, created by a uniform random process or a clustered [2] process. With both the uniform and the clustered process, three datasets were generated: a dense one, where the set elements ranged between 0 and 29,999; a moderately sparse one, where the set elements ranged between 0 and 999,999; and a sparse one, where the set elements ranged up to 9,999,999. The names of the synthetic datasets encode the parameters: [Clustered;1111;10000; r] and [Uniform;1111;10000; r] ($|B_i| = 10000$ and value 1111 was used to seed the random-number generator.)

The moderate or sparse uniform datasets would not be good candidates for EWAH compression: when the elements present in a set are sorted, an element and its successor will usually not be within 64 values of each other, and therefore most set elements require a whole machine word for storage (plus the overhead to specify the run of zeros). Thus the moderate and sparse uniform data would be better stored as sorted lists of integers.

Our dense uniform datasets are well suited for bitmap representation. Since runs of zero (or one) will rarely be long, bitmap compression is not useful.

5.4 Queries Used

For our experiments, we will have an intended value of N . A similarity query takes some row-id and determines the bitmaps whose associated sets contain that rid. If there were exactly N bitmaps, we would then use them in a threshold computation. Even if $T = N$, we will obtain a nonempty answer to a threshold computation, as the original rid meets the threshold.

Unfortunately, this may be fewer or more than N bitmaps. If there are more than N bitmaps, we simply take the first N . If we have N' bitmaps, where $N' < N$, we will take $\lfloor N/N' \rfloor$ or $\lceil N/N' \rceil$ copies of each bitmap, in order to obtain a collection of N bitmaps. The trick of taking repeated copies is a known approach to obtaining a *weighted* threshold computation by transforming it to our unweighted thresholds [21]. In our case, we are simulating having weights $\lfloor N/N' \rfloor$ and $\lceil N/N' \rceil$.

We have a second approach to boost the number of bitmaps in a similarity query. Instead of taking a single row-id, we take 10 or 100. For each row id, we proceed as before, determining the set of bitmaps that have 1 for that row-id. The union of all these sets of bitmaps is then considered, and we either select the first N of them (if the union has more than N), or we take multiple copies as needed to obtain a collection of N . We use the notation “similarity(10)” and “similarity(100)” to indicate the use of this second approach. Note that threshold computations with $T \approx N$ will now have the (very likely) possibility of returning empty results.

Note that the frequencies of various q -grams differ widely, and the frequencies of words in the PGDVD dataset will also follow Zipf’s law. An implication is that if we randomly select a word from the dataset and take its q -grams, we will, on average, be looking at frequent q -grams. Thus the last two columns in Table 9 differ: the first shows the average density of bitmaps from the dataset, whereas the second shows the average density of the bitmaps actually selected by similarity queries.

There is one subtle but important difference, involving binary attributes, between similarity queries against CensusIncome and the other datasets. The other datasets are based only on binary (Boolean) attributes, and the similarity queries are based only on *true* values. For example, a similarity query on string ‘Sam’ will involve the bitmap for bigram ‘am’, but for the edit-distance application of Sarawagi and Kirpal, it will not involve a bitmap for “does not contain bigram ‘pq’”. However, if we had encoded the relationship of strings and bigrams in a table, there would have been an attribute for each possible bigram. Two values (*true* and *false*) would appear in the column. Thus, there would be a (presumably sparse) bitmap for the true value, and a (presumably dense) bitmap for the false value. A

similarity query for 'Sam' over such a table *would* involve the bitmap for “does not contain bigram ‘pq’”, because ‘Sam’ does meet the condition of this bitmap. Since the Sarawagi and Kirpal approach is based only on the bigrams actually present, our solution has been to treat binary attributes specially. Yet there are other cases (perhaps a gender attribute with values ‘M’ and ‘F’) where binary attributes should be treated the same as other attributes. This may indicate that similarity queries should allow users to specify how to handle ‘False’ values of Boolean attributes.

Note that including the dense bitmaps would have drastically favoured algorithms that do not iterate over the 1 bits (such as the circuit-based approaches or RBMRG).

Competitions: We assess the effectiveness of the various algorithms by measuring their wall-clock times on a variety of test runs, each called a competition. A competition consists of a dataset, specific values of N and T , and a randomly selected rid (or set of rids) that will determine which N bitmaps are selected in a similarity query ¹¹.

Each algorithm is assigned a rank that depends on its speed, with rank 0 being the fastest algorithm. Each algorithm is also compared, for each competition, to see whether it is no more than 50% or 100% slower than the rank-0 algorithm.

Results are then tabulated for a related collection of competitions. Currently, we have one collection (SMALL-COMPETITIONS) of competitions to reflect cases where N is small. The queries correspond to a single row. Pairs N and T are as follows: (4,3), (8,3), (8,4), (8,6), (8,7), (16,3), (16,4), (16,5), (16,6), (16,9), (16,12), (16,13), (16,14), (16,15), (32,3), (32,4), (32,6), (32,9), (32,13), (32,15), (32,19), (32,21), (32,28), (32,30), (32,31). These pairs are generated by doubling N and using T values that are either T' or $N + 2 - T'$ where $T' = 3, 4, 6, \dots$ is generated by $T'_1 = 3$ and $T'_k = \lfloor \frac{3}{2}T'_{k-1} \rfloor$. This choice of T values favours especially large and especially small thresholds. Especially large thresholds, for moderate sizes of N , should be typical of certain applications, including that of Li et al. [25]. On these small competitions, we used similarity queries for IMDB-2gr, IMDB-3gr, PGDVD and CensusIncome.

We also run MEDIUM-COMPETITIONS, a collection of competitions using a wider range of N and T values. The values of N are still obtained by repeated doubling, and the values of T are still obtained as before. However, N goes up to

¹¹In our experiments the choice of N , random seed and dataset uniquely determines the set of bitmaps chosen. This means that as T is varied, we can clearly see the effect of T on that particular set of N bitmaps, as long as we use the same seed for the random number generator. However, if we hold T constant and look at the effect of varying N , we may get a collection of three sparse bitmaps for $T = 3$, but four dense bitmaps for $T = 4$, and so forth. To reduce this effect, we use 10 different runs and report their averages when showing how time varies with N .

128 (and T can go up to 127). For MEDIUM-COMPETITIONS, we used similarity(10) queries for IMDB-2gr, IMDB-3gr, PGDVD and CensusIncome.

Finally, we have LARGE-COMPETITIONS, where N can go up to 512 and T can go to 511. We used similarity(100) queries for IMDB-2gr, IMDB-3gr, CensusIncome and PGDVD, but similarity queries were used for PGDVD-2gr and PGDVD-3gr. Due to the nature of our synthetic datasets, it does not really matter which type of query we used, except we note that we did not duplicate any bitmaps.

5.5 Scalability of Algorithms

As previewed in Tables 3 and 4, the various algorithms' running times are all affected¹² by N . Some are affected by T and others are highly sensitive to the characteristics of the datasets being processed.

Although we later present more details on the effect of these factors on each algorithm, a few examples on compressed bitmaps first illustrate these effects.

Fig. 3 shows how several algorithms behaved as N was changed. For each value of N , we took 10 similarity queries and averaged their running times, holding T constant at $N/2$. Note that we did *not* count the time to compute the appropriate threshold circuit, for the circuit-based approaches. This is justified by the discussion in § 4.4.5. To focus on the growth rate, the time for an algorithm has been normalized by dividing it by that algorithm's speed when $N = 32$.

Fig. 4 shows the effect of varying T , on one particular set of 64 bitmaps. Absolute times are shown, but on a logarithmic scale.

5.6 'w' and Non-'w' Algorithms

We have two main implementation styles. Algorithms whose names begin with 'w' were implemented by converting the compressed bitmaps into sorted lists of integers, and then processing these lists. Some of the algorithms in question require the manipulation of such lists and seem to demand all of their data in memory in such a format. Examples would be w2CTI or wSORT. Thus, there is no native bitmap implementation of such an algorithm. Other algorithms were implemented using both implementation styles, and thus have a 'w' version and a native bitmap version. We did not implement a native bitmap version of WMGSK, having observed that

- the other 'w' implementations almost always outperformed it, and

¹² For table entries (such as that for SCANCOUNT) where B is given but N is not explicit, note that B grows as N grows: given a set of N bitmaps with B ones, if a new nonzero bitmap is added, the total number of ones increases.

- the overheads of converting a bitmap into a sorted list of integers always outweighed whatever gains might be obtained by processing integer arrays.

With these ‘w’ algorithms, there are limitations to which datasets and queries can be processed, due to the requirement of storing the input as (frequently huge) integer lists. Algorithm `WSORT` particularly had difficulties, and many data points for $N \geq 128$ are missing. `WMGSK` had trouble for $N = 512$ on `PGDVD-3gr`. Even when larger N values were handled by such algorithms, the running times were often much higher than one might anticipate, and also the CPU utilization for the single-threaded tests were frequently noted to exceed 100%. This presumably indicates concurrent work by the garbage collector, and such results may not represent the behaviour we would find on a machine with more memory.

5.7 Uncompressed bitmaps

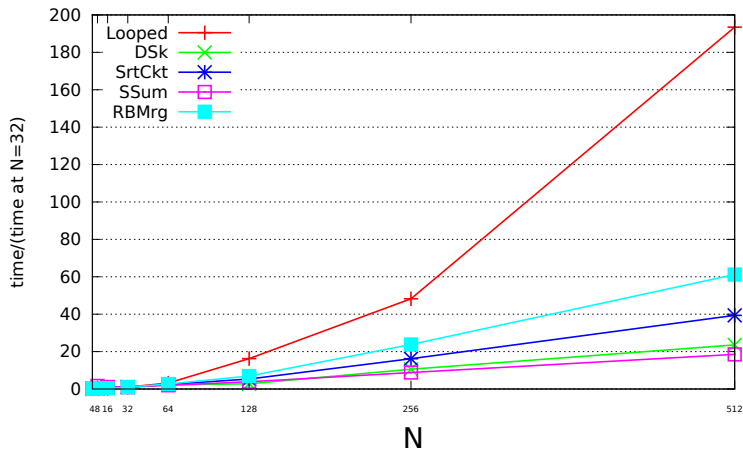
While our primary interest is in word-aligned RLE bitmaps, it is useful to look at the simpler case of uncompressed bitmaps. Therefore, we experimented with algorithms operating over `JAVA.UTIL.BITSET`. We implement `LOOPED`, `DSK` with various choices of parameter μ , `SCANCOUNT` (see Appendix D), `TREEADD`, `SSUM`, `SOPCKT` and `SRTCKT`.

The technique used by `SCANCOUNT` to iterate through only the set bits means that it does less work when there are few set bits. Thus we experiment with queries where the `BITSETS` are taken from the index, as well as cases where the same `BITSETS` are negated prior to threshold computations.

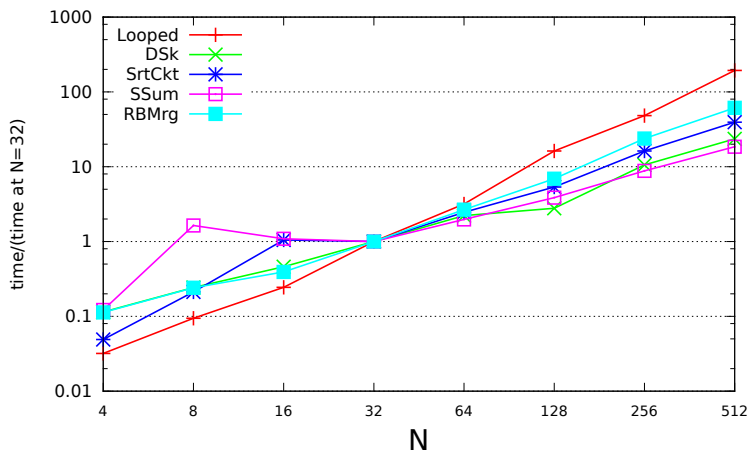
For display purposes we are comparing only a few algorithms, and thus we can associate each one with a colour. Then for each dataset we generate two different sequences of queries. The first randomly chooses $\log N$ uniformly from 2.0 to 10.0. From that, we compute the nearest integer N . We then randomly choose an integer threshold T from 2 to $N - 1$ inclusive. Finally, we choose N bitmaps corresponding to a similarity query. Note that if a particular value of N is chosen several times, we do not (usually) generate the same N bitmaps. The query is executed using each of the algorithms, and we record which one was fastest. We also keep track of the total time taken by each algorithm. Since the choice of N and T often determines which algorithm is fastest, we place the winner’s coloured marker on an N, T grid.

The second sequence of queries is similar, except that every bitmap has been negated.

Table 10 gives results for similarity queries. We would usually select the bitmap for the comma-space bigram in each test for `IMDB-2gr`, and this bitmap’s high density hurts `SCANCOUNT` enough that `TREEADD` can overcome it. These



(a) linear axes



(b) logarithmic axes

Figure 3: Effect of N on running times of several algorithms on EWAH compressed bitmaps. $T = N/2$, and the chosen dataset is PGDVD-3gr. To focus on scalability, each algorithm’s running time is normalized so that it takes unit time when $N = 32$.

effects are shown visually in Fig. 5. Each marker shows which algorithm was fastest for a query of a given N and T in the workload. As noted, we presume the comma-space bigram’s bitmap was involved in most queries for IMDB-2gr. Thus we see the adder circuits performed well for moderate and large values of T , whereas SCANCOUNT never was best. For small values of T , LOOPED is usually

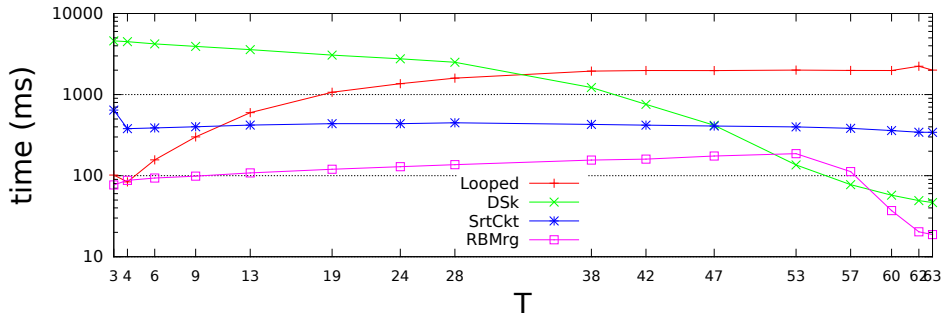


Figure 4: Effect of T on running times of several algorithms on EWAH compressed bitmaps. $N=64$, and the dataset is PGDVD-3gr. SSUM took about 200 ms except for $T = 3$, where it took about 400 ms.

Table 10: Total workload times (seconds), uncompressed bitmaps (BITSET)

Algorithm	As Given			Negated		
	IMDB-2	IMDB-3	PGDVD	IMDB-2	IMDB-3	PGDVD
SCANCOUNT	23.1	8.6	3.3	112.7	124.2	105.3
LOOPED	208.2	203.0	113.9	219.1	218.1	170.4
DSK	61.5	18.4	8.0	619.0	586.3	493.0
TREEADD	6.4	6.1	3.0	6.4	6.5	3.9
SSUM	6.5	6.4	3.8	7.2	7.9	4.8
SRTCCT	26.6	25.8	16.3	26.0	25.6	21.1
WMGOPT	106.1	28.6	12.0	–	–	–
w2CTI	55.5	16.3	5.0	–	–	–

the fastest technique when $T \leq 3$. With IMDB-3gr and PGDVD we see the adders competing with SCANCOUNT once N is larger than about 60. Depending on the dataset, the pruning-based approaches DSK and w2CTI are sometimes effective (DSK requires $T \approx N$ to be successful, whereas w2CTI can handle cases when T and N differ more).

Using BITSET, we found that the sideways-sum adder was frequently slower than the tree adder for certain datasets. For instance, with PGDVD and $N = 119$, $T = 60$ it took 55.1 ms for the sideways-sum adder, but only 46.6 ms for the other. Other combinations of N and T were similar. We found this surprising, because the tree adder requires about 40% more operations than the sideways-sum adder. Investigating the OpenJDK source code for BITSET [16], we found that operations such as AND and OR are optimized to avoid work after the word containing the last set bit in a bitmap. By setting a sentinel bit after the last valid row-id in the index, we can force all BITSETS to have their maximum length. In that case, both kinds

of adder became significantly slower: for $N = 119$ and $T = 60$ the sideways-sum and tree-adder speeds were 71.8 ms and 113 ms, respectively. Thus, the speed ratio between adders was much closer to what we expected. Since BITSET is not a fixed-length vector of bits, we see how its implementation makes the determination of the faster algorithm become data dependent. While we know the tree-adder circuit manipulates more BITSETS, presumably they were much shorter ones when processing our datasets for small values of N : the pattern in Fig. 5 is that SSUM was the faster Adder circuit for smaller values of N , whereas TREEADD was faster for large N .

When the BITSETS were negated, we obtained extremely dense bitmaps. It is not surprising that SCANCOUNT was negatively affected by the density of the bitmaps, as it iterates over the ones. It may be surprising that LOOPED, TREEADD, SSUM and SRTCKT were affected, because should have been (more or less) oblivious to their data. However, the BITSET representation, as implemented in OpenJDK, only stores bitmap words until the word with until the largest one bit. In negating the bitmaps, we used `BitSet.flip(0, numRows)`. Suppose that `numRows` was 1000, but we had a bitmap whose last set bit was 20. After the flip, it would have required 50 times more data to store. Presumably it would also have taken longer to process.

The poor performance for LOOPED arose because the workload included queries with large values of T , and the algorithm’s running time depends strongly on T . However, it frequently outperformed the other algorithms when T was extremely small. Unfortunately, the total workload times were dominated by the times of the queries where N and T were large¹³. For similar reasons, it appears that TREEADD was always to be preferred to SRTCKT. However, for smaller N and T , SRTCKT frequently outperformed TREEADD.

Under BITSET negation, we see a pattern for IMDB-2gr (Fig. 5d) much like Fig. 5a, except that DSK is *never* best. (Due to memory limitations, none of the ‘w’ algorithms could be run.) Results for BITSET negation on IMDB-2gr and PGDVD were almost indistinguishable from the pattern seen in Fig. 5d, except in which adder circuit was better (they preferred the sideways-sum adder).

Discussion: If one does not know much about the data and does not know the values of N and T to expect, the adder circuits are safe bets (see Table 10. If T is known to be very small, LOOPED is a reasonable choice, and SRTCKT may also fare well. Algorithms SCANCOUNT, DSK and the ‘w’ algorithms can be good choices if the data is known to be very sparse. For w2CTI and DSK, we need to have effective opportunities for pruning, and thus T needs to be very large. How-

¹³ The query-generation process tends to produce large T values when N is large.

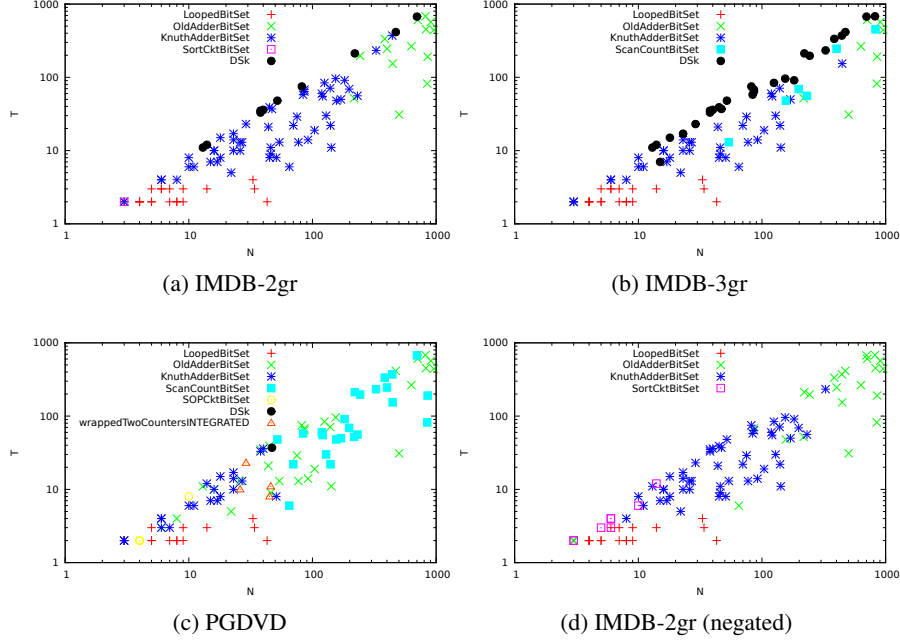


Figure 5: The fastest algorithm for each of the 100 queries in the workload are shown. Similarity queries were used over BITSETS.

ever, SCANCOUNT is too slow when the data is dense, DSK can perform very poorly unless $T \approx N$, and the ‘w’ algorithms will fail if the integer-list representation requires too much memory (each bit can turn into a 32-bit quantity, for a 32-fold space expansion).

5.8 Comparing Algorithms on EWAH

Our experiments first focus on the individual algorithms. For each algorithm, we show how it scales with N and T on similarity queries involving both synthetic and real datasets. We omit SOPCKT because it cannot be run with most N and T combinations. We omit w2CTN and w2CTA because the better pruning done by w2CTI means they are usually worse than w2CTI.

The experiments varying T were done with one particular set of bitmaps. It corresponds to $N = 32$ and SMALL-COMPETITIONS. The logarithmic y scale can make differences look small, but this is needed to show the drastic differences that T can make for some algorithms.

To study scaling with N , we ran a series of competitions using $N = 4, 8, 16, \dots$

up to 512 for $T = 3$, $T = N/2$ and $T = N - 1$. Ten similarity queries (each with one prototypical item) were generated for each value of N . The 10 times were then averaged, and the averaged time was then normalized by dividing it by the average time for $N = 32$.

To allow a comparison between algorithms, we show heat maps indicating the conditions (N and T) when that algorithm performed well on our real datasets. (We also show when its performance is *terrible*, which we define as 10 times longer than the fastest algorithm.) This data included SMALL-COMPETITIONS, MEDIUM-COMPETITIONS, LARGE-COMPETITIONS as well as the competitions used when varying N .

Unfortunately, the heat map aggregates results from our various real datasets, and the algorithm performance can be greatly influenced by the dataset used. The heat maps do not provide a way to see the effect of the dataset. Thus, these heat maps might be appropriate for a workload in which all datasets were used equally, and with N and T distributions that were independent of the dataset.

After these per-algorithm results are given and discussed, § 5.9 ranks the algorithms by supposing a workload that gives equal importance to queries over each dataset, but in which a fixed N and T are used. A stacked bar chart is then used. An algorithm's overall slowness on the workload is shown by the overall height of the bar. However, it is illustrative to see the individual contributions from the various datasets. From this we can assess the sensitivity of the various algorithms to the characteristics of their datasets. We show such stacked bar charts for a few representative (N, T) combinations.

Appendix C provides yet another view into the outcome of the competitions. Here, results for the various (N, T) combinations are aggregated, but we focus on the individual suboptimalities ((measured time - best time)/best time) observed. They are shown as points on a per-algorithm badness column. The problem with this view is that one cannot tell which N and K values correspond to a given point.

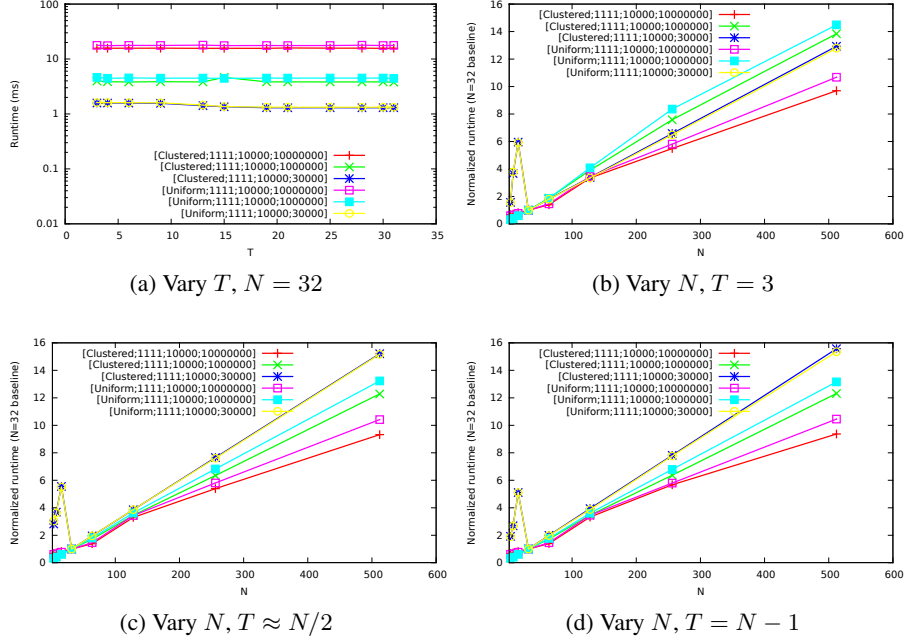


Figure 6: Varying T and N on SCANCOUNT, synthetic data (effect of varying N uses time relative to $N = 32$)

5.8.1 Algorithm SCANCOUNT

The effect of varying T on SCANCOUNT are shown in Figs. 6a and 7a.

1. The effects of varying N are shown in Figs. 6b–6d and 7b–8c.
2. The percentage of
 - (a) cases where the algorithm achieved the fastest results is shown in Fig. 9a;
 - (b) cases where it was within 50% of the fastest result (including the fastest cases) is in Fig. 9b;
 - (c) cases within 100% is shown in Fig. 9c.
 - (d) disastrous cases is shown in Fig. 9d. In such cases, the algorithm took at least 10 times as long as the fastest algorithm.

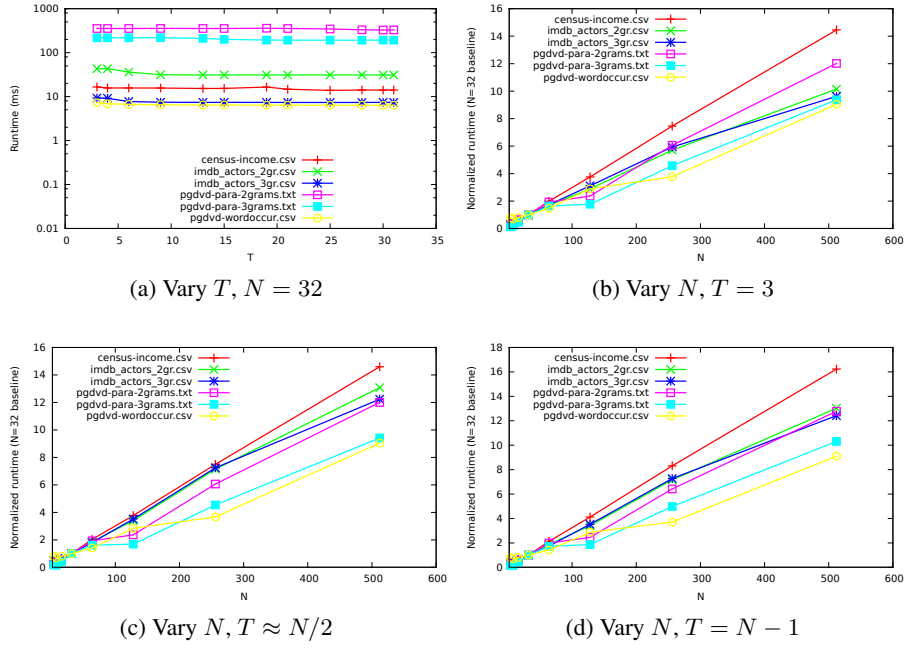


Figure 7: Varying T and N on SCANCOUNT, real data (effect of varying N uses time relative to $N = 32$)

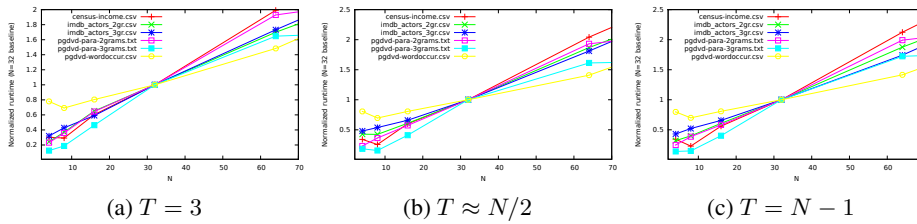
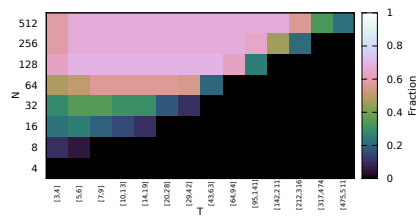
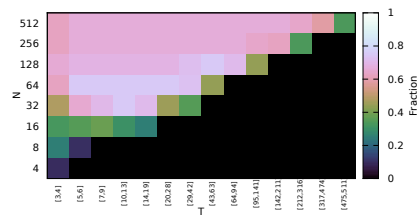


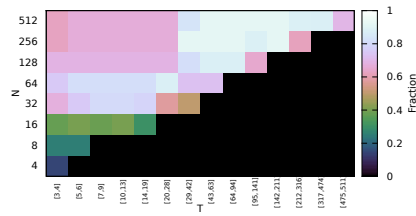
Figure 8: Effect of N (times relative to $N = 32$) for smaller values of N , on ScnCnt



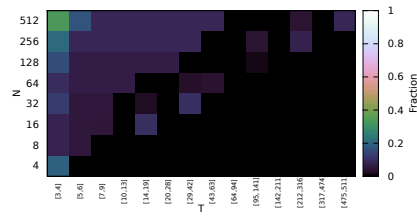
(a) Wins



(b) Good



(c) Fair



(d) Terrible

Figure 9: Heat map showing when to use and when to avoid ScnCnt

Several algorithms showed little effect from T . This include SCANCOUNT, WSORT, WHEAP, HASHCNT and (to some extent) TREEADD.

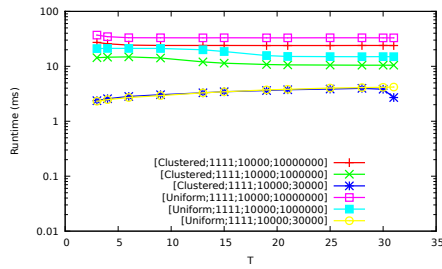
SCANCOUNT had strong overall performance, and was strongest when $N \geq 32$ and T was neither particularly big or particularly small. The number of terrible cases was few, and they tended to arise when N was large and $T < N/2$. Since SCANCOUNT was not much affected by T , these results tend to highlight values of N and T where competitors were particularly strong.

Synthetic data clearly shows the dependence on r , and also dense cases had an unusual situation at $N = 4$, $N = 8$ (and peaking at $N = 16$) where the algorithm was substantially slower than for $N = 32$. This effect remains unexplained. Nothing similar was observed on real data.

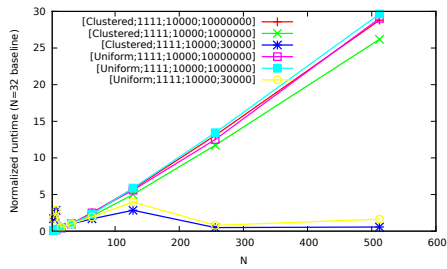
5.8.2 Algorithm RBMRG

The effect of varying T on RBMRG are shown in Figs. 10a and 11a.

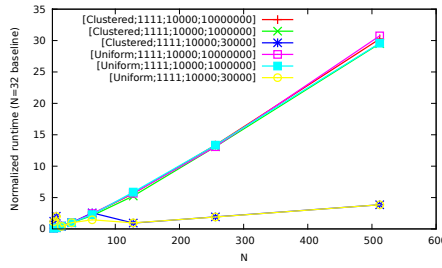
1. The effects of varying N are shown in Figs. 10b–10d and 11b–12c.
2. The percentage of
 - (a) cases where the algorithm achieved the fastest results is shown in Fig. 13a;
 - (b) cases where it was within 50% of the fastest result (including the fastest cases) is in Fig. 13b;
 - (c) cases within 100% is shown in Fig. 13c.
 - (d) disastrous cases is shown in Fig. 13d. In such cases, the algorithm took at least 10 times as long as the fastest algorithm.



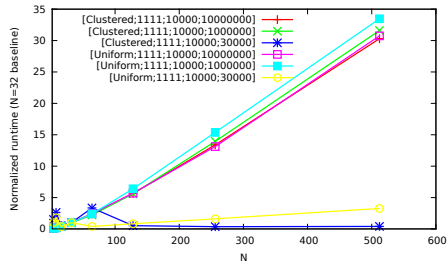
(a) Vary T , $N = 32$



(b) Vary N , $T = 3$



(c) Vary N , $T \approx N/2$



(d) Vary N , $T = N - 1$

Figure 10: Varying T and N on RBMRG, synthetic data (effect of varying N uses time relative to $N = 32$)

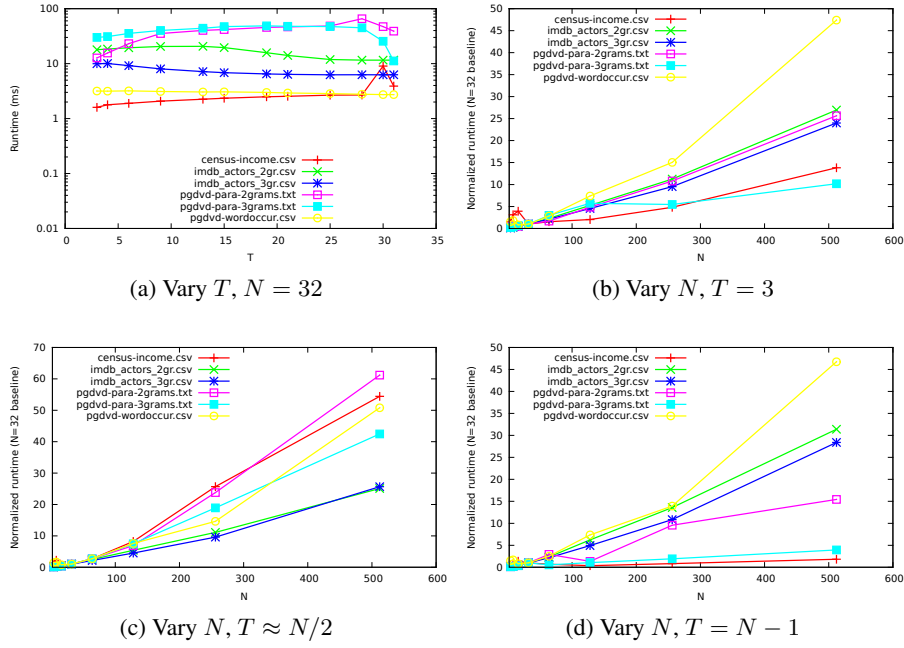


Figure 11: Varying T and N on RBMRG, real data (effect of varying N uses time relative to $N = 32$)

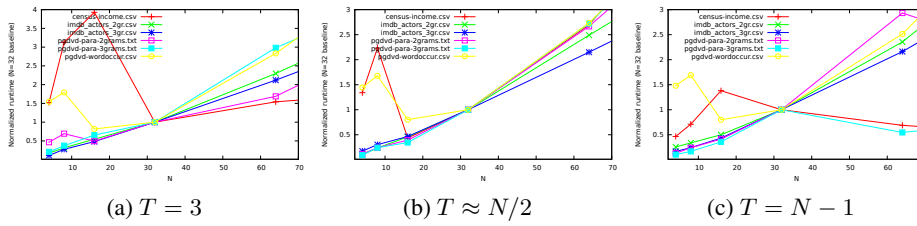
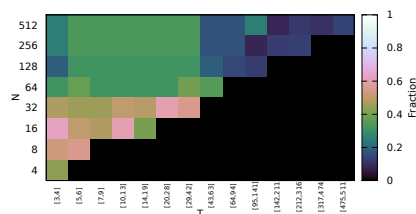
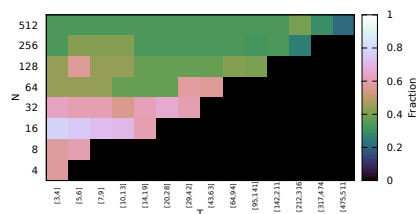


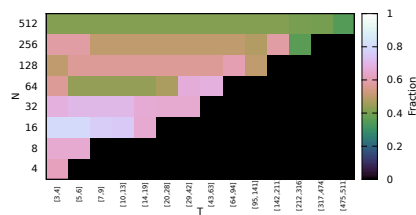
Figure 12: Effect of N (times relative to $N = 32$) for smaller values of N , on RBMRG



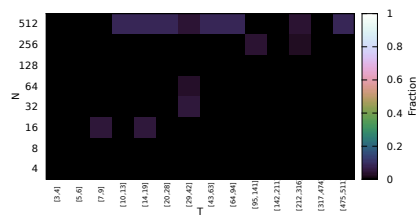
(a) Wins



(b) Good



(c) Fair



(d) Terrible

Figure 13: Heat map showing when to use and when to avoid RBMrg

The most complex behaviour with respect to T was with RBMRG (Fig. 11a.) On one real dataset, its performance was not affected by T . On two others, time dropped substantially when T was large enough. The growth rates of CensusIncome, PGDVD-2gr and PGDVD-3gr resembled the growth observed for the dense synthetic data: an increase in running time, followed by a reduction at the largest T . IMDB-2gr and IMDB-3gr more resembled the moderately sparse synthetic data.

Synthetic data shows that RBMRG’s run-based performance benefited from the clustered dense data, which presumably had few runs. The improvement with T may be surprising, as the input runs processed are clearly independent of T . However, we compute an output, which is more quickly done if there are fewer runs. When T is large, we are typically just coalescing runs of zeros, a fast operation for a compressed bitmap. Similarly, when T is small, we may be quickly coalescing runs of ones. For in-between values of T we have to solve a threshold problem involving the dirty words.

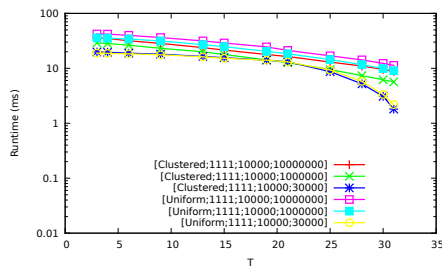
The complexity of the output bitmap, in terms of the number of its runs, could be as high as the total RUNCOUNT of its inputs. Thus, while the processing of the input’s RUNCOUNT runs may be unaffected by T , the number of output runs (after coalescing) may vary dramatically. If the cost of constructing a compressed bitmap is substantially higher than the cost of reading one, we could see results where the threshold makes these kinds of differences (factors near 10).

Its strengths seem to be with $N = 16$ and $N = 32$ for larger values of T . It was only infrequently terrible, even more so than SCANCOUNT.

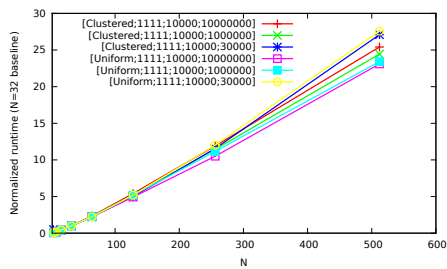
5.8.3 Algorithm DSK

The effect of varying T on DSK are shown in Figs. 14a and 15a.

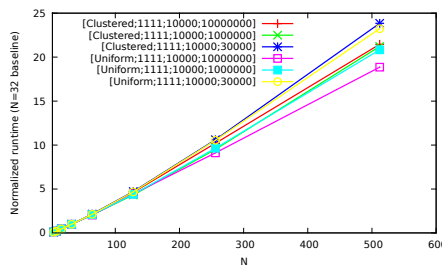
1. The effects of varying N are shown in Figs. 14b–14d and 15b–16c.
2. The percentage of
 - (a) cases where the algorithm achieved the fastest results is shown in Fig. 17a;
 - (b) cases where it was within 50% of the fastest result (including the fastest cases) is in Fig. 17b;
 - (c) cases within 100% is shown in Fig. 17c.
 - (d) disastrous cases is shown in Fig. 17d. In such cases, the algorithm took at least 10 times as long as the fastest algorithm.



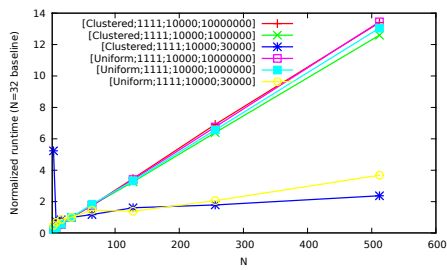
(a) Vary T , $N = 32$



(b) Vary N , $T = 3$



(c) Vary N , $T \approx N/2$



(d) Vary N , $T = N - 1$

Figure 14: Varying T and N on DSK, synthetic data (effect of varying N uses time relative to $N = 32$)

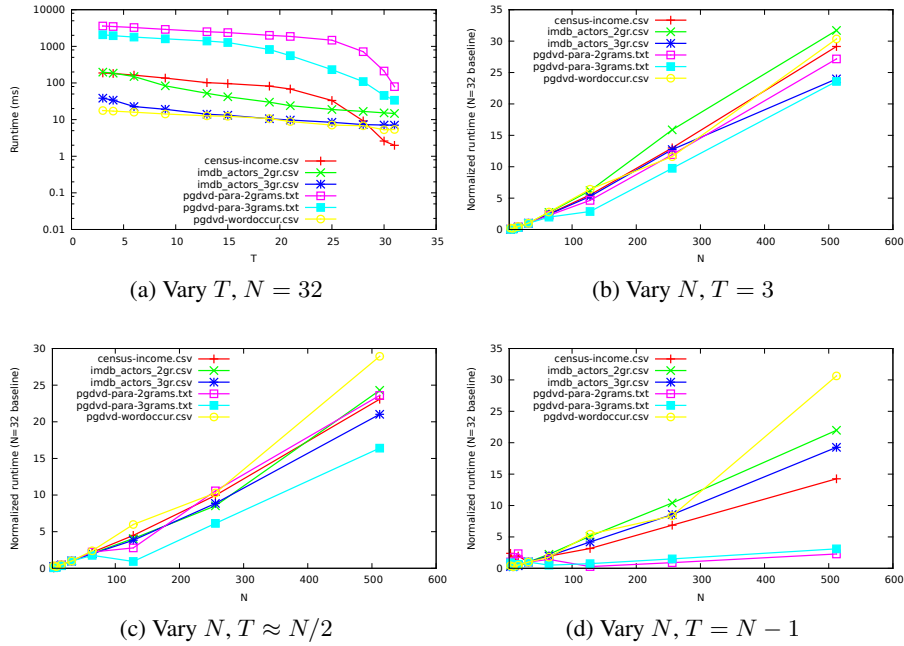


Figure 15: Varying T and N on DSK, real data (effect of varying N uses time relative to $N = 32$)

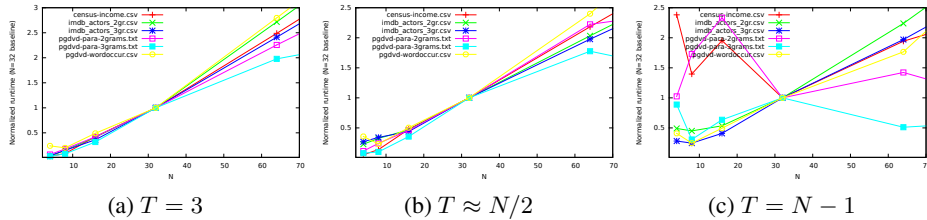
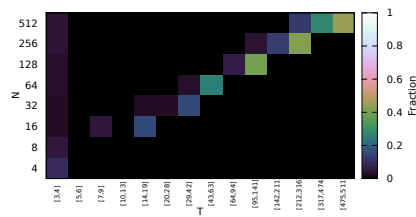
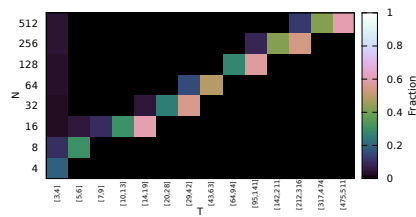


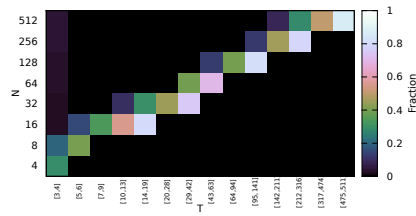
Figure 16: Effect of N (times relative to $N = 32$) for smaller values of N , on DSK



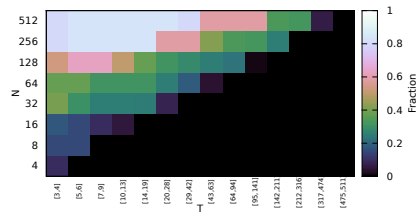
(a) Wins



(b) Good



(c) Fair



(d) Terrible

Figure 17: Heat map showing when to use and when to avoid DSk

Table 11: Values of μ recommended.

Dataset	1 row, $N = 16$	10 rows, $N = 128$	100 rows, $N = 512$
PGDVD	0.0343	0.0226	0.5820
CensusIncome	0.0432	0.0162	0.0144
IMDB-2gr	0.0508	0.0495	0.0536
IMDB-3gr	0.1170	0.0731	0.1390

The algorithms that use pruning (DSK, WMGSK, MGOPT) benefited greatly from large thresholds. Typical differences were between 1 and 2 orders of magnitude. However, the shape of the drop-off curve varied by dataset.

Synthetic data shows that the density of a dataset was important in determining how steep the drop-off curve from pruning is. (We see this both in Figs. 14a and 15d.) It seems that denser data led to more benefit from pruning.

When $T = N - 1$, we see a very complex behaviour on several real datasets that peaked early with N . PGDVD-2gr peaks at 16 and then became faster with larger N , until $N = 128$. Thereafter, its time very gradually increased with N .

DSK depends significantly on the choice of an appropriate parameter μ that controls L . The suggested approach from [25] was to determine this experimentally, for each dataset, using a collection of representative queries. We chose a single sample of size N as discussed above, then ran queries with a collection of different threshold values. The selected values of μ are shown in Table 11. Note that the best value for μ depends significantly on the threshold, and thus the values in the tables are thus compromises that may work poorly for many thresholds. For instance, when $N = 512$, $T = 369$, IMDB-3gr preferred $\mu = 0.00490$. Yet the approach in [25] would have us use $\mu = 0.139$ whenever $N = 512$, because many smaller thresholds preferred it.

We see a wide range of μ values. For experiments, we chose four representative values: $\mu \in \{0.005, 0.02, 0.05, 0.1\}$, labelling DSK with these choices as DSk.005, DSk.02, DSk.05 and DSk.1. We also report (as DSk) on the *best* result achieved by any of the 4 μ values, which is what is shown here. This gives the algorithm an unfair advantage, as we do not know how to obtain these results without multiple attempts using different values of μ . In our experience, the difference between a good and a poor choice of μ (within the range discussed above) is usually less than an order of magnitude.

The heat maps show that DSK was a good choice when T was close to N . However, when this was not the case, DivideSkip was frequently terrible.

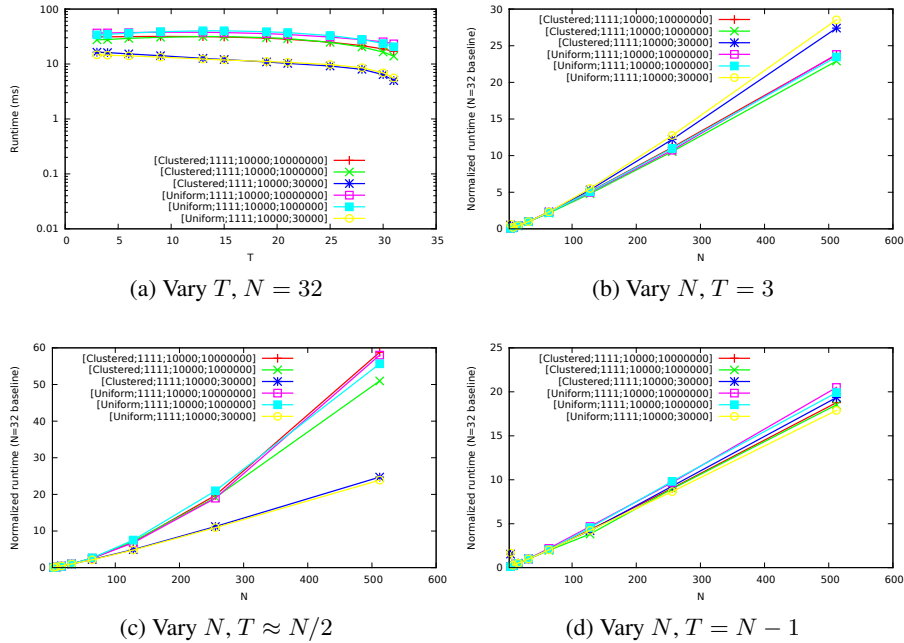


Figure 18: Varying T and N on MGOPT, synthetic data (effect of varying N uses time relative to $N = 32$)

5.8.4 Algorithm MGOPT

The effect of varying T on MGOPT are shown in Figs. 18a and 19a.

1. The effects of varying N are shown in Figs. 18b–18d and 19b–20c.
2. The percentage of
 - (a) cases where the algorithm achieved the fastest results is shown in Fig. 21a;
 - (b) cases where it was within 50% of the fastest result (including the fastest cases) is in Fig. 21b;
 - (c) cases within 100% is shown in Fig. 21c.
 - (d) disastrous cases is shown in Fig. 21d. In such cases, the algorithm took at least 10 times as long as the fastest algorithm.

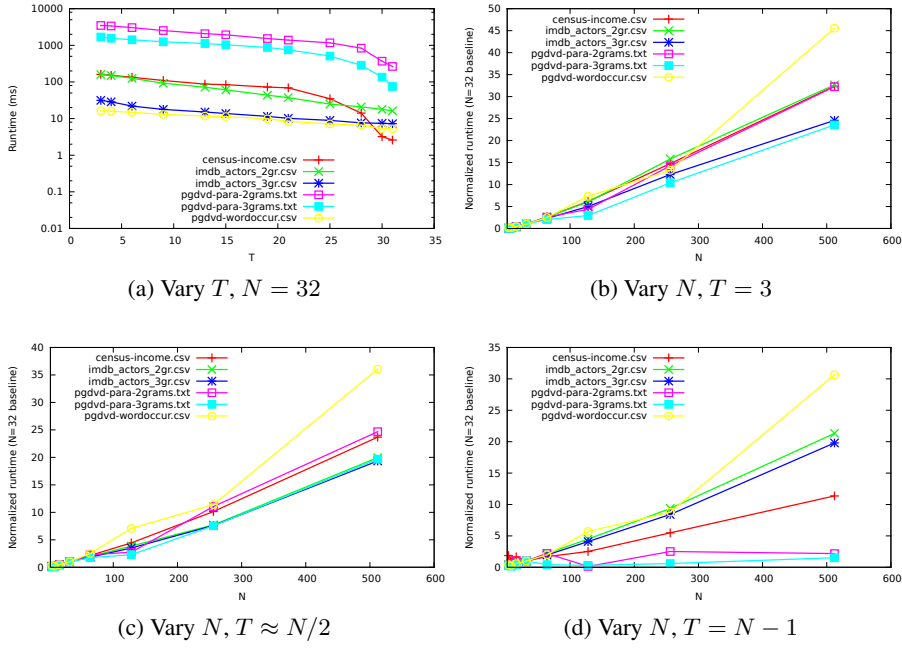


Figure 19: Varying T and N on MGOPT, real data (effect of varying N uses time relative to $N = 32$)

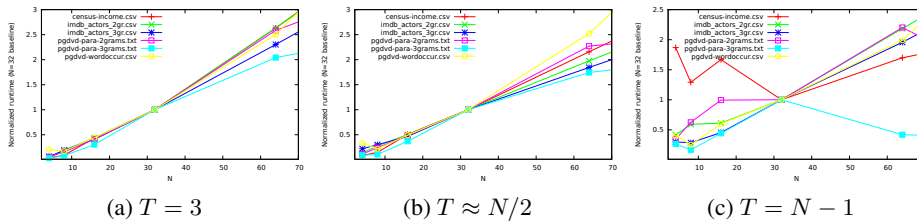
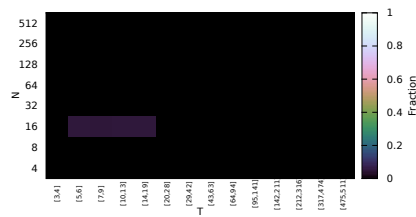
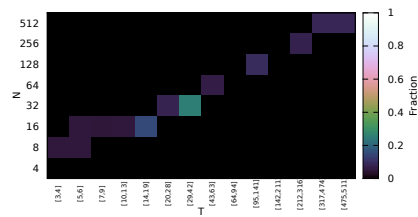


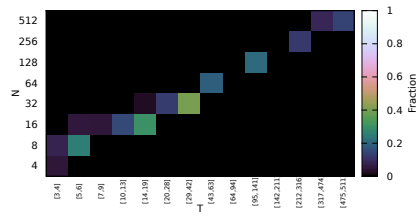
Figure 20: Effect of N (times relative to $N = 32$) for smaller values of N , on MgOpt



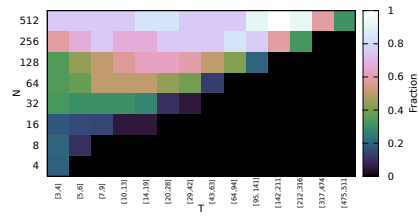
(a) Wins



(b) Good



(c) Fair



(d) Terrible

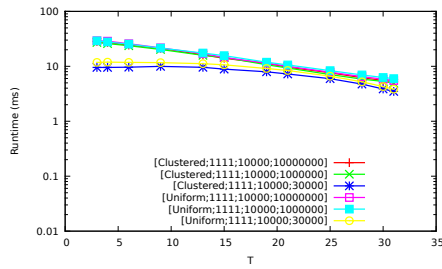
Figure 21: Heat map showing when to use and when to avoid MgOpt

MGOPT has performance similar to (but weaker than) DSK. It seems to have more trouble on non-dense synthetic data than DSK when $T \approx N/2$. On real data, with $T = N - 1$ it has many of the same behaviours as DSK.

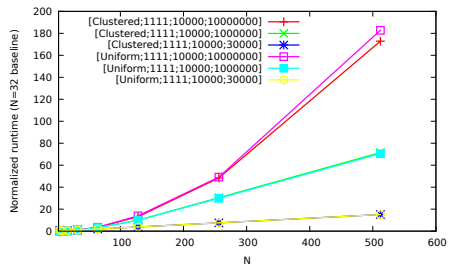
5.8.5 Algorithm w2CTI

The effect of varying T on w2CTI are shown in Figs. 22a and 23a.

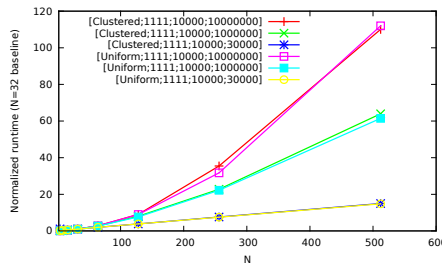
1. The effects of varying N are shown in Figs. 22b–22d and 23b–24c.
2. The percentage of
 - (a) cases where the algorithm achieved the fastest results is shown in Fig. 25a;
 - (b) cases where it was within 50% of the fastest result (including the fastest cases) is in Fig. 25b;
 - (c) cases within 100% is shown in Fig. 25c.
 - (d) disastrous cases is shown in Fig. 25d. In such cases, the algorithm took at least 10 times as long as the fastest algorithm.



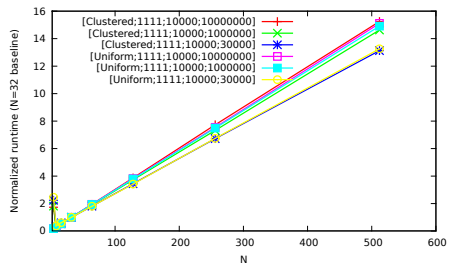
(a) Vary T , $N = 32$



(b) Vary N , $T = 3$



(c) Vary N , $T \approx N/2$



(d) Vary N , $T = N - 1$

Figure 22: Varying T and N on w2CTI, synthetic data (effect of varying N uses time relative to $N = 32$)

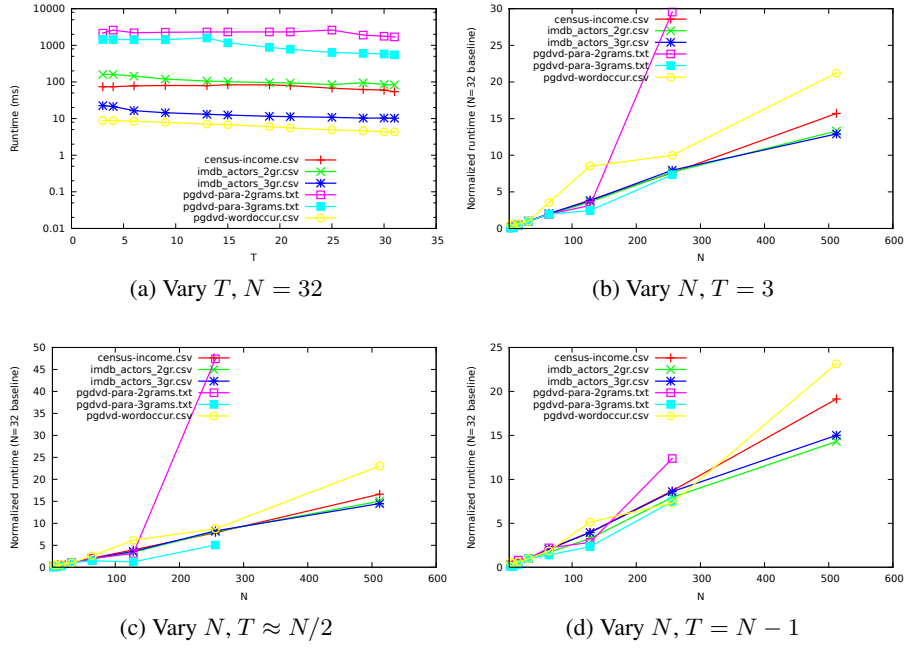


Figure 23: Varying T and N on w2CtI, real data (effect of varying N uses time relative to $N = 32$)

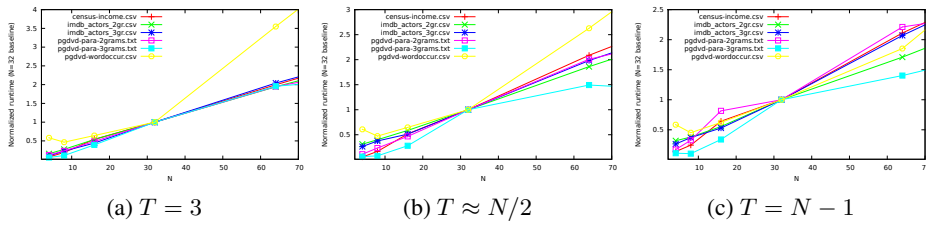
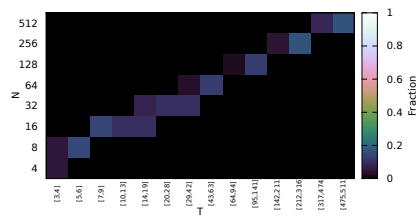
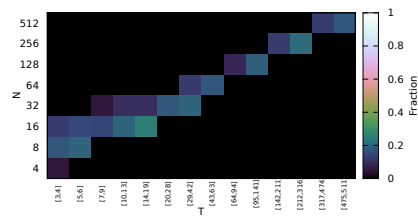


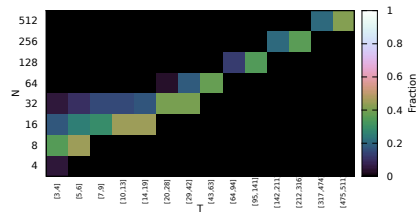
Figure 24: Effect of N (times relative to $N = 32$) for smaller values of N , on w2CtI



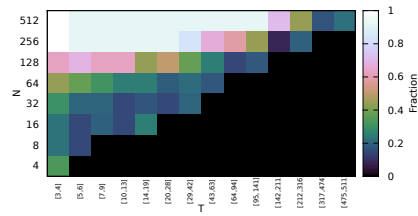
(a) Wins



(b) Good



(c) Fair



(d) Terrible

Figure 25: Heat map showing when to use and when to avoid w2CtI

Algorithm w2CTI appears to have had superlinear (in N) running time on synthetic data. Recall that its worst-case running time is $\Theta(BN)$ and that B , on average, increases linearly with N . Thus it might not be surprising to see super-linear increases. We also see that this algorithm was fastest for dense data. With such data, there is a good chance for items to have occurred in both lists being merged, resulting in a smaller output and less data being processed in future merges. Similar effects were observed (but are not shown) for w2CTA or w2CTN which do less (or no) pruning.

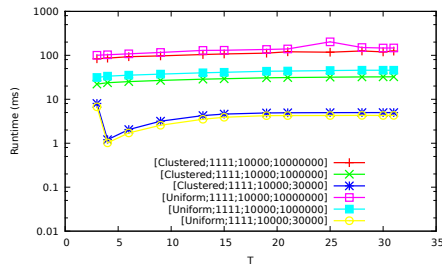
All ‘w’ implementations suffered from memory problems that affected their performance when N was large, for some of the larger datasets. In particular, on PGDVD-2gr, the computation for w2CTI took excessive time for $N = 256$ and failed for $N = 512$.

On real data, w2CTI heat maps show that this was a very poor algorithm for large N and small T . It did have some wins and some good behaviour when $T \approx N$.

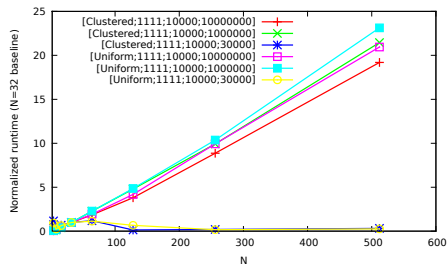
5.8.6 Algorithm LOOPED

The effect of varying T on LOOPED are shown in Figs. 26a and 27a.

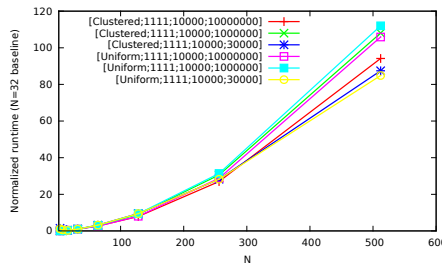
1. The effects of varying N are shown in Figs. 26b–26d and 27b–28c.
2. The percentage of
 - (a) cases where the algorithm achieved the fastest results is shown in Fig. 29a;
 - (b) cases where it was within 50% of the fastest result (including the fastest cases) is in Fig. 29b;
 - (c) cases within 100% is shown in Fig. 29c.
 - (d) disastrous cases is shown in Fig. 29d. In such cases, the algorithm took at least 10 times as long as the fastest algorithm.



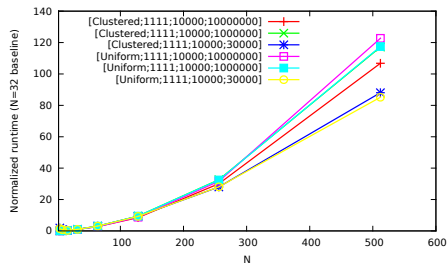
(a) Vary T , $N = 32$



(b) Vary N , $T = 3$



(c) Vary N , $T \approx N/2$



(d) Vary N , $T = N - 1$

Figure 26: Varying T and N on LOOPED, synthetic data (effect of varying N uses time relative to $N = 32$)

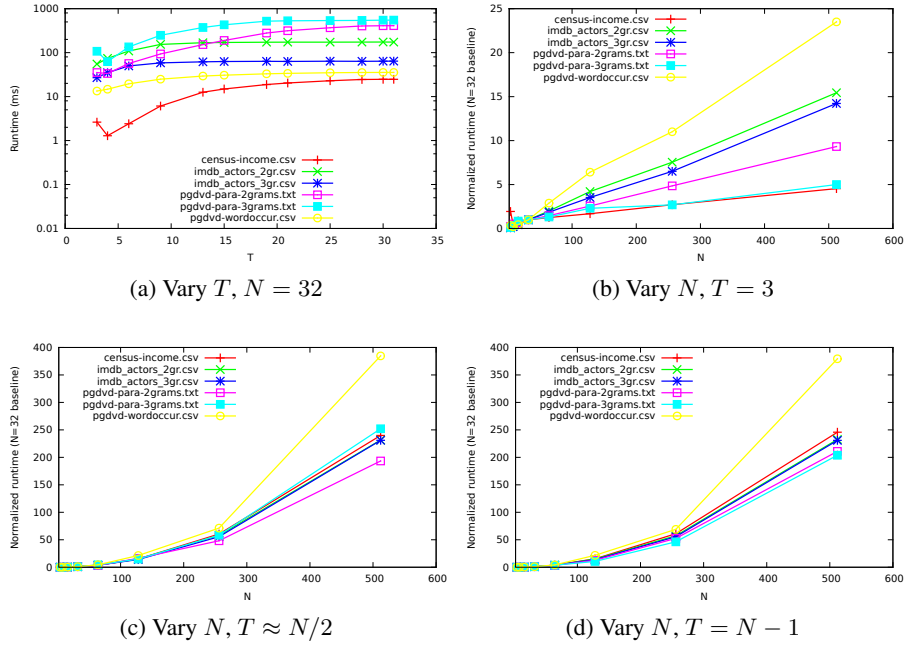


Figure 27: Varying T and N on LOOPED, real data (effect of varying N uses time relative to $N = 32$)

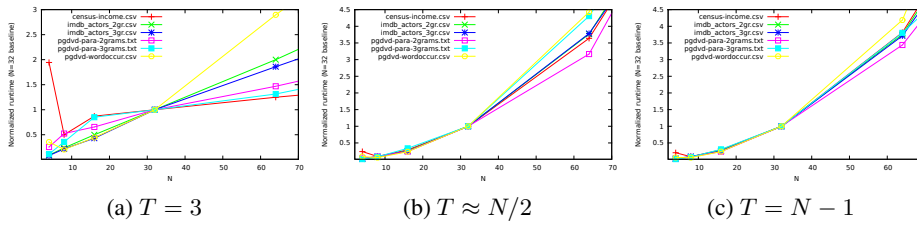
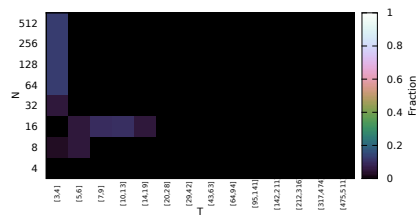
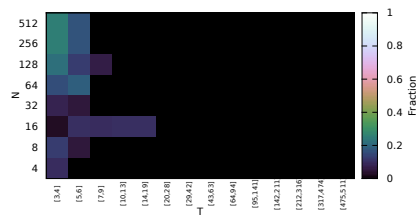


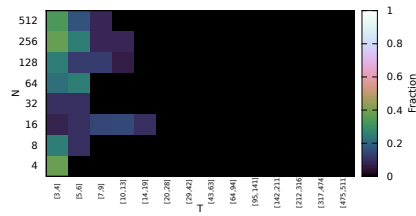
Figure 28: Effect of N (times relative to $N = 32$) for smaller values of N , on Looped



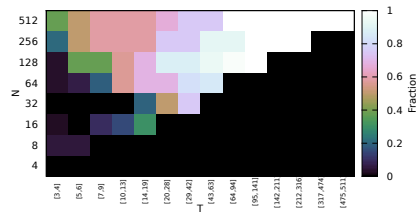
(a) Wins



(b) Good



(c) Fair



(d) Terrible

Figure 29: Heat map showing when to use and when to avoid Looped

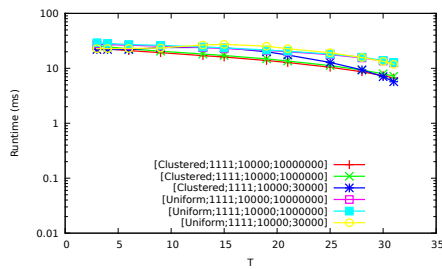
As expected, LOOPED usually became worse with T , although the effect was much more pronounced on real data. The large dip from $T = 3$ to $T = 4$ on the dense synthetic data is unexplained. The algorithm for LOOPED does the operations for $T = 3$ in the course of computing $T = 4$. We see the same surprising effect on real data, for CensusIncome. When N is varied with $T = 3$ we again see unusual behaviour for the dense synthetic data. This may be due to the efficiency with which JavaEWAH can OR bitmaps that have long runs of ones. Otherwise, for synthetic data we see curves that make sense, given our $O(NT)$ analysis.

Heatmaps confirm that the approach, which does not win particularly often, does so for smaller values of T , even with larger N . It is almost always terrible when both N and T are large.

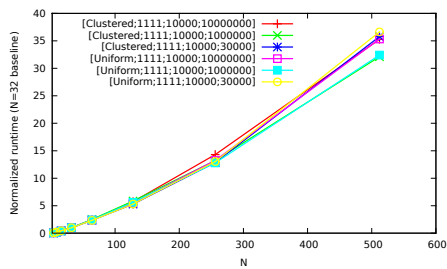
5.8.7 Algorithm wMergeSkip

The effect of varying T on wMergeSkip are shown in Figs. 30a and 31a.

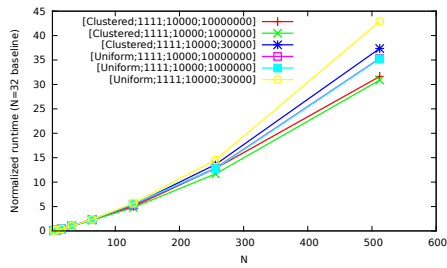
1. The effects of varying N are shown in Figs. 30b–30d and 31b–32c.
2. The percentage of
 - (a) cases where the algorithm achieved the fastest results is shown in Fig. 33a;
 - (b) cases where it was within 50% of the fastest result (including the fastest cases) is in Fig. 33b;
 - (c) cases within 100% is shown in Fig. 33c.
 - (d) disastrous cases is shown in Fig. 33d. In such cases, the algorithm took at least 10 times as long as the fastest algorithm.



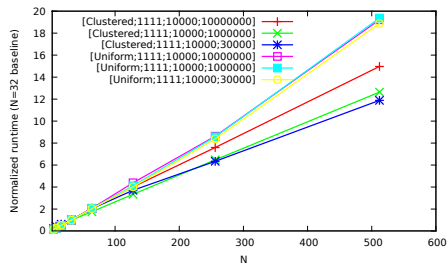
(a) Vary T , $N = 32$



(b) Vary N , $T = 3$



(c) Vary N , $T \approx N/2$



(d) Vary N , $T = N - 1$

Figure 30: Varying T and N on wMergeSkip, synthetic data (effect of varying N uses time relative to $N = 32$)

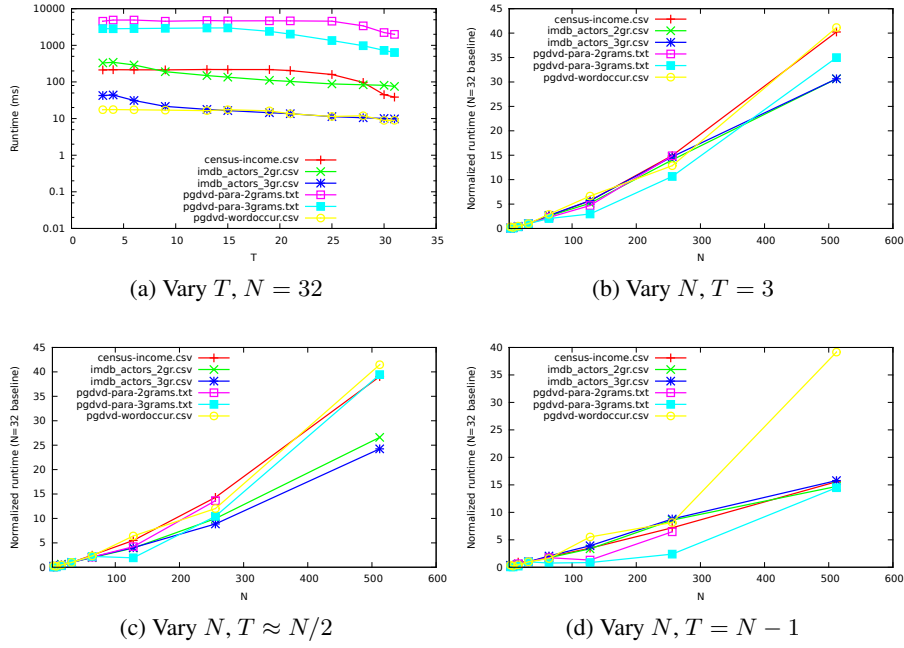


Figure 31: Varying T and N on wMergeSkip, real data (effect of varying N uses time relative to $N = 32$)

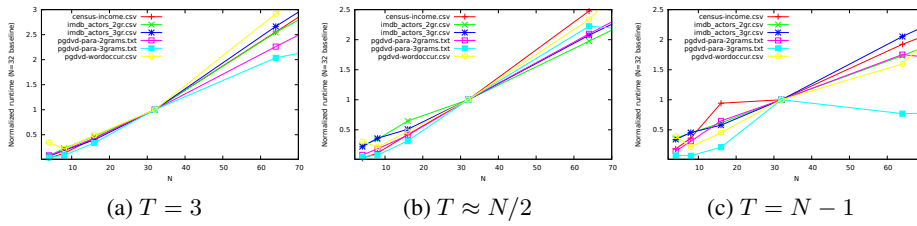
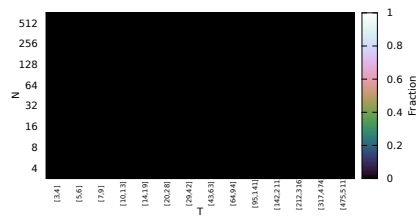
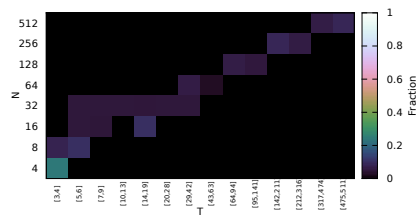


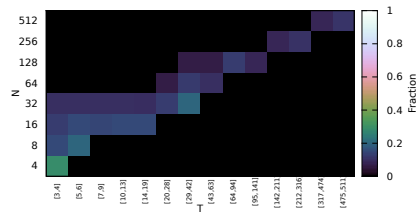
Figure 32: Effect of N (times relative to $N = 32$) for smaller values of N , on wMgSk



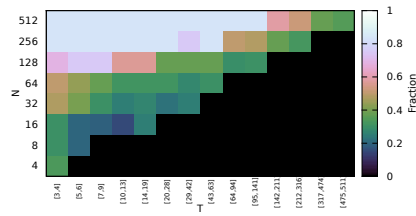
(a) Wins



(b) Good



(c) Fair



(d) Terrible

Figure 33: Heat map showing when to use and when to avoid wMgSk

The ‘w’ version of MergeSkip is outperformed by the ‘w’ version of DivideSkip (which is in turn outperformed by the bitmap version of DivideSkip). On synthetic and real data, we see that larger T values improve time: pruning is working.

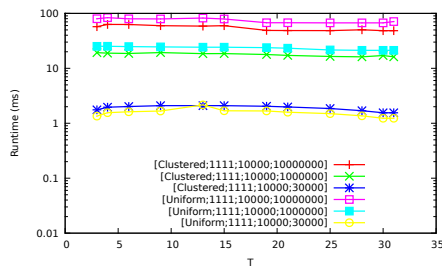
On real data, we see the memory problems faced by many ‘w’ implementations: for several datasets, $N = 512$ results could not be obtained.

Examining heatmaps, we see the algorithm was never best. Again, its (limited) strength is along the $T \approx N$ diagonal and it is frequently terrible.

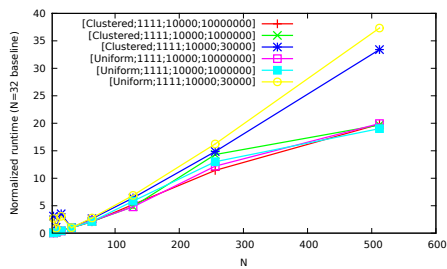
5.8.8 Algorithm SRTCKT

The effect of varying T on SRTCKT are shown in Figs. 34a and 35a.

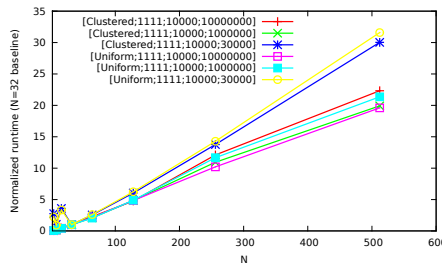
1. The effects of varying N are shown in Figs. 34b–34d and 35b–36c.
2. The percentage of
 - (a) cases where the algorithm achieved the fastest results is shown in Fig. 37a;
 - (b) cases where it was within 50% of the fastest result (including the fastest cases) is in Fig. 37b;
 - (c) cases within 100% is shown in Fig. 37c.
 - (d) disastrous cases is shown in Fig. 37d. In such cases, the algorithm took at least 10 times as long as the fastest algorithm.



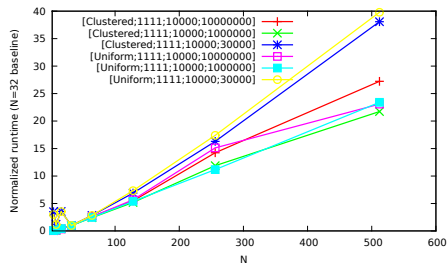
(a) Vary T , $N = 32$



(b) Vary N , $T = 3$

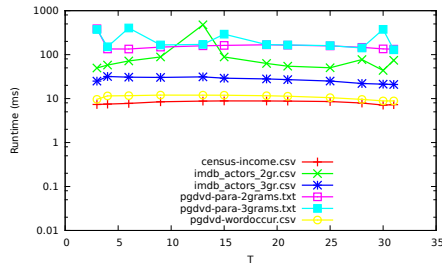


(c) Vary N , $T \approx N/2$

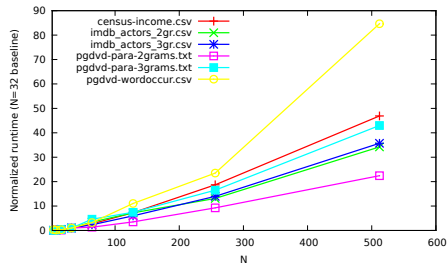


(d) Vary N , $T = N - 1$

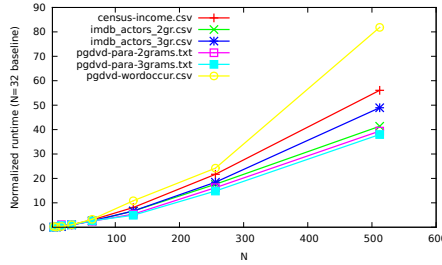
Figure 34: Varying T and N on SRTCKT, synthetic data (effect of varying N uses time relative to $N = 32$)



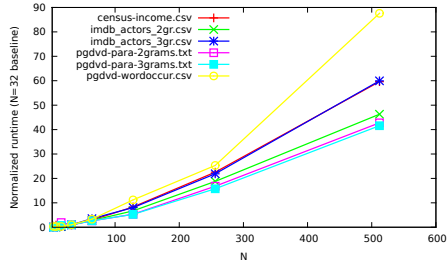
(a) Vary T , $N = 32$



(b) Vary N , $T = 3$

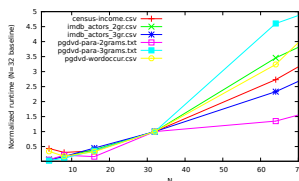


(c) Vary N , $T \approx N/2$

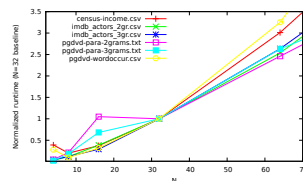


(d) Vary N , $T = N - 1$

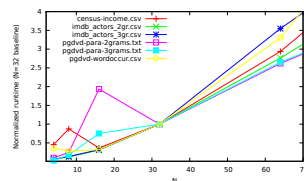
Figure 35: Varying T and N on SRTCKT, real data (effect of varying N uses time relative to $N = 32$)



(a) $T = 3$

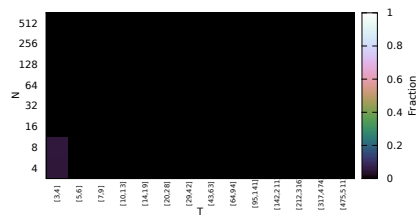


(b) $T \approx N/2$

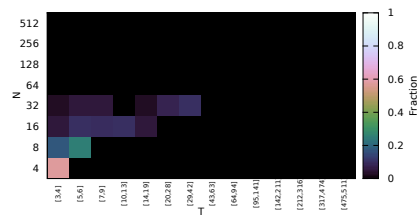


(c) $T = N - 1$

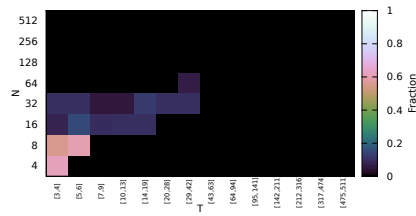
Figure 36: Effect of N (times relative to $N = 32$) for smaller values of N , on SrtCkt



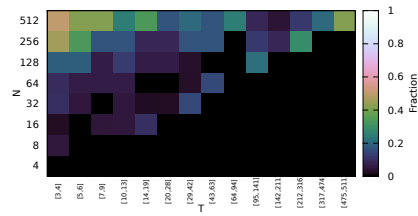
(a) Wins



(b) Good



(c) Fair



(d) Terrible

Figure 37: Heat map showing when to use and when to avoid SrtCkt

On synthetic data, `SRTCKT` is not much affected by T , but it prefers dense data. Such bitmaps compress better and there is more opportunity for bit-level parallelism than with extremely sparse data. For dense synthetic data, there is an initial peak when N varies, similar to `SCANCOUNT`.

On some real datasets, varying T makes a significant difference without an obvious trend. Since the circuits differ according to T , this may not be too surprising. However, the same circuit behaves differently for different datasets.

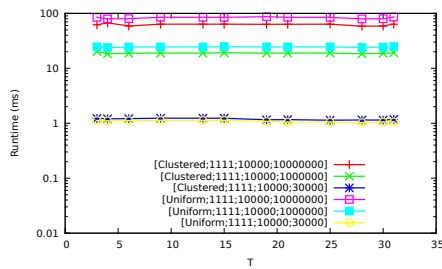
On real datasets, increasing N appears to lead to superlinear time increases. We may be seeing the extra $\log^2 N$ factor, or the slowdown may be due to memory use (`SRTCKT` seems to require more space for its temporary results than the adder circuits).

`SRTCKT` is strongest when both N and T are small. It becomes increasingly terrible with N and is frequently terrible when $N = 512$, but is rarely terrible when $N \leq 32$.

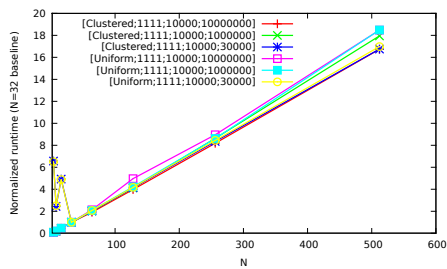
5.8.9 Algorithm `TREEADD`

The effect of varying T on `TREEADD` are shown in Figs. 38a and 39a.

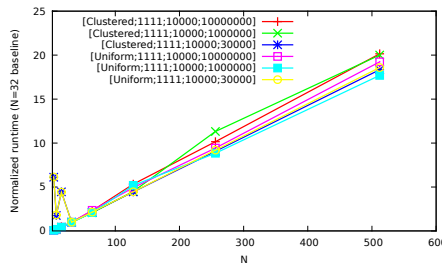
1. The effects of varying N are shown in Figs. 38b–38d and 39b–40c.
2. The percentage of
 - (a) cases where the algorithm achieved the fastest results is shown in Fig. 41a;
 - (b) cases where it was within 50% of the fastest result (including the fastest cases) is in Fig. 41b;
 - (c) cases within 100% is shown in Fig. 41c.
 - (d) disastrous cases is shown in Fig. 41d. In such cases, the algorithm took at least 10 times as long as the fastest algorithm.



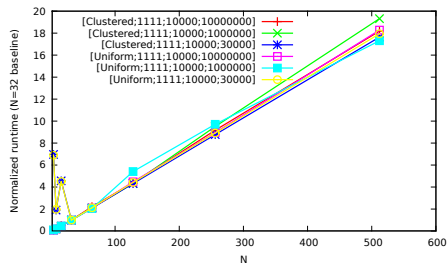
(a) Vary T , $N = 32$



(b) Vary N , $T = 3$

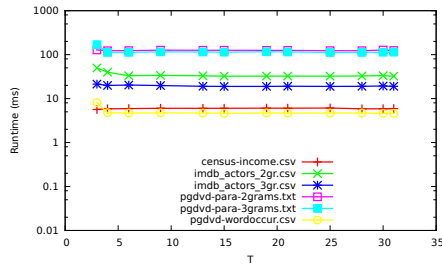


(c) Vary N , $T \approx N/2$

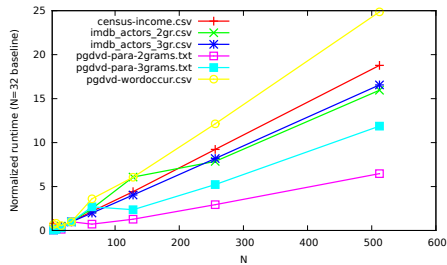


(d) Vary N , $T = N - 1$

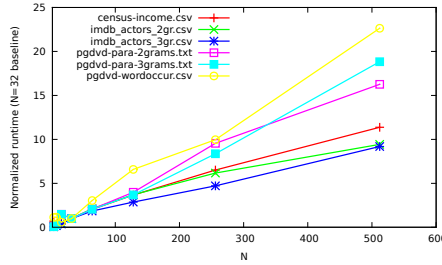
Figure 38: Varying T and N on TREEADD, synthetic data (effect of varying N uses time relative to $N = 32$)



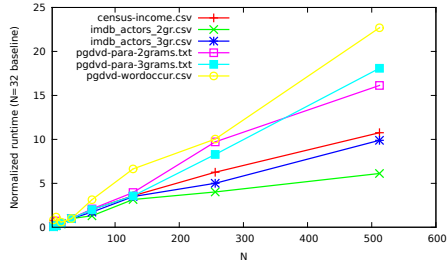
(a) Vary T , $N = 32$



(b) Vary N , $T = 3$

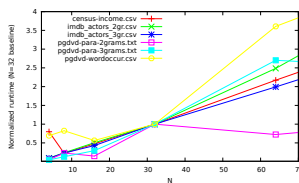


(c) Vary N , $T \approx N/2$

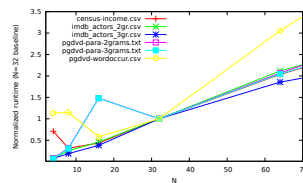


(d) Vary N , $T = N - 1$

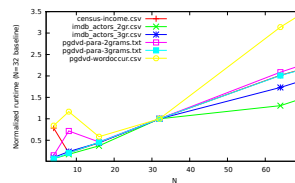
Figure 39: Varying T and N on TREEADD, real data (effect of varying N uses time relative to $N = 32$)



(a) $T = 3$

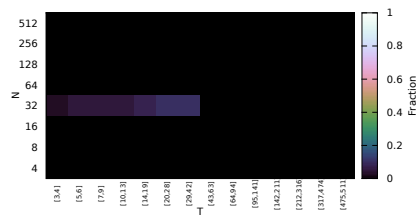


(b) $T \approx N/2$

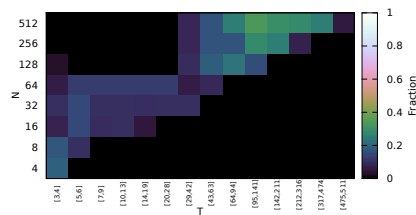


(c) $T = N - 1$

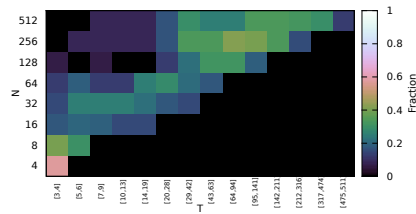
Figure 40: Effect of N (times relative to $N = 32$) for smaller values of N , on TreeAdd



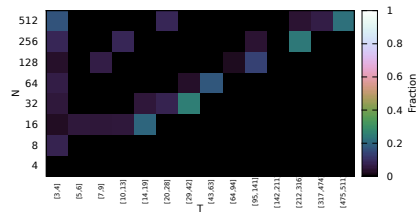
(a) Wins



(b) Good



(c) Fair



(d) Terrible

Figure 41: Heat map showing when to use and when to avoid TreeAdd

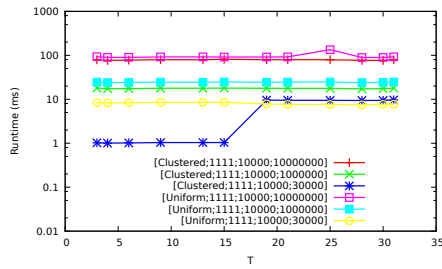
On synthetic data, TREEADD preferred dense data, but its scaling was very little affected by density. It had erratic behaviour for the three smallest values of N (4, 8 and 16) on dense synthetic data, and real data shows similarly erratic behaviour for small N .

This circuit is a good choice when N and T are both small. It is infrequently terrible; when it is, the situation is that the pruning-based algorithms have become especially strong. TREEADD has not really degraded.

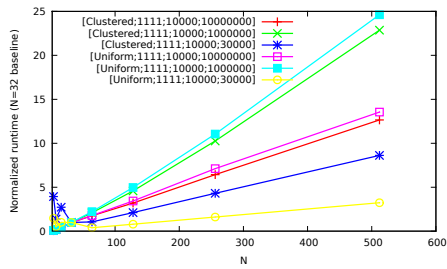
5.8.10 Algorithm SSUM

The effect of varying T on SSUM are shown in Figs. 42a and 43a.

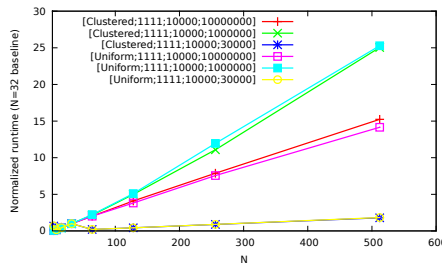
1. The effects of varying N are shown in Figs. 42b–42d and 43b–44c.
2. The percentage of
 - (a) cases where the algorithm achieved the fastest results is shown in Fig. 45a;
 - (b) cases where it was within 50% of the fastest result (including the fastest cases) is in Fig. 45b;
 - (c) cases within 100% is shown in Fig. 45c.
 - (d) disastrous cases is shown in Fig. 45d. In such cases, the algorithm took at least 10 times as long as the fastest algorithm.



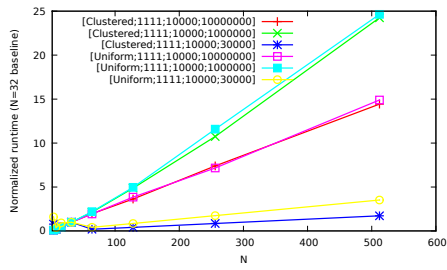
(a) Vary T , $N = 32$



(b) Vary N , $T = 3$



(c) Vary N , $T \approx N/2$



(d) Vary N , $T = N - 1$

Figure 42: Varying T and N on SSUM, synthetic data (effect of varying N uses time relative to $N = 32$)

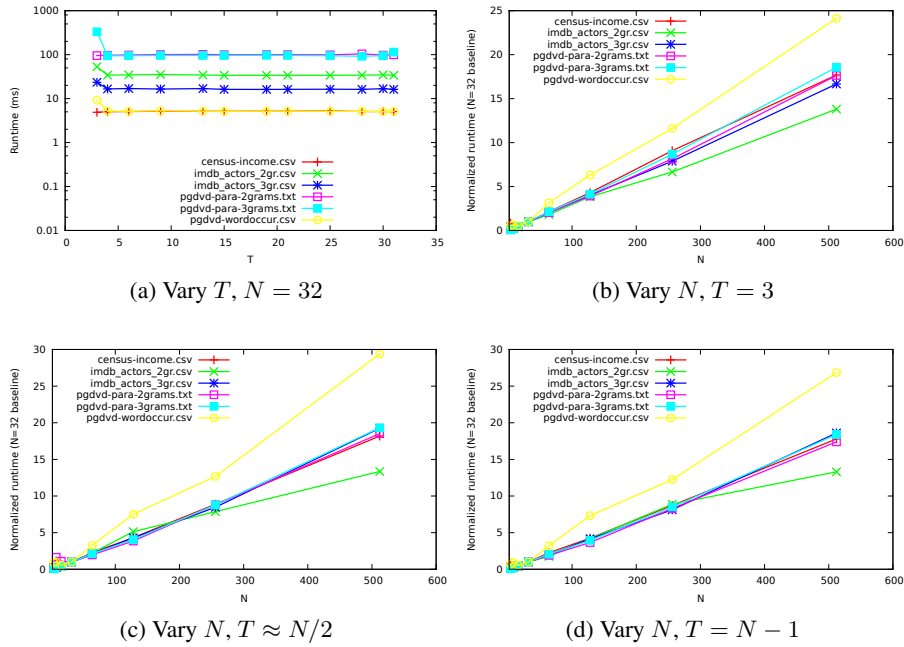


Figure 43: Varying T and N on SSUM, real data (effect of varying N uses time relative to $N = 32$)

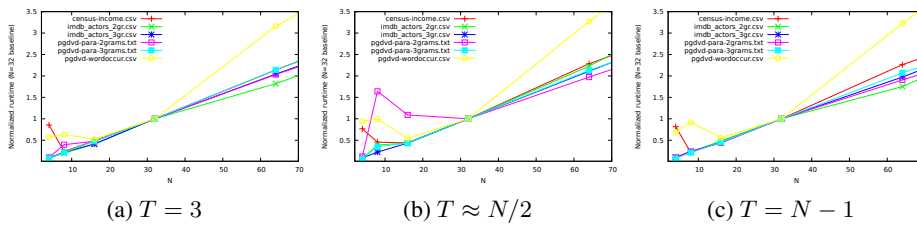
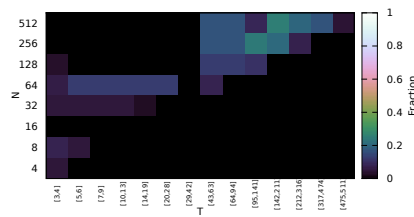
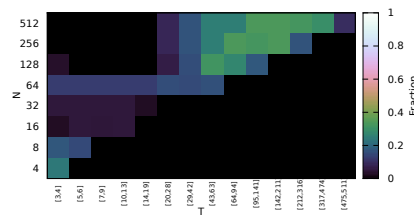


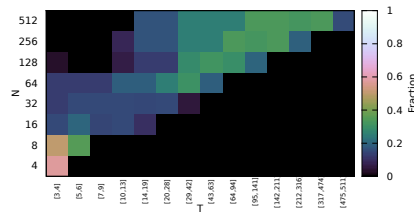
Figure 44: Effect of N (times relative to $N = 32$) for smaller values of N , on SSUM



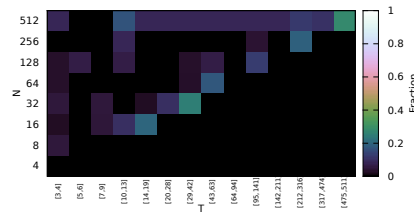
(a) Wins



(b) Good



(c) Fair



(d) Terrible

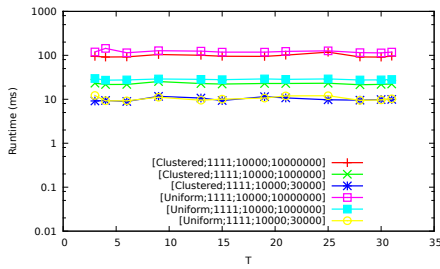
Figure 45: Heat map showing when to use and when to avoid SSum

The sideways-sum circuit behaved much differently for dense synthetic data than did TREEADD. The odd behaviour for clustered dense data, as T varies, is unexplained. There seems to be no similar behaviour on our real data, however. The heatmaps show that it won many competitions across a wide range of T and N , and was at least frequently fair (except when N was large and T was small, when LOOPED often made it look worse than fair). Terrible cases were limited (but more frequent when $N = 512$) and appeared mostly on the diagonal, where pruning algorithms could sometimes make it look bad.

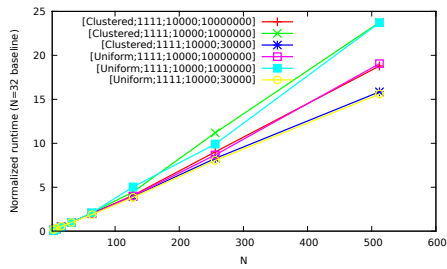
5.8.11 Algorithm CSVCKT

The effect of varying T on CSVCKT are shown in Figs. 46a and 47a.

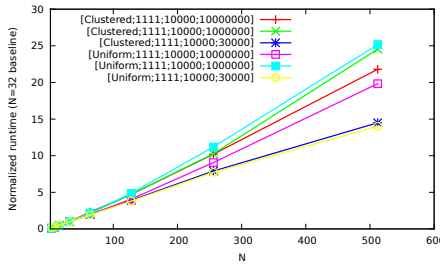
1. The effects of varying N are shown in Figs. 46b–46d and 47b–48c.
2. The percentage of
 - (a) cases where the algorithm achieved the fastest results is shown in Fig. 49a;
 - (b) cases where it was within 50% of the fastest result (including the fastest cases) is in Fig. 49b;
 - (c) cases within 100% is shown in Fig. 49c.
 - (d) disastrous cases is shown in Fig. 49d. In such cases, the algorithm took at least 10 times as long as the fastest algorithm.



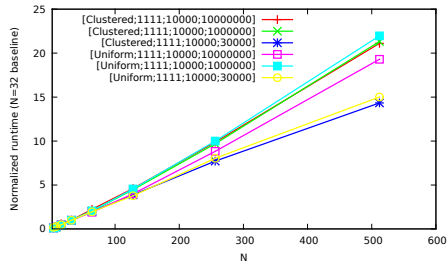
(a) Vary T , $N = 32$



(b) Vary N , $T = 3$



(c) Vary N , $T \approx N/2$



(d) Vary N , $T = N - 1$

Figure 46: Varying T and N on CSVCKT, synthetic data (effect of varying N uses time relative to $N = 32$)

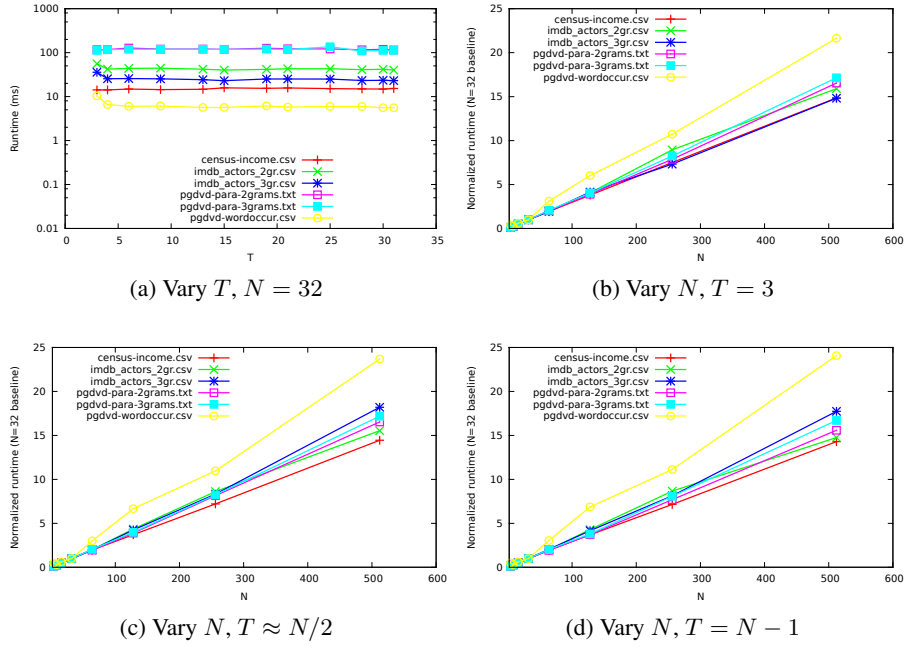


Figure 47: Varying T and N on CSVCKT, real data (effect of varying N uses time relative to $N = 32$)

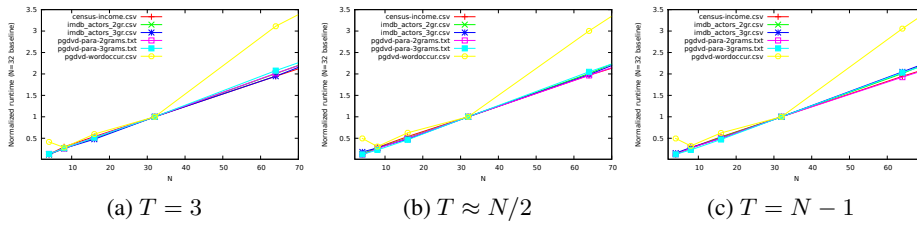
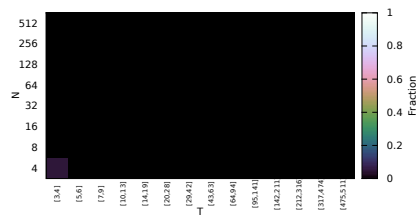
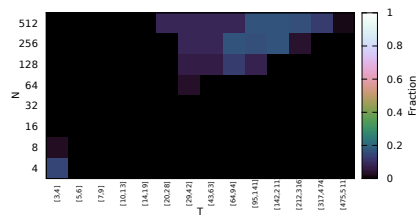


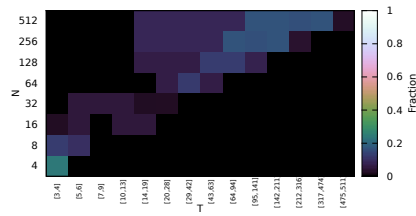
Figure 48: Effect of N (times relative to $N = 32$) for smaller values of N , on CSVCKT



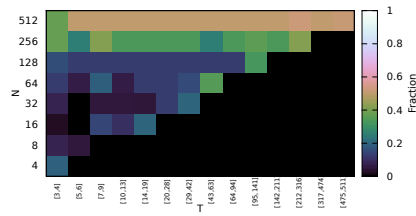
(a) Wins



(b) Good



(c) Fair



(d) Terrible

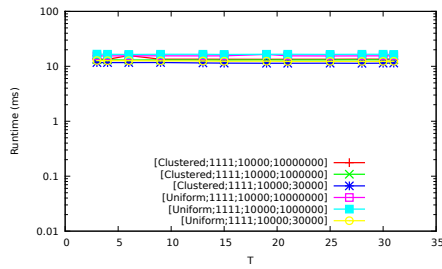
Figure 49: Heat map showing when to use and when to avoid CSvCkt

The carry-save adder approach was not much affected by T or by whether the synthetic data was uniform or clustered. It was somewhat slower than the other adder approaches and therefore had fewer wins. It was more frequently terrible (but in similar situations) when compared to the other adders.

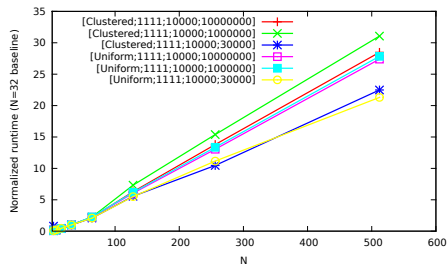
5.8.12 Algorithm wSORT

The effect of varying T on wSORT are shown in Figs. 50a and 51a.

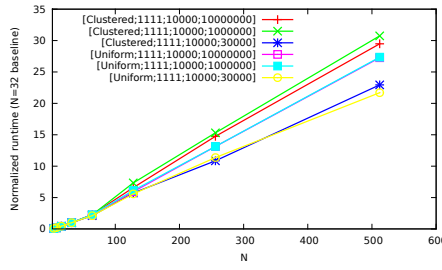
1. The effects of varying N are shown in Figs. 50b–50d and 51b–52c.
2. The percentage of
 - (a) cases where the algorithm achieved the fastest results is shown in Fig. 53a;
 - (b) cases where it was within 50% of the fastest result (including the fastest cases) is in Fig. 53b;
 - (c) cases within 100% is shown in Fig. 53c.
 - (d) disastrous cases is shown in Fig. 53d. In such cases, the algorithm took at least 10 times as long as the fastest algorithm.



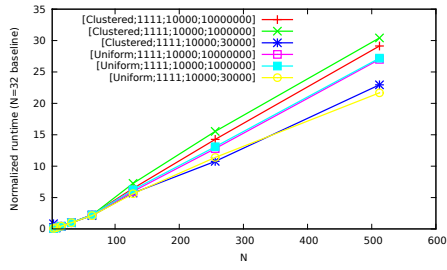
(a) Vary T , $N = 32$



(b) Vary N , $T = 3$



(c) Vary N , $T \approx N/2$



(d) Vary N , $T = N - 1$

Figure 50: Varying T and N on WSORT, synthetic data (effect of varying N uses time relative to $N = 32$)

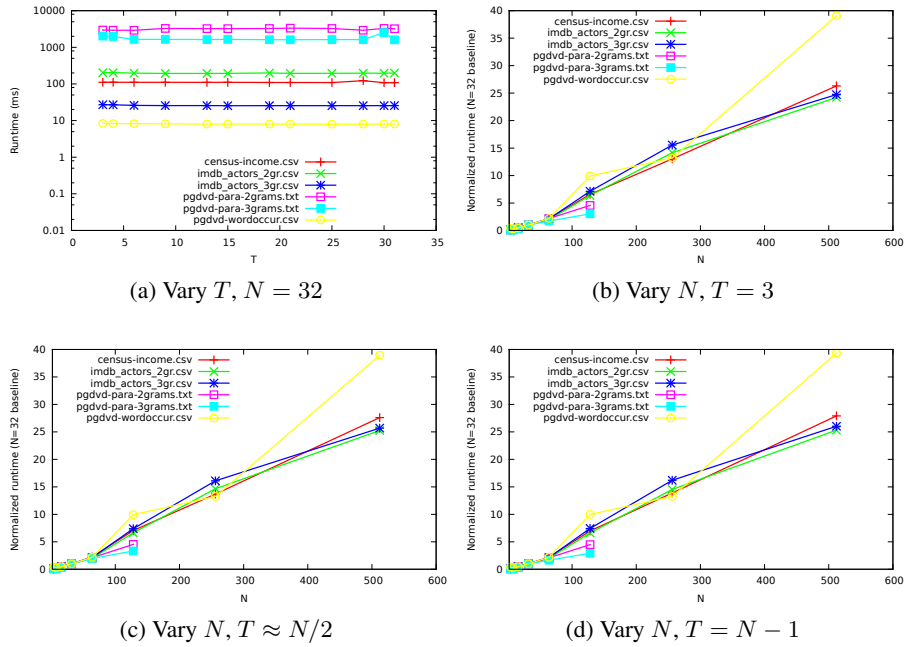


Figure 51: Varying T and N on wSORT, real data (effect of varying N uses time relative to $N = 32$)

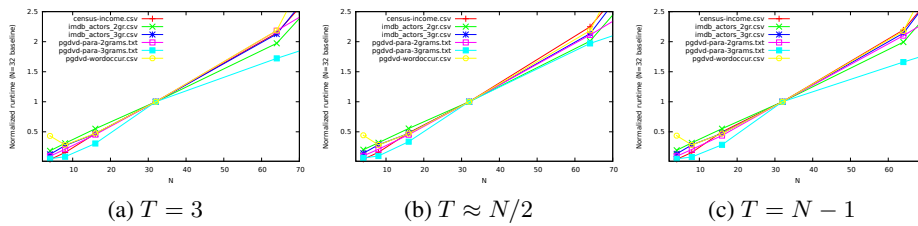
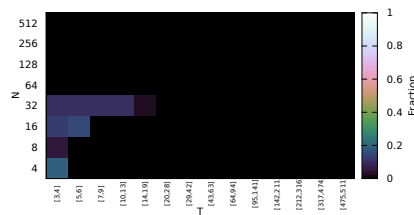
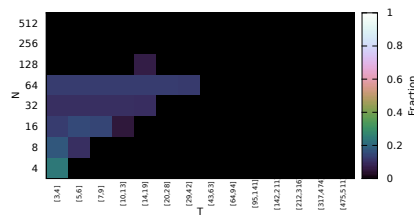


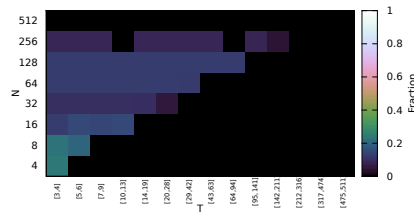
Figure 52: Effect of N (times relative to $N = 32$) for smaller values of N , on wSort



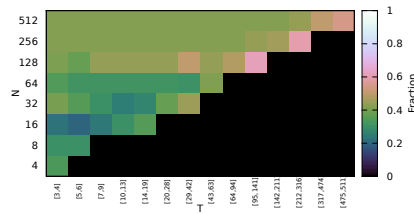
(a) Wins



(b) Good



(c) Fair



(d) Terrible

Figure 53: Heat map showing when to use and when to avoid wSort

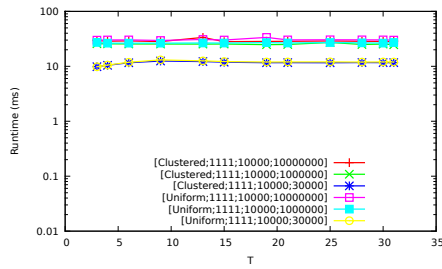
Algorithm wSORT is not much affected by density, for synthetic data. This makes sense. The behaviour is very consistent as N is increased. Since we use T only after most of the work (sorting) has been done, we should not be surprised to see that T has fairly little effect.

Despite being a ‘w’ algorithm, it won a few cases for smaller N . However, this algorithm lead to more memory-exhaustion failures than any other, as PGDVD-3gr and PGDVD-2gr are not successful for $N \geq 256$.

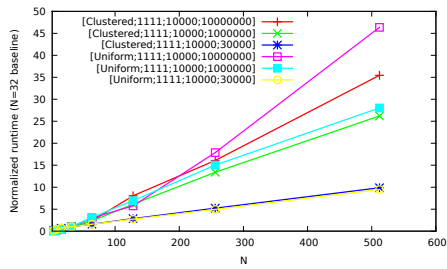
5.8.13 Algorithm HASHCNT

The effect of varying T on HASHCNT are shown in Figs. 54a and 55a.

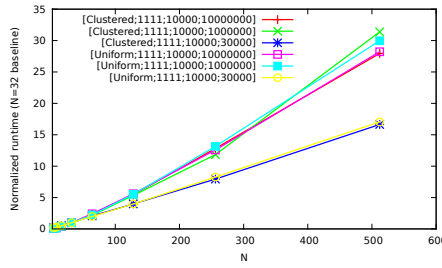
1. The effects of varying N are shown in Figs. 54b–54d and 55b–56c.
2. The percentage of
 - (a) cases where the algorithm achieved the fastest results is shown in Fig. 57a;
 - (b) cases where it was within 50% of the fastest result (including the fastest cases) is in Fig. 57b;
 - (c) cases within 100% is shown in Fig. 57c.
 - (d) disastrous cases is shown in Fig. 57d. In such cases, the algorithm took at least 10 times as long as the fastest algorithm.



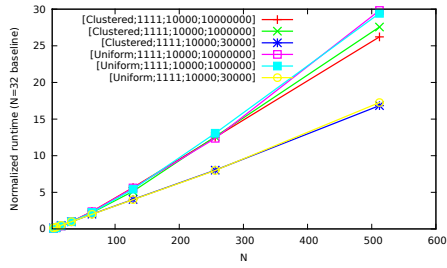
(a) Vary T , $N = 32$



(b) Vary N , $T = 3$



(c) Vary N , $T \approx N/2$



(d) Vary N , $T = N - 1$

Figure 54: Varying T and N on HASHCNT, synthetic data (effect of varying N uses time relative to $N = 32$)

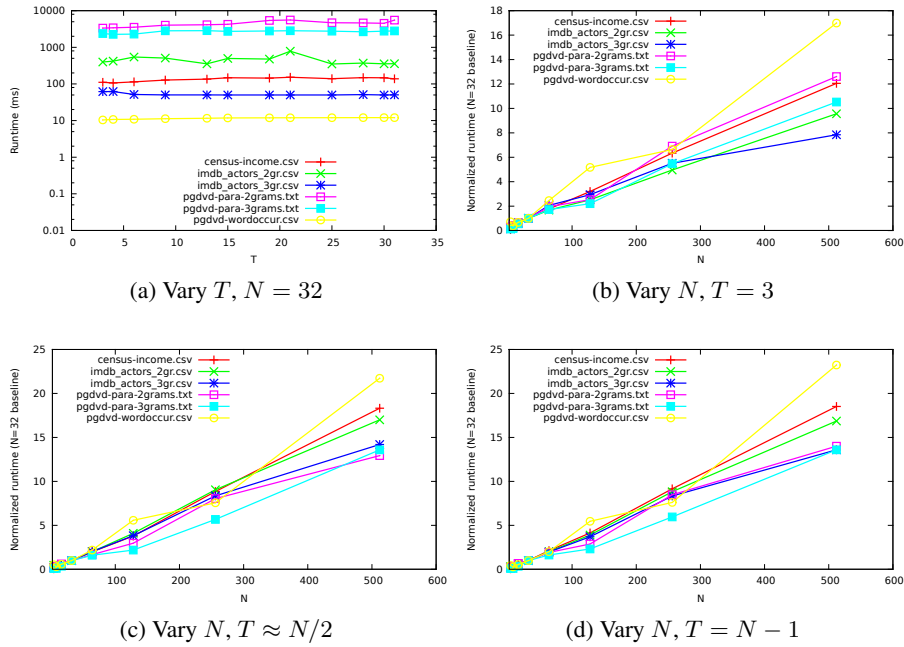


Figure 55: Varying T and N on HASHCNT, real data (effect of varying N uses time relative to $N = 32$)

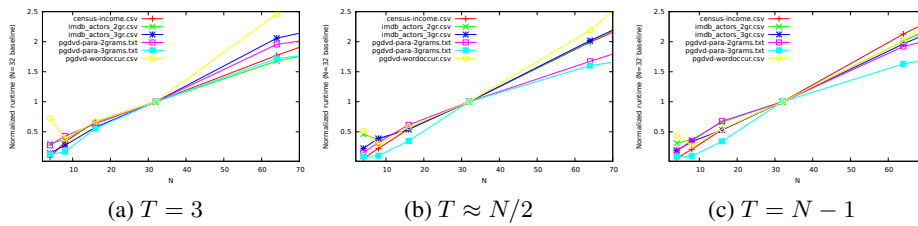
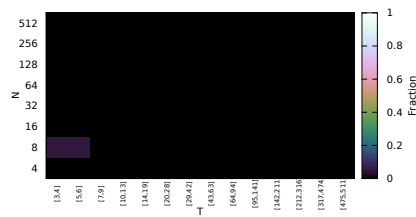
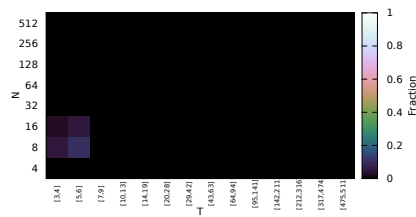


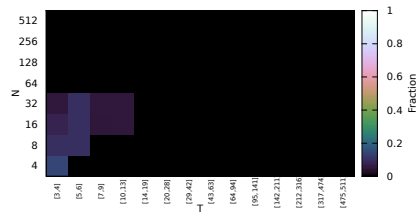
Figure 56: Effect of N (times relative to $N = 32$) for smaller values of N , on HashCnt



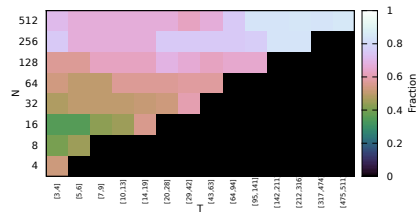
(a) Wins



(b) Good



(c) Fair



(d) Terrible

Figure 57: Heat map showing when to use and when to avoid HashCnt

On synthetic data, HASHCNT preferred dense data. Fewer distinct counters needed to be maintained, and thus the required hash table was smaller, leading to cache benefits.

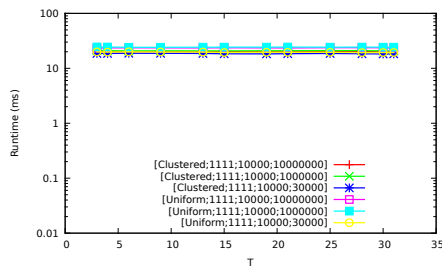
The HASHCNT approach was usually terrible. This is somewhat surprising, considering how strong SCANCOUNT was. If the range of items was too big for SCANCOUNT, a typical programmer would consider this route instead.

To see why this approach might be so ineffective, we have to compare the costs of hashing the counter number to the cost of indexing into an array. Also, the `HashMap` implementation will require boxing and unboxing integer values, although that can be avoided with more specialized int-to-int hash libraries. Worse, the hashing process means that the efficient ascending scan through counter numbers will turn into irregular accesses through the heap, even with the more specialized libraries. Finally, constructing the compressed bitmap index requires iterating over the keys in sorted order. Sorting them is expensive.

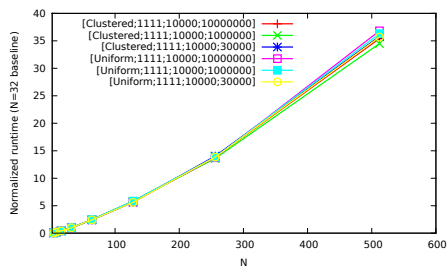
5.8.14 Algorithm WHEAP

The effect of varying T on WHEAP are shown in Figs. 58a and 59a.

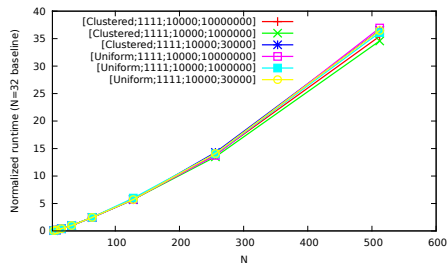
1. The effects of varying N are shown in Figs. 58b–58d and 59b–60c.
2. The percentage of
 - (a) cases where the algorithm achieved the fastest results is shown in Fig. 61a;
 - (b) cases where it was within 50% of the fastest result (including the fastest cases) is in Fig. 61b;
 - (c) cases within 100% is shown in Fig. 61c.
 - (d) disastrous cases is shown in Fig. 61d. In such cases, the algorithm took at least 10 times as long as the fastest algorithm.



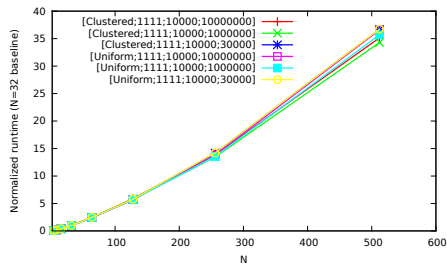
(a) Vary T , $N = 32$



(b) Vary N , $T = 3$



(c) Vary N , $T \approx N/2$



(d) Vary N , $T = N - 1$

Figure 58: Varying T and N on WHEAP, synthetic data (effect of varying N uses time relative to $N = 32$)

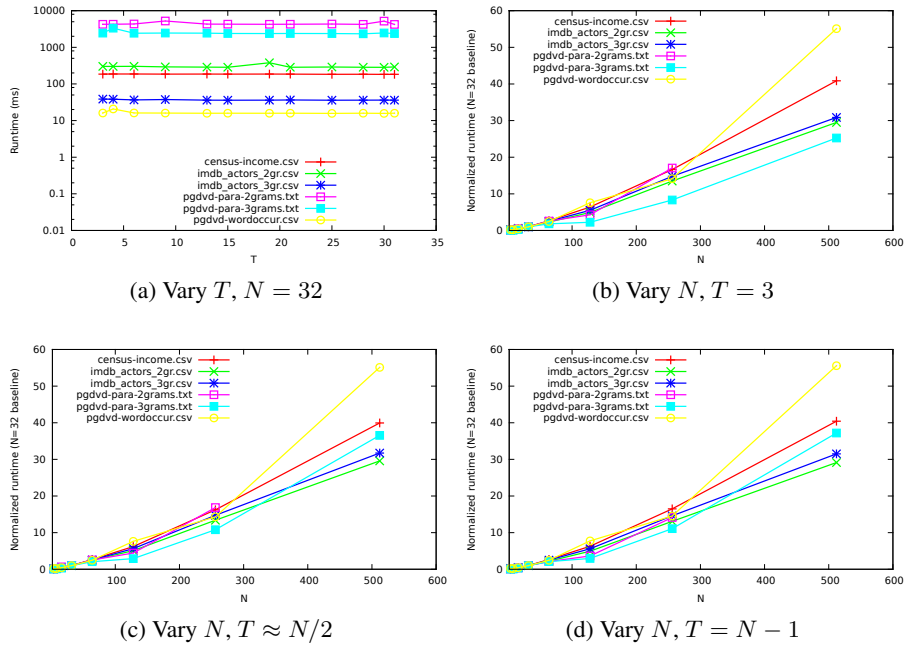


Figure 59: Varying T and N on wHEAP, real data (effect of varying N uses time relative to $N = 32$)

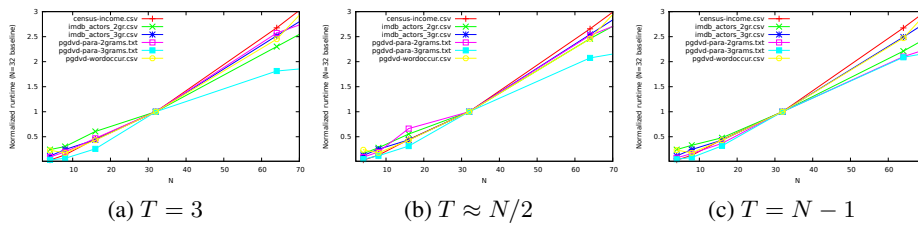
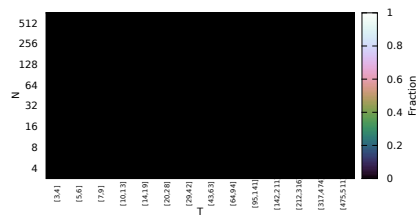
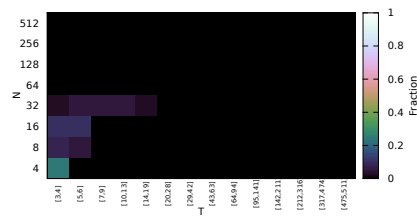


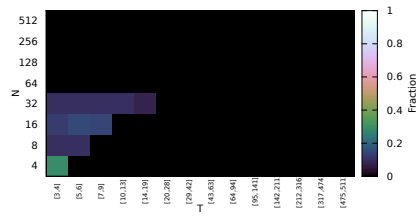
Figure 60: Effect of N (times relative to $N = 32$) for smaller values of N , on wHeap



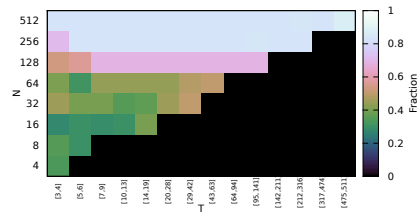
(a) Wins



(b) Good



(c) Fair



(d) Terrible

Figure 61: Heat map showing when to use and when to avoid wHeap

On synthetic data, the characteristics of the data were insignificant.

The time complexity has a $\log N$ factor, which presumably accounts for the shape of the curves on synthetic data. As one of the ‘w’ algorithms, we could not run all datasets with queries for $N = 512$. The wHEAP algorithm was usually terrible.

5.9 Workload

Although we have seen the algorithms in isolation, we still want some way to say that “Algorithm X is better than Algorithm Y”. To do this, we can examine total time taken on a particular set of queries (workload). However, we wish to control for the different sizes of the datasets—otherwise, performance on small datasets will be disregarded. Therefore, we use a workload that assumes fast-running (for *some* algorithm) queries are issued more often than queries that are slow (for *all* algorithms).

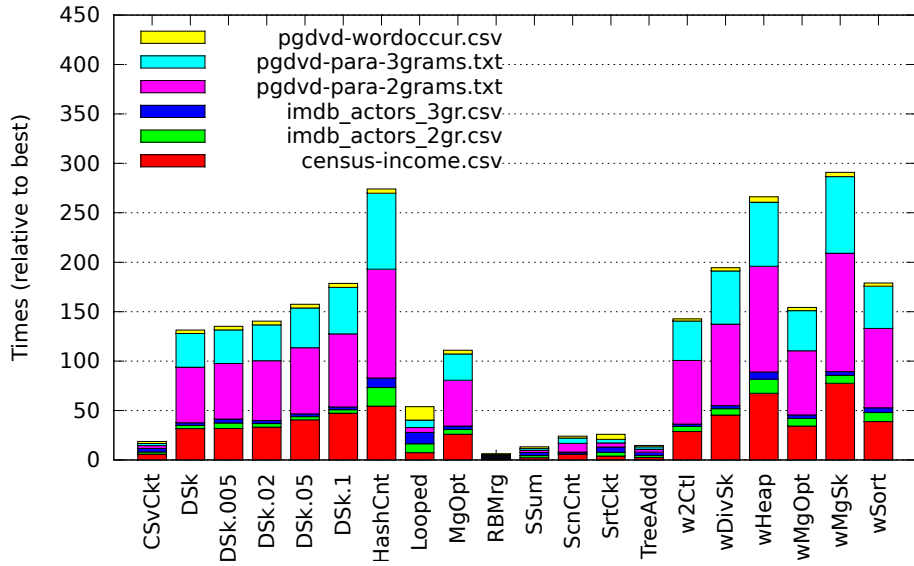
Fig. 62 shows how the various algorithms fare for a threshold of 19 over 32 bitmaps. Since the datasets are of varying size and we do not want the largest datasets to dominate the effects, we normalize the running times on a dataset D by dividing the running time by the fastest running time of any algorithm on D . I.e., if $t_{\mathcal{A}}(D)$ denotes the actual running time when algorithm \mathcal{A} processes a given collection of queries on dataset D , then its normalized time is

$$t_{\mathcal{A}}^{\text{norm}}(D) = t_{\mathcal{A}}(D) / \min_{\mathcal{A}'} t_{\mathcal{A}'}(D).$$

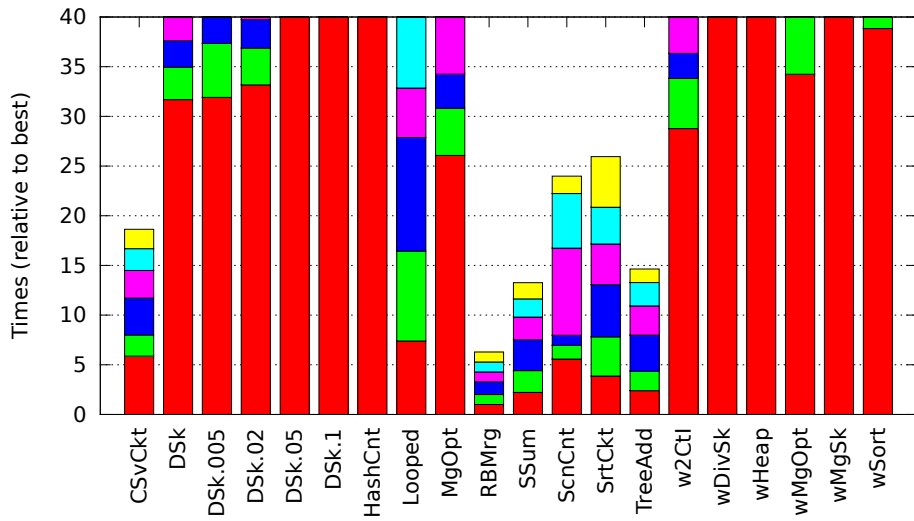
This is similar to saying that we have a workload where queries against the smaller datasets are more frequent. It makes equal each dataset, in that the total time spent on all queries (executed by the fastest algorithm) for two different datasets would be equal. If one algorithm were fastest in all 6 cases, its total bar height would be 6. We see no bar is quite that low, but SCANCOUNT, RBMRG, TREEADD and SRTCKT look promising. (Many of the other algorithms look bad because they performed very poorly on one dataset, PGDVD-2gr.)

Looking at bars whose colours are unequal, we identify several algorithms that are sensitive to the characteristics of the datasets (for instance, the various wrapped algorithms seem to do more poorly on PGDVD-2gr and PGDVD-3gr than other datasets, whereas LOOPED finds IMDB-3gr difficult. RBMRG, the adder and sorting circuits, and SCANCOUNT seem less sensitive to the datasets than other algorithms.

However, if we repeat the process for thresholds 3 or 31 on 32 bitmaps, results differ (see Figs. 63 and 64. For $T = 31$, DSK works particularly well and LOOPED is about 10 times slower than optimal, whereas for $T = 3$ LOOPED performs



(a) Full y range



(b) Reduced y

Figure 62: Relative speeds of algorithms over a collection of queries with $T = 16$ and $N = 32$.

best and DSK is roughly 40 (250/6) times slower than optimal. (Note that the y range changes in these figures). Algorithms RBMRG and LOOPED are relatively insensitive to the dataset. For $T = 31$ we see that the value μ for DSK affects whether the PGDVD-2gr dataset is difficult.

5.10 Discussion

If we are to recommend only one threshold algorithm for similarity queries on run-length compressed bitmaps, then RBMRG should be used. It was frequently the fastest algorithm, and it rarely behaved disastrously. However, if T is very small, LOOPED may perform better. As well, the sideways-sum adder circuit (SSUM) performed well overall and was infrequently disastrous. Both LOOPED and SSUM have the advantage that they can use an unmodified (perhaps closed-source) bitmap library, whereas RBMRG would require adding code to the bitmap library. The LOOPED algorithm has the advantage of simplicity, since a substantial implementation effort is required with any of the circuit-based approaches.

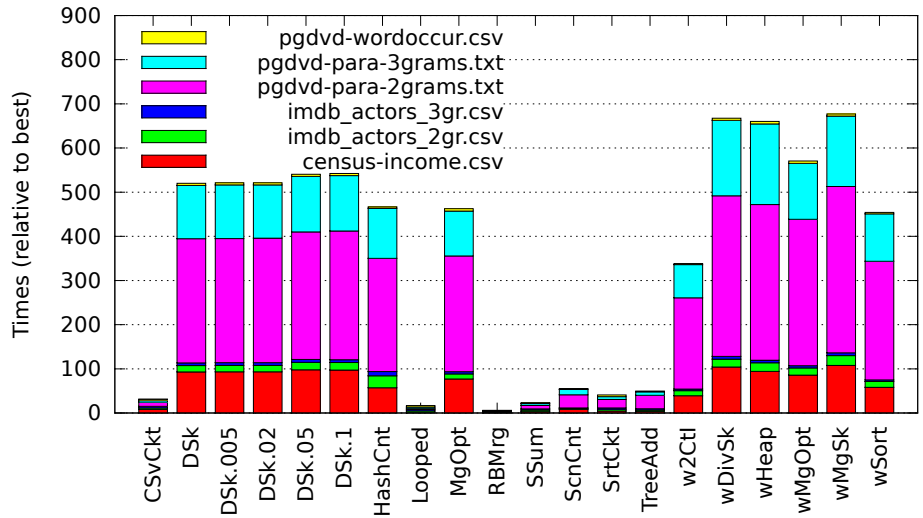
The simple SCANCOUNT depends heavily on the dataset. On some datasets, its performance is frequently best, whereas in others, it is frequently terrible. Its use is risky. The hash-map variant, HASHCNT, is almost always disastrous.

For similarity queries over run-length compressed bitmaps, the ‘w’ implementation approach (transform the data into lists of sorted integers) cannot be recommended. We observed many cases where the list of integers was much larger, thus creating memory problems. Also, the time cost in doing the conversion is too high.

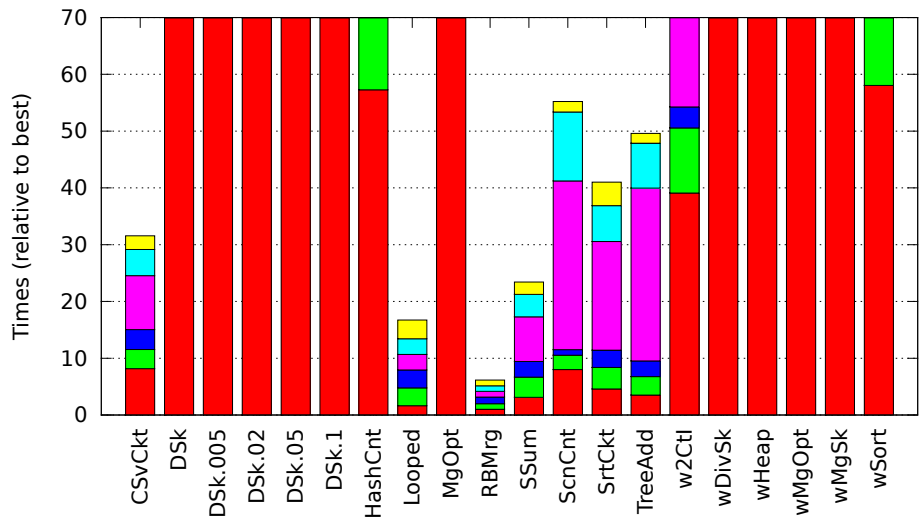
Well-known pruning-based algorithms such as MGOPT and DSK are not suitable for general threshold computations over bitmaps. In cases where $T \approx N$, they often do well (but many times, so does RBMRG). There are some applications where the requirement for a large T can be met. For instance, using the formula in [25] (which they credit to Sarawagi and Kirpal [35]) with strings of length 64, if we are interested in finding the strings of edit distance at most two from some target using trigrams, the appropriate threshold is $64 + 3 - 1 - 2 * 3 = 60$.

5.10.1 Performance counters results.

Execution times include factors other than the number of instructions executed. Pipeline stalls due to cache or translation-lookaside-buffer (TLB) misses can lead to unexpectedly poor running times. To assess our implementations, we generated 10 “Random attributes” queries (such as those used in the top of Table 5) and used the Linux `perf stat` tool to monitor various cache-miss rates as well the overall instructions-per-cycle figure of merit. Our focus was on the most promising algorithms. Although the data generation phase was included, it took much less

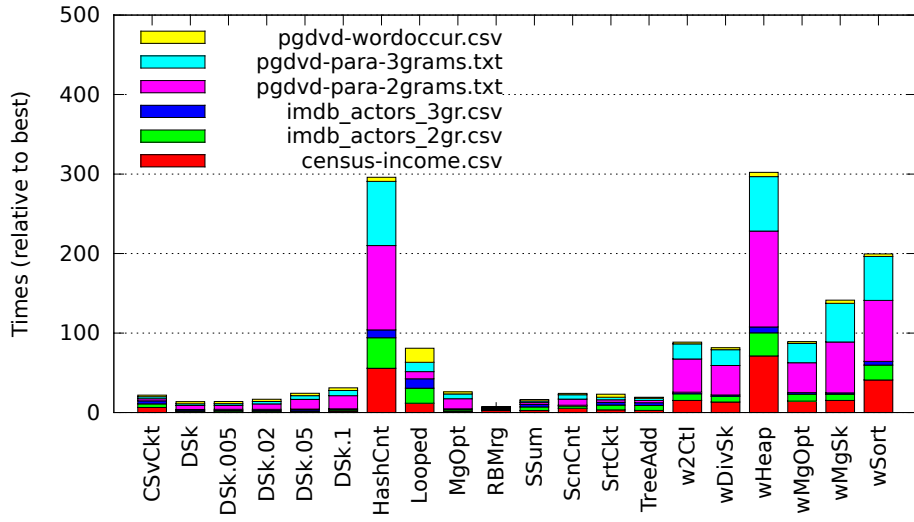


(a) Full y range

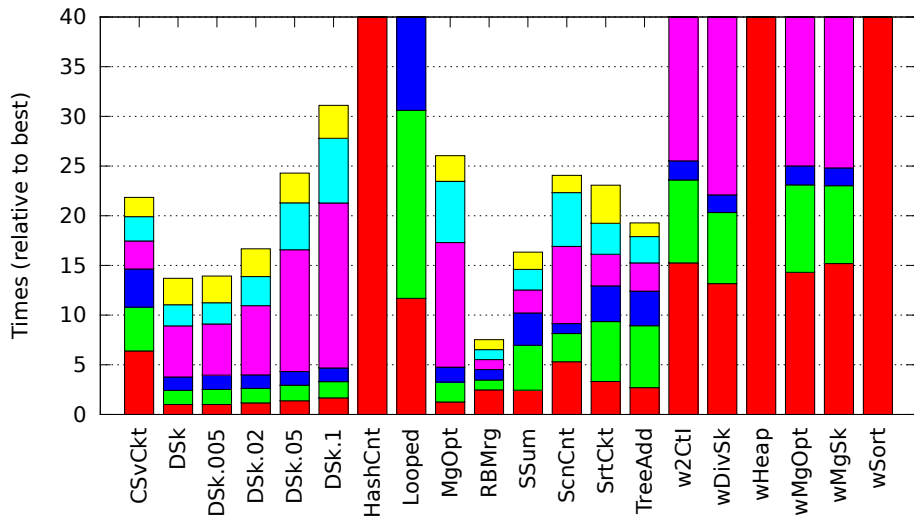


(b) Reduced y

Figure 63: Relative speeds of algorithms over a collection of queries with $T = 3$ and $N = 32$.



(a) Full y range



(b) Reduced y

Figure 64: Relative speeds of algorithms over a collection of queries with $T = 31$ and $N = 32$.

Table 12: Hardware performance counter results.

Algorithm	IPC	Miss rates (%)			
		L2	L3	TLB-load	TLB-store
SCANCOUNT	1.9	5.0	0.31	4.2×10^{-3}	7.4×10^{-4}
w2CTI	2.0	11.9	0.90	3.6×10^{-2}	6.7×10^{-2}
MGOPT	2.2	1.7	0.16	5.7×10^{-2}	8.0×10^{-4}
DSK	2.2	1.8	0.17	3.8×10^{-2}	7.4×10^{-4}
SSUM	2.1	5.9	0.43	7.1×10^{-3}	2.1×10^{-2}
LOOPED	2.1	8.4	0.31	5.0×10^{-3}	2.3×10^{-2}
RBMRG	2.1	6.1	0.17	1.9×10^{-1}	4.4×10^{-3}

than 1 s, and the query was repeatedly executed for 100 s. Query input volumes ranged between 103 kB and 43 MB, so the computation cannot be done entirely in cache. The formulae used to calculate the L2 and L3 miss rates were non-obvious and found on an Intel forum [6, 17], which indicates there is no way to calculate the L1 miss rate. Results are in Table 12.

The table shows remarkable consistency in Instructions Per Cycle (IPC). Algorithms DSK and MGOPT put the least load on the memory system, whereas—unsurprisingly—w2CTI put the most load on it. The RBMRG algorithm had the worst TLB performance, but very good results for L3. Understanding the behaviour of an algorithm on different cache levels is important for parallel computing. In a multithreaded environment, we will want to do most of our computation within L1 and L2 (on our processor, L3 cache is shared between all cores, unlike L1 and L2).

6 Conclusion and Future Work

This report has considered algorithms for threshold (and more generally, symmetric Boolean functions) on bitmaps, both compressed (EWAH) and uncompressed (BITSET). The algorithms both include known algorithms that have been adapted so they work with bitmaps (rather than sorted lists of integers), and also include a number of novel algorithms.

Experiments were conducted using small synthetic datasets, as well as several moderately large real datasets. The use of similarity queries and the choices of real datasets mean that our results can be related to those in previous work, such as that by Li et al.

We have seen that the most straightforward algorithm, SCANCOUNT, can often be outperformed on similarity queries over bitmap indexes. This observation is consistent with previous results reported by Li et al. when the data was represented as sorted lists of integers. Nevertheless, it is not disastrous if the bitmaps are sufficiently sparse. We have also seen that the other algorithms from Li et al.

are highly dependent on the characteristics of the data and the selected threshold. When T is near N , they are frequently good. However, for other values of T they can behave very poorly. For EWAH compressed bitmaps, the RBMRG algorithm exploits the runs in the data and rarely behaves badly. For both compressed and uncompressed (BITSET) bitmaps, the algorithms based on Boolean circuits perform well. Of TREEADD, SSUM and SRTCKT, we recommend SSUM. It uses fewest operations for large N and seems to be less dependent on the data characteristics than TREEADD or SRTCKT. These algorithms are not affected much by the choice of T , and can make use of an unmodified bitmap library. A disadvantage is that considerable implementation effort is required. An alternative adder design, CSVCKT, has a much simpler implementation. However, its performance does not match SSUM or TREEADD. It should be possible to implement SSUM following the general style of CSVCKT, rather than using the explicit circuit approach. The simple LOOPED algorithm also can use an unmodified bitmap library, and it is an excellent choice when T is very small. While it becomes worse as T grows, the growth on actual data may be significantly better than our theoretical worst-case analysis suggests.

For future work, we should broaden the threshold computations to include those needed to answer queries other than similarity queries. We have seen that similarity queries tend to use bitmaps that are significantly denser than the average bitmap present in an index. We have identified another class of queries as being interesting, wherein a random attribute value is selected for each of N attributes, as we did in Table 5. This will end up choosing sparser bitmaps and is likely to favour SCANCOUNT.

Our work has considered N values up to 512. Yet we use datasets whose indexes have tens of thousands of bitmaps, and datasets with millions of bitmaps are not out of the question. Would there be applications where $N = 1,000,000$ would be useful? If so, which algorithms should be used? The circuit-based algorithms will become infeasible for extremely large N , but which of the others can be used? Can new algorithms be developed for this case?

We have seen that several algorithms need certain characteristics of the data in order to be successful. To date, we have mostly looked at the sparseness of the bitmaps or their RUNCOUNT. Are there other data characteristics that can determine whether a given algorithm should be recommended? If so, can we find ways to compute these characteristics or maintain them in the DBMS?

Finally, algorithms can be parallelized, and while most of our threshold computations take only a few milliseconds, we have some that may take tens of seconds. If we try extremely large N values, this may increase. At some point, it may become important to have one threshold computation run faster than is possible using a single core. For multicore processing, a particular challenge is that all cores

compete for access to L3 and RAM. E.g., this means that it is best if intermediate results fit in L2 cache.

References

- [1] M. Ajtai, J. Komlós, and E. Szemerédi. Sorting in $c \log n$ parallel steps. *Combinatorica*, 3(1):1–19, 1983.
- [2] Vo Ngoc Anh and Alistair Moffat. Index compression using 64-bit words. *Software—Practice and Experience*, 40(2):131–147, 2010.
- [3] G. Antoshenkov. Byte-aligned bitmap compression. In *Data Compression Conference (DCC'95)*, page 476, Washington, DC, USA, 1995. IEEE Computer Society.
- [4] Peter J. Ashenden. *Digital Design (Verilog): An Embedded Systems Approach Using Verilog*. Elsevier, 2007.
- [5] Alexander Behm, Shengyue Ji, Chen Li, and Jiaheng Lu. Space-constrained gram-based indexing for efficient approximate string search. In *Proceedings IEEE 25th International Conference on Data Engineering (ICDE'09)*, pages 604–615. IEEE, 2009.
- [6] Shannon Cepeda. How to get the L1,L2 cache miss of an intel[sic] i5 Sandy Bridge (response). online, Intel Developer Zone, <http://software.intel.com/en-us/forums/topic/280087>, 2012. last checked 2014-02-17.
- [7] Alessandro Colantonio and Roberto Di Pietro. Concise: Compressed 'n' composable integer set. *Information Processing Letters*, 110(16):644–650, July 2010.
- [8] Thomas Cormen, Charles Leiserson, Ronald Rivest, and Clifford Stein. *Introduction to Algorithms*. MIT Press, 3rd edition, 2009.
- [9] J. Shane Culpepper and Alistair Moffat. Efficient set intersection for inverted indexing. *ACM Transactions on Information Systems*, 29(1):1:1–1:25, December 2010.
- [10] Rob Eden. GNU TROVE high performance collections for Java. online: <https://bitbucket.org/robeden/trove/>. last checked 2014-02-17.

- [11] Erling Ellingsen. Bit tricks, part III: Fast vertical counter. online:<http://www.steike.com/code/bits/vertical-counter/>, 2009. last checked 2014-02-17.
- [12] Alfredo Ferro, Rosalba Giugno, Piera Laura Puglisi, and Alfredo Pulvirenti. An efficient duplicate record detection using q-grams array inverted index. In *12th International Conference on Data Warehousing and Knowledge Discovery (DaWaK'10), LNCS 6263*, pages 309–323. Springer, 2010.
- [13] A. Frank and A. Asuncion. UCI machine learning repository. <http://archive.ics.uci.edu/ml> (checked 2014-02-17), 2010.
- [14] F. Fusco, M. P. Stoecklin, and M. Vlachos. NET-FLi: On-the-fly compression, archiving and indexing of streaming network traffic. *Proceedings of the VLDB Endowment*, 3:1382–1393, 2010.
- [15] Michael R. Garey and David S. Johnson. *Computers and Intractability: A Guide to the Theory of NP-Completeness*. W. H. Freeman, New York, 1979.
- [16] GrepCode. Grepcode: java.util.bitset(.java)-class-source code view. online: <http://grepcode.com/file/repository.grepcode.com/java/root/jdk/openjdk/7-b147/java/util/BitSet.java#BitSet>. last checked 2014-02-17.
- [17] Intel Corporation. *Intel 64 and IA-32 Software Developer's Manual: System Programming Guide, Part 2*, volume 3B. Intel Corporation, September 2013. <http://www.intel.com/Assets/PDF/manual/253669.pdf> last checked 2014-02-17.
- [18] Lianyin Jia, Jianqing Xi, Mengjuan Li, Yong Liu, and Decheng Miao. ETI: an efficient index for set similarity queries. *Frontiers of Computer Science*, 6(6):700–712, 2012.
- [19] Owen Kaser, Steven Keith, and Daniel Lemire. The LitOLAP project: Data warehousing with literature. In *Proceedings, CaSTA'06 : The 5th Annual Canadian Symposium on Text Analysis*, pages 93–96, 2006.
- [20] Donald E. Knuth. *Searching and Sorting*, volume 3 of *The Art of Computer Programming*. Addison-Wesley, Reading, Massachusetts, 1997.
- [21] Donald E. Knuth. *Combinatorial Algorithms, Part 1*, volume 4A of *The Art of Computer Programming*. Addison-Wesley, Boston, Massachusetts, 2011.

- [22] Daniel Lemire and Owen Kaser. Reordering columns for smaller indexes. *Information Sciences*, 181(12):2550–2570, June 2011.
- [23] Daniel Lemire, Owen Kaser, and Kamel Aouiche. Sorting improves word-aligned bitmap indexes. *Data & Knowledge Engineering*, 69(1):3–28, 2010.
- [24] Daniel Lemire, Cliff Moon, David McIntosh, Robert Becho, Colby Ranger, Veronika Zenz, and Owen Kaser. JavaEWAH - GitHub page. online: <https://github.com/lemire/javaewah>, 2014. last checked 2014-02-13.
- [25] Chen Li, Jiaheng Lu, and Yiming Lu. Efficient merging and filtering algorithms for approximate string searches. In *Proceedings of the 2008 IEEE 24th International Conference on Data Engineering (ICDE'08)*, pages 257–266, Washington, DC, USA, 2008. IEEE Computer Society.
- [26] Mengjuan Li, Lianyin Jia, Jinguo You, Jianqing Xi, HaiFei Qin, and Rui Zeng. Fast T-overlap query algorithms using graphics processor units and its applications in web data query. *World Wide Web*, pages 1–17, 2013.
- [27] Alistair Moffat and Justin Zobel. Self-indexing inverted files for fast text retrieval. *ACM Transactions on Information Systems*, 14(4):349–379, 1996.
- [28] Daniele Montanari and Piera Laura Puglisi. Near duplicate document detection for large information flows. In *IFIP WG 8.4, 8.9, TC 5 International Cross Domain Conference and Workshop on Availability, Reliability, and Security, CD-ARES 2012, LNCS 7465*, pages 203–217. Springer, August 2012.
- [29] Gonzalo Navarro and Eliana Provedel. Fast, small, simple rank/select on bitmaps. In *Proceedings, 11th International Symposium on Experimental Algorithms (SEA 2012), LNCS 7276*, pages 295–306. Springer, 2012.
- [30] Shirley A. Perry and Peter Willett. A review of the use of inverted files for best match searching in information retrieval systems. *Journal of Information Science*, 6(2-3):59–66, 1983.
- [31] Project Gutenberg Literary Archive Foundation. July 2006 Gutenberg DVD. http://www.gutenberg.org/wiki/Gutenberg:The_CD_and_DVD_Project, 2006. (Last checked 2014-02-13).
- [32] Willard van Orman Quine. Two theorems about truth functions. *Boletín de la Sociedad Matemática Mexicana*, 10, 1953.

- [33] Denis Rinfret, Patrick O’Neil, and Elizabeth O’Neil. Bit-sliced index arithmetic. In *Proceedings of the 2001 ACM SIGMOD International Conference on Management of Data*, pages 47–57. ACM, May 2001.
- [34] Peter Sanders and Frederik Transier. Intersection in integer inverted indices. In *2007 Proceedings of the Ninth Workshop on Algorithm Engineering and Experiments (ALENEX07)*, volume 7, pages 71–83, Philadelphia, PA, USA, 2007. SIAM.
- [35] Sunita Sarawagi and Alok Kirpal. Efficient set joins on similarity predicates. In *Proceedings of the 2004 ACM SIGMOD International Conference on Management of Data*, pages 743–754, New York, NY, USA, 2004. ACM.
- [36] Ravi Sethi. Complete register allocation problems. *SIAM Journal on Computing*, 4:226–248, 1975.
- [37] Mike Stonebraker, Daniel J. Abadi, Adam Batkin, Xuedong Chen, Mitch Cherniack, Miguel Ferreira, Edmond Lau, Amerson Lin, Sam Madden, Elizabeth O’Neil, Pat O’Neil, Alex Rasin, Nga Tran, and Stan Zdonik. C-Store: a column-oriented DBMS. In *VLDB’05, Proceedings of the 31st International Conference on Very Large Data Bases*, pages 553–564, New York, NY, USA, 2005. ACM.
- [38] Henry S. Warren, Jr. *Hacker’s Delight*. Addison Wesley, 2nd ed. edition, 2013.
- [39] Hazel Webb, Daniel Lemire, and Owen Kaser. Diamond dicing. *Data & Knowledge Engineering*, 86:1–18, 2013.
- [40] K. Wu, K. Stockinger, and A. Shoshani. Breaking the curse of cardinality on bitmap indexes. In *SSDBM’08: Proceedings of the 20th International Conference on Scientific and Statistical Database Management, LNCS 5069*, pages 348–365. Springer, 2008.
- [41] Kesheng Wu, Ekow Otoo, and Arie Shoshani. On the performance of bitmap indices for high cardinality attributes. In *VLDB’04, Proceedings of the 30th International Conference on Very Large Data Bases*, pages 24–35. Morgan Kaufmann, 2004.
- [42] Kesheng Wu, Ekow J. Otoo, and Arie Shoshani. Optimizing bitmap indices with efficient compression. *ACM Transactions on Database Systems*, 31(1):1–38, 2006.

A IMDB dataset

The IMDB dataset was used in [25], but the details necessary to prepare an identical copy of the dataset were not given. The IMDb organization makes its data available for noncommercial use, but it is not free data. The conditions also explicitly forbid using it to make an online database: this may prevent us from distributing the final dataset we obtained. However, the following steps can be followed:

1. Download `actors.list.gz` from `ftp://ftp.sunet.se/pub/tv+movies/imdb/`. In autumn 2013, the gzipped file was 223 MB; uncompressed it was 803,MB. Li et al. noted the actors list was 22MB [25].
2. Find the line `Name\s+Title`, skip the following line, then process lines until a line consisting of at least 60 '-'s is reached (several hundred lines from the end of the file).
3. For the processed part of the file, take every line that is non-blank in column 1, and extract from column 1 to the first tab character as an actor name, using the sed pipeline

```
sed '/^ .*/d' actorslistmiddle.txt | sed '/^\s*/d' | sed 's/./\s/'
```

where the apparent spaces are tabs. In autumn 2013, the result was 35 MB with 1783816 actors. No other attempts to clean data or regularize punctuation should be made. The number of unique bigrams was 4276 and the number of unique trigrams was 50663. The number of unique bigrams is larger than one might expect, because the actor list is international and has many non-English names and stage names. Names can include punctuation and other symbols. Also, our n-grams are case sensitive.

Note that the comma-space bigram occurs in almost every name due to the heavy use of the "surname, firstname" pattern. There may be some other extremely common bigrams. The majority of n-grams occur very rarely, however.

The database has grown: [25] report 1,199,299 names with total size 22 MB, and the number of unique grams was 34737. (They used 3-grams.) We determined that the bitmap indexes would have about 35 million set bits. Considering the 1.7 million actors, this means about 20 bigrams or trigrams per actor on average, very similar to the 19 reported by Li et al. [25].

B Compiled code

Our experiments compiled Boolean circuits into a number of different targets: Java (using either the EWAH or BitSet libraries), C++ (uncompressed bitmaps stored in arrays), or a custom byte-code that a Java program interprets (using either BitSet or EWAH). We finally used the last approach, but the other targets are human-readable and carry out the same logical operations.

The C++ code has a each bitmap as a fixed-size array of 64-bit words. Using AVX, we could instead work with 256 (or 512, with AVX2) bit words.

For $N = 5$, $T = 2$ and the SSUM circuit we get the following. The function is vertical, in that it takes complete input vectors and produces a complete output vector. Internally, the computation is carried out in a memory-efficient, horizontal (word at a time) manner.

```
void compiledFunc(long long **inputs, int vectLen,
long long *output) {
int ctr=0;
for (ctr=0; ctr < vectLen; ++ctr) {
long long gate2=inputs[0][ctr];
long long gate3=inputs[1][ctr];
long long gate4=inputs[2][ctr];
long long gate5=inputs[3][ctr];
long long gate6=inputs[4][ctr];
long long gate7=gate2 ^ gate3;
long long gate8=gate7 ^ gate4;
long long gate9=gate7 & gate4;
long long gate10=gate2 & gate3;
long long gate11=gate9 | gate10;
long long gate12=gate8 ^ gate5;
long long gate14=gate12 & gate6;
long long gate15=gate8 & gate5;
long long gate16=gate14 | gate15;
long long gate17=gate11 & gate16;
long long gate18=gate11 ^ gate16;
long long gate19=gate17 | gate18;
output[ctr] = gate19;
}
}
```

The same example compiled to Java, for EWAH, is given below. Internally, a vertical implementation is used. A last-use analysis removes references to bitmaps that are no longer needed, to reduce memory use. A more sophisticated approach would remove the null assignments for gates 2–6 (since references to these bitmaps would be held by the caller), and 17 and 18 (since these references will be lost before any more memory is required).

```
public static EWAHCompressedBitmap compiledFunc(
    EWAHCompressedBitmap [] inputs) {
    EWAHCompressedBitmap g2 = inputs[0];
    EWAHCompressedBitmap g3 = inputs[1];
    EWAHCompressedBitmap g4 = inputs[2];
    EWAHCompressedBitmap g5 = inputs[3];
    EWAHCompressedBitmap g6 = inputs[4];
    EWAHCompressedBitmap g7 = EWAHCompressedBitmap.xor(g2,g3);
    EWAHCompressedBitmap g8 = EWAHCompressedBitmap.xor(g7,g4);
    EWAHCompressedBitmap g9 = EWAHCompressedBitmap.and(g7,g4);
    g4= null;
    g7= null;
    EWAHCompressedBitmap g10 = EWAHCompressedBitmap.and(g2,g3);
    g2= null;
    g3= null;
    EWAHCompressedBitmap g11 = EWAHCompressedBitmap.or(g9,g10);
    g9= null;
    g10= null;
    EWAHCompressedBitmap g12 = EWAHCompressedBitmap.xor(g8,g5);
    EWAHCompressedBitmap g14 = EWAHCompressedBitmap.and(g12,g6);
    g6= null;
    g12= null;
    EWAHCompressedBitmap g15 = EWAHCompressedBitmap.and(g8,g5);
    g5= null;
    g8= null;
    EWAHCompressedBitmap g16 = EWAHCompressedBitmap.or(g14,g15);
    g14= null;
    g15= null;
    EWAHCompressedBitmap g17 = EWAHCompressedBitmap.and(g11,g16);
    EWAHCompressedBitmap g18 = EWAHCompressedBitmap.xor(g11,g16);
    g11= null;
    g16= null;
    EWAHCompressedBitmap g19 = EWAHCompressedBitmap.or(g17,g18);
    g17= null;
    g18= null;
    return g19;
}
```

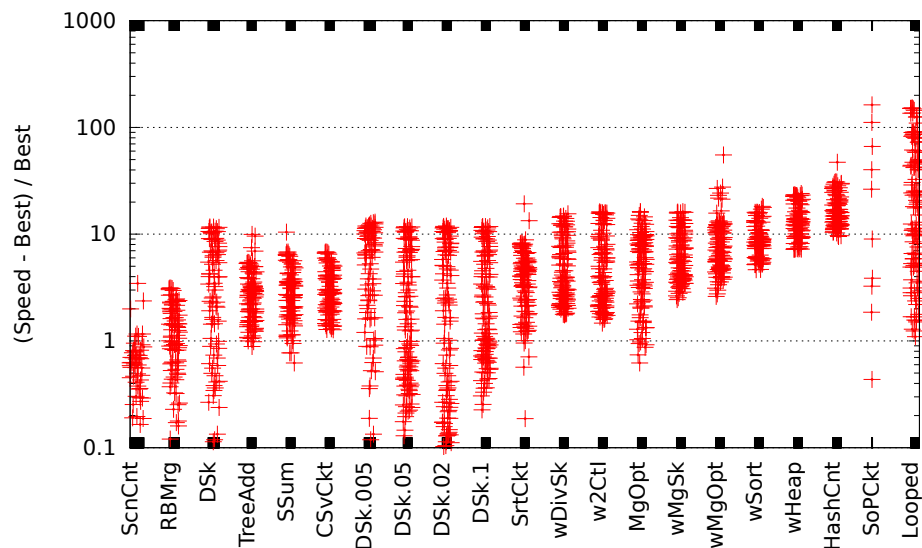


Figure 65: Suboptimality (for cases when the algorithm was at least 10% slower than the fastest algorithm). IMDB-2gr, $N \leq 512$, Similarity(100) queries.

C Suboptimality plots

We compare, for each competition, each algorithm’s running time to the best running time. The suboptimality is the additional running time the algorithm requires, compared to the best running time of any of the algorithms, divided by that best running time. For each algorithm, we show the distribution of its suboptimality scores on the competitions. Since the y axis is logarithmic, we do not show the cases where the algorithm’s running time was within 10% of the best running time. The order of algorithms on the x axis is by increasing mean suboptimality.

C.1 Wide range of N

Some cases were omitted, when too much memory was required. See Figs. 65–69.

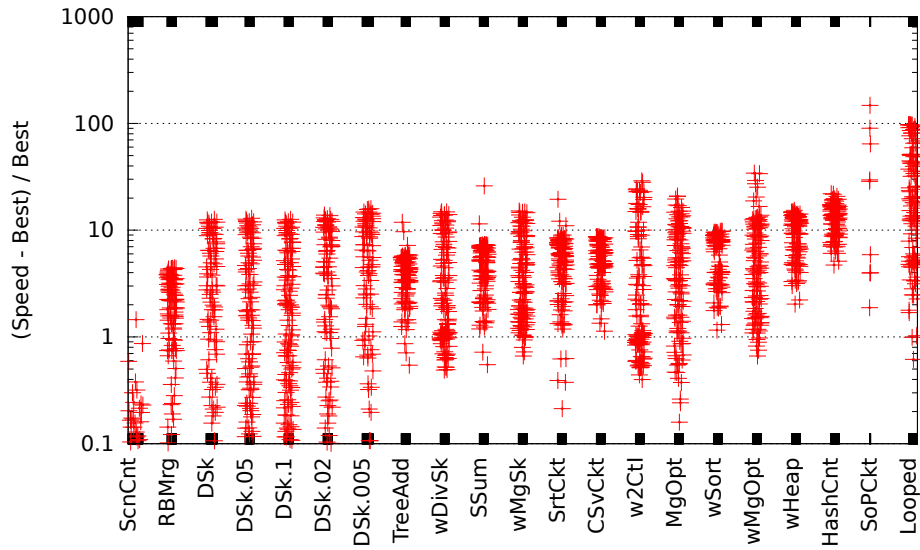


Figure 66: Suboptimality. IMDB-3gr, $N \leq 512$, Similarity(100) queries.

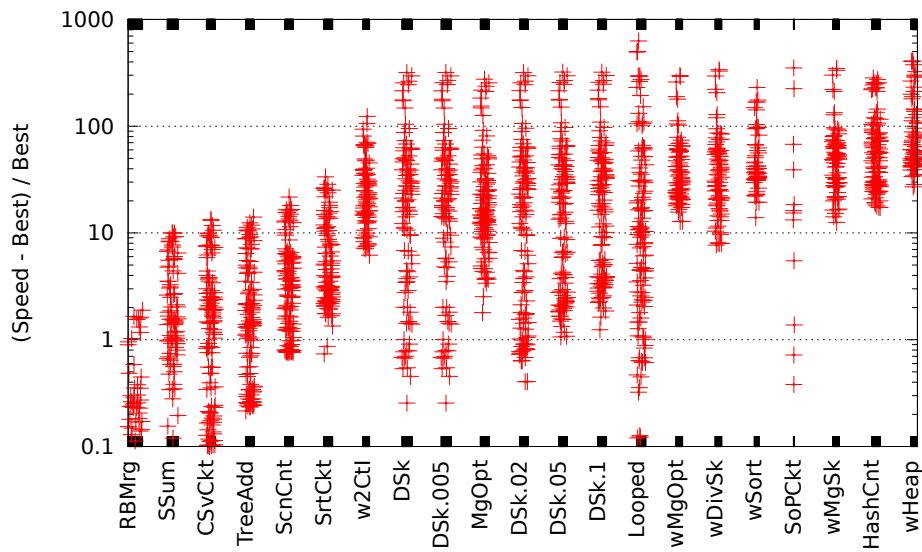


Figure 67: Suboptimality. PGDVD-3gr, $N \leq 512$, Similarity queries.

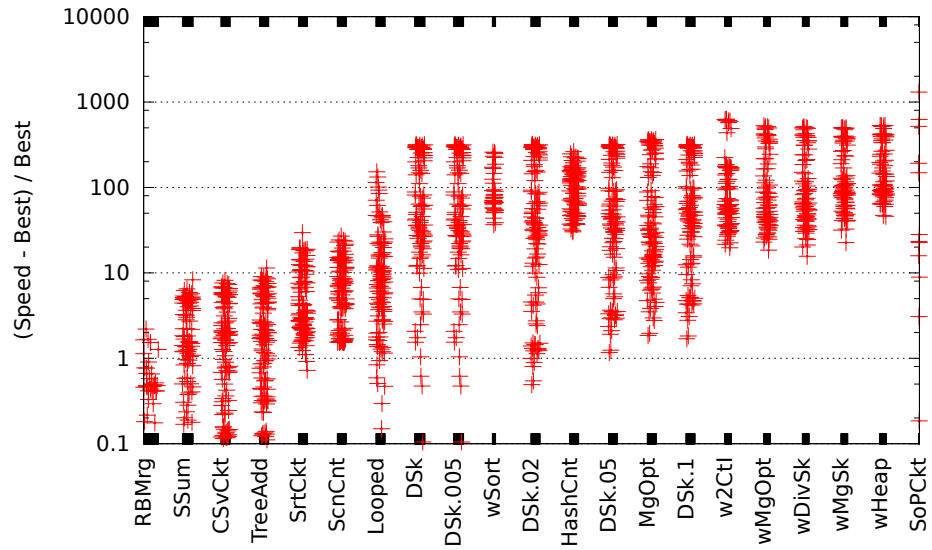


Figure 68: Suboptimality. PGDVD-2gr, $N \leq 512$, Similarity queries.

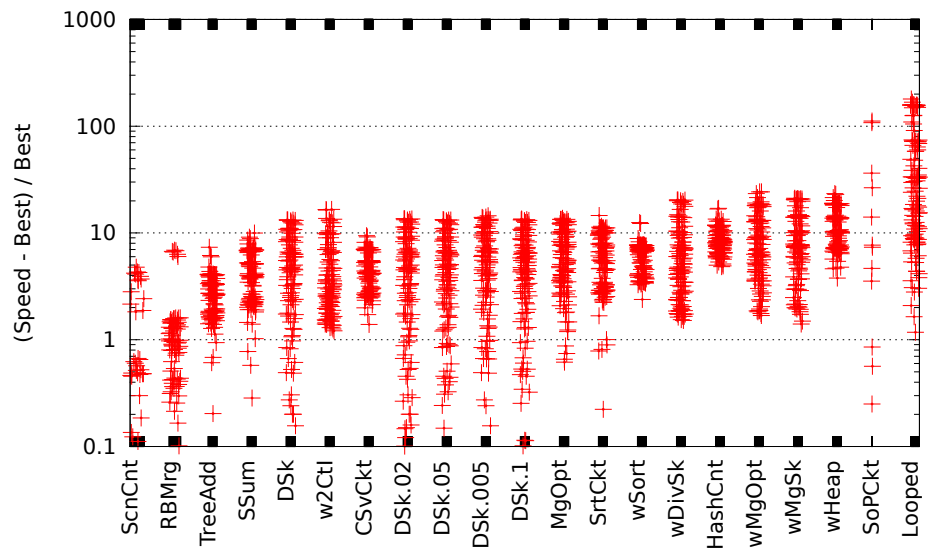


Figure 69: Suboptimality. PGDVD, $N \leq 512$, Similarity(100) queries.

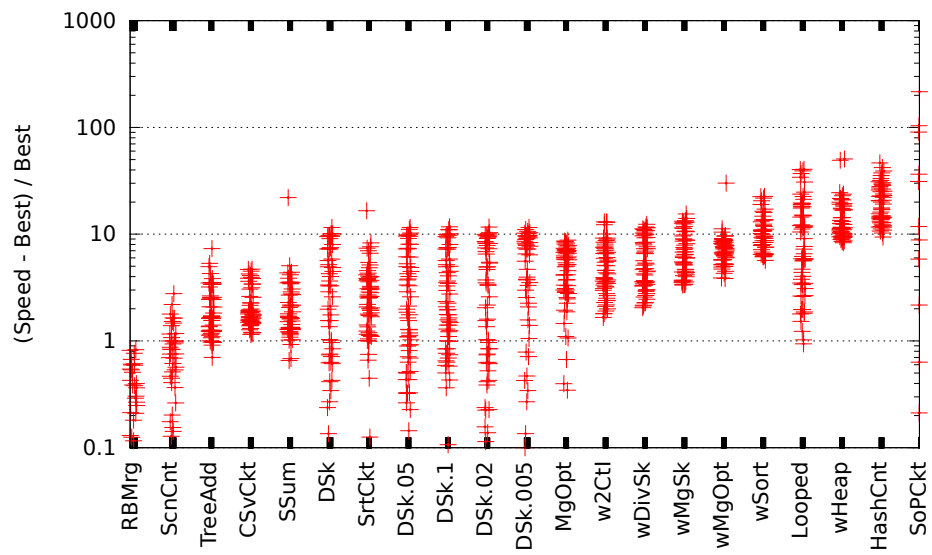


Figure 70: Suboptimality. IMDB-2gr, $N \leq 128$, Similarity(10) queries.

C.2 Narrower range of N

See Figs. 70–73.

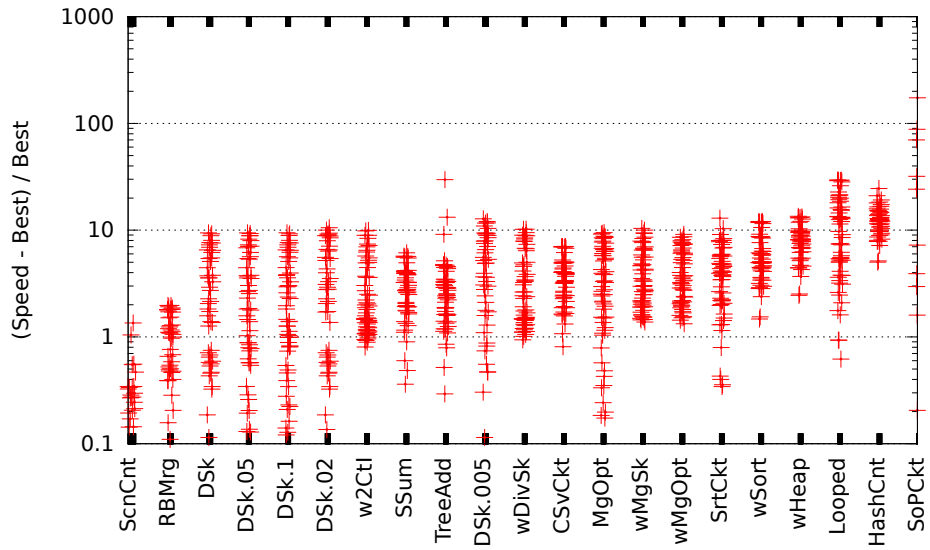


Figure 71: Suboptimality. IMDB-3gr, $N \leq 128$, Similarity(10) queries.

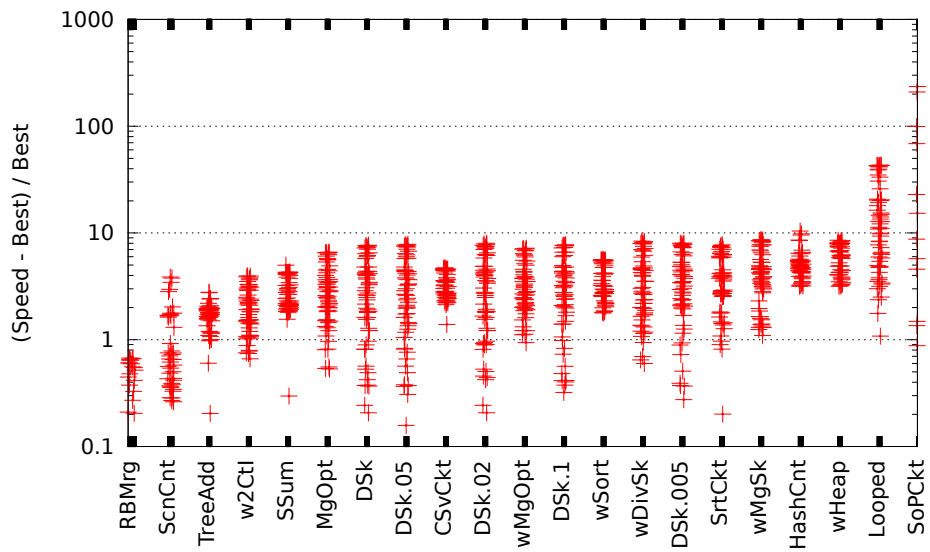


Figure 72: Suboptimality. PGDVD, $N \leq 128$, Similarity(10) queries.

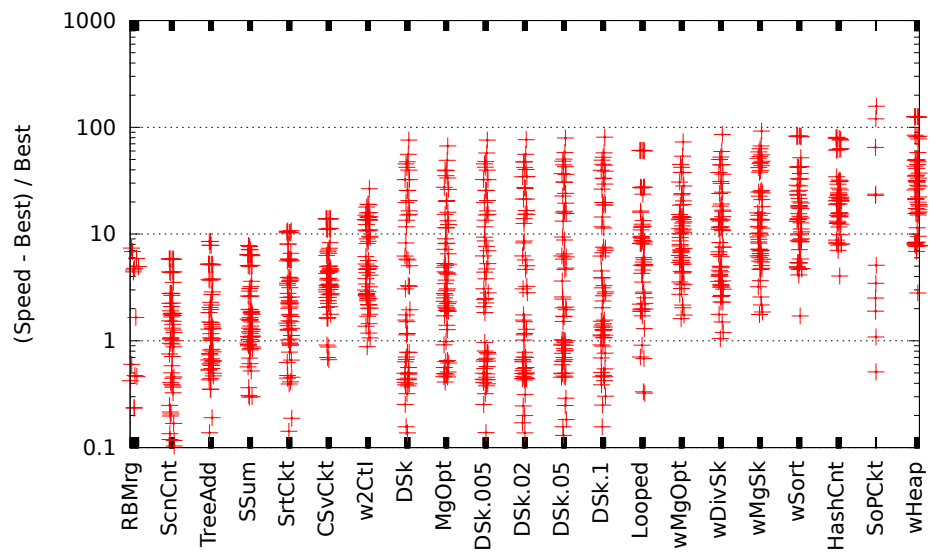


Figure 73: Suboptimality. CensusIncome, $N \leq 128$, Similarity(10) queries.

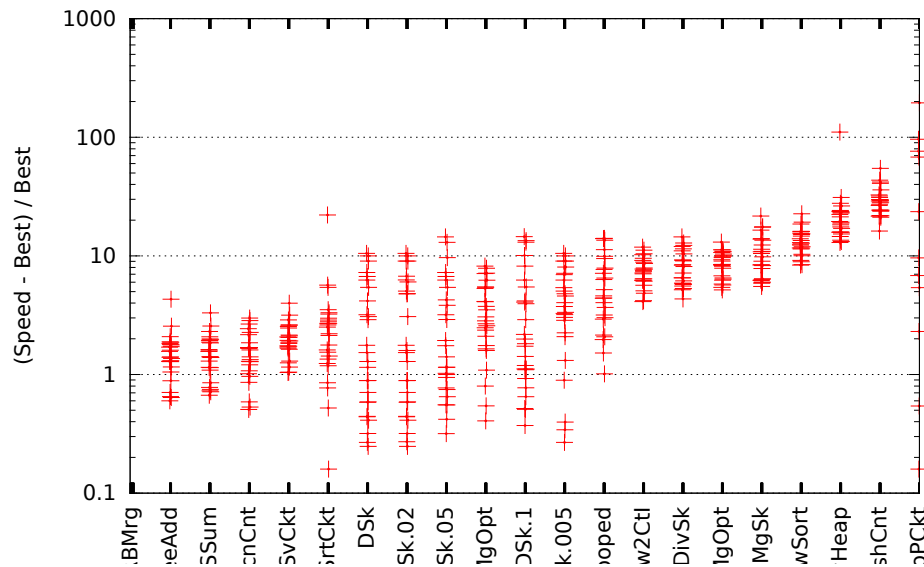


Figure 74: Suboptimality. IMDB-2gr, $N \leq 32$, Similarity queries.

C.3 Narrowest range of N

See Figs. 74–77.

D SCANCOUNT on BitSet

The code for SCANCOUNT on BitSet inputs is particularly simple.

```

Arrays.fill(counts, 0);
for (BitSet bs : inputsAsBitSets)
    for (int k = bs.nextSetBit(0); k >= 0;
         k = bs.nextSetBit(k+1))
        counts[k]++;
scanCountAns.clear();
for (int k=0; k < counts.length; ++k)
    if (counts[k] >= K) scanCountAns.set(k);

```

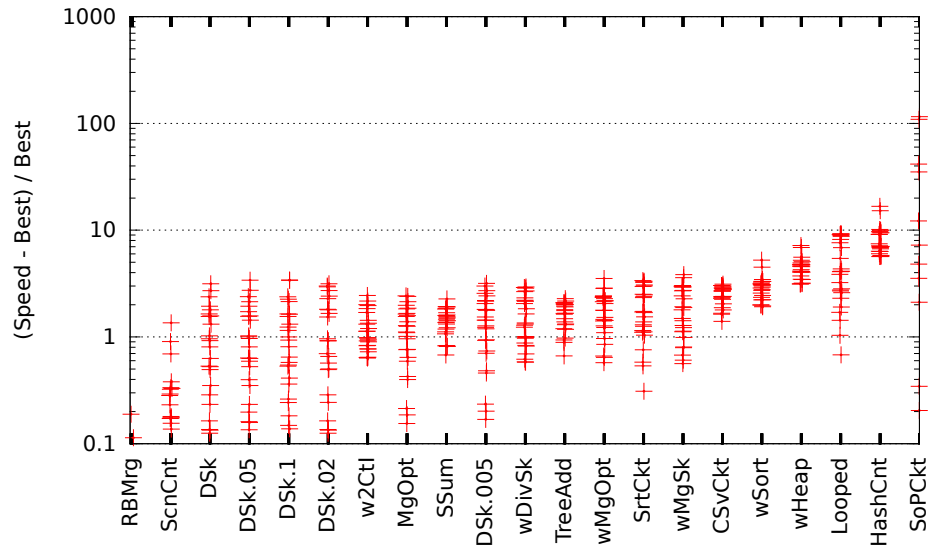


Figure 75: Suboptimality. IMDB-3gr, $N \leq 32$, Similarity queries.

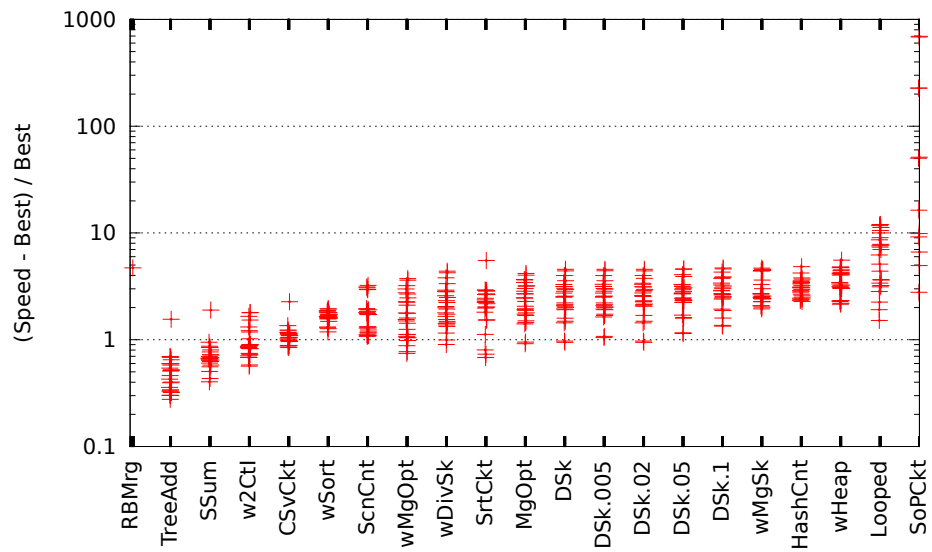


Figure 76: Suboptimality. PGDVD, $N \leq 32$, Similarity queries.

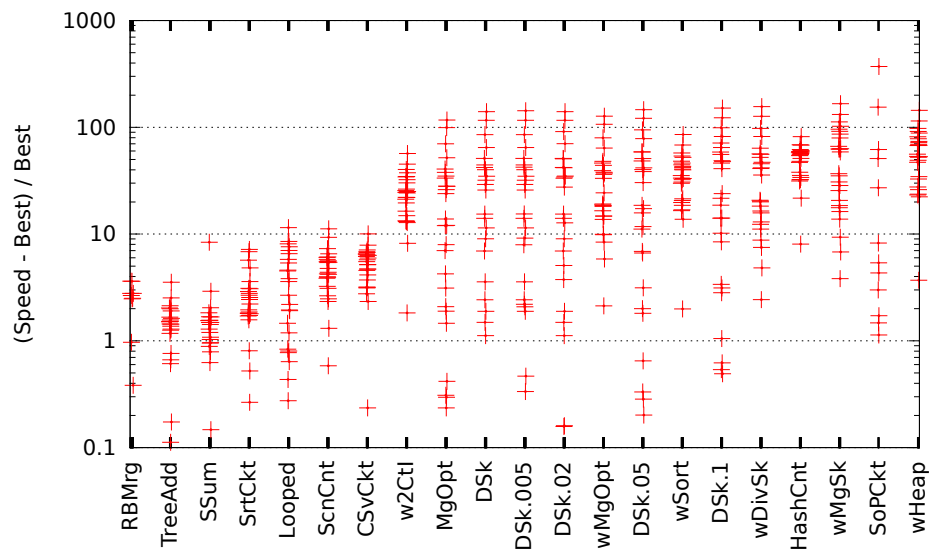


Figure 77: Suboptimality. CensusIncome, $N \leq 32$, Similarity queries.